ENCAPSULATION OF PROCYANIDINS IN DOUBLE EMULSIONS STABILIZED BY PROTEIN–POLYSACCHARIDE COMPLEXES

Rikkert Berendsen

Dipòsit Legal: T 1926-2014

Encapsulation of procyanidins in double emulsions stabilized by protein–polysaccharide complexes

Universitat Rovira i Virgili

Doctoral Thesis

Rikkert Berendsen

Rikkert Berendsen

Encapsulation of procyanidins in double emulsions stabilized by protein–polysaccharide complexes

DOCTORAL THESIS

Supervised by
Dr. Montserrat Ferrando Cogollos

Co-supervised by
Dr. Carme Güell Saperas

UNIVERSITAT ROVIRA I VIRGILI
Department of Chemical Engineering

Tarragona, 2014

UNIVERSITAT ROVIRA I VIRGILI

Departament d'Enginyeria Química, ETSEQ
Avinguda Països Catalans 26
Campus Sescelada, Spain
tel. +34 977 55 8505

I STATE that the present study, entitled "Encapsulation of procyanidins in double emulsions stabilized by protein–polysaccharide complexes", presented by Rikkert Berendsen, has been carried out under my supervision at the Department of Chemical Engineering of the University of Rovira i Virgili, and that it fulfills all requirements to obtain the doctoral degree.

Tarragona, September 8, 2014

Doctoral Thesis Supervisors

Dr. Montserrat Ferrando Cogollos   Dr. Carme Güell Saperas

Thesis committee

Dr. Marilyn Rayner   *(President)*
Lund University
Department of Food Technology,
Engineering and Nutrition
Lund, Sweden

Dr. Maria Paz Romero Fabregat   *(Secretary)*
Universitat de Lleida
Departament de Tecnologia d'Aliments
Lérida, Spain

Dr. Juan Carlos Arboleya Payo   *(Vocal)*
Azti-Tecnalia
Unidad de Investigación Alimentaria
Derio, Spain

Acknowledgments

First, I would like to express my gratitude towards Montse, who convinced me to come to Tarragona and do the doctorate under her supervision. You always stood open for my ideas, which made our discussions very pleasant and fruitful. Giving me the freedom to discover was something which I wouldn't want to have missed.

Carme was always involved and showed her concern for my integration in Tarragona. And you are totally right, working abroad extents to living abroad.

When Sílvia and I started doing experiments with the FTIR and already obtaining the first results, the device broke. Sadly enough we didn't continue this topic. Thank you for your warmth and humor.

I am very grateful to Tamara and Jaume, who have been very patient with me while I was, and still am, learning to express myself in Spanish. It has been a great pleasure spending time with you, in and outside the university.

Also my non-Spanish colleagues, Abreham, Tilahun, Worku, Sarathi and Osmar, and the many students who have passed the lab, Vanessa and Fernanda, Ukamaka, Rana, Caroline, Samara, Joana, Jordi, Sonia, and Marta made my stay a pleasant one. I have spend some good times in the lab with you all.

And of course all the other doctorate students and colleagues from other groups with whom I shared coffees, lunches and barbecues.

Furthermore, I would like to thank Professor Thomas Schäfer from POLY-MAT at The University of the Basque Country and Núria Canela from CTNS for their first discussions and help on adsorption experiments. Ciara O'Sullivan, Olivier Henry and Josep Lluis Acero from the Group of Nanobiotechnology and Bioanalysis with their help and support on the SPRi measurements. And Daniel Salavera from CREVER for his help on the osmotic pressure measurements.

Por tres años Neus y Lidón han sido mis compañeras de piso, hemos compartido más que solo un piso. Desde el primer momento me habéis dado muchísima confianza y fue un honor de haber podido conoceros.

Claramente tengo que doy las gracias a mis amigos; Angi y David, Susana, Ana, Ívan y Balya, Cate, Rúben, Albert, Visen y Montse, Samu, David y Ivan. No podría haber deseado mejores amigos.

Sergi, Angelica y Esther, gracias por vuestra hospitalidad, cariño y música.

My Dutch friends, who I could fall back on when visiting the Netherlands, and who have visit me in Spain, it is a pleasure to have such friends.

And finally, I would like to thank my parents and brothers for their support and never failing to believe in me.

"Afstand scheidt enkel de lichamen, niet de geesten."
Desiderius Erasmus Roterodamus,
Dutch humanist and philosoph
(1466 – 1536)

"Observar sin pensar es tan peligroso como pensar sin observar."
Santiago Ramón y Cajal,
Spanish neuroscientist
(1852 – 1934)

Contents

List of symbols and abbreviations

Symbols

a_w	[-]	wateractivity
BS	[%]	backscattering
C_{p,W_2}^n	[μg mL^{-1}]	procyanidin in W_2 after n^{th} cycle
$C_{p,\mu capsule}^{total}$	[g kg^{-1}]	total procyanidin in microcapsules
$C_{p,\mu capsule}^{wall}$	[g kg^{-1}]	procyanidin in the microcapsule wall
d_p	[μm]	pore diameter
d_d	[μm]	droplet size
$d_{d,f}$	[μm]	droplet size after emulsifying
$d_{d,i}$	[μm]	droplet size before emulsifying
$d_{4,3}$	[μm]	volume-weighted mean diameter
d_{10}	[μm]	10% of droplets below this value
d_{50}	[μm]	50% of droplets below this value
d_{90}	[μm]	90% of droplets below this value
$EEemulsion$	[%]	emulsion encapsulation efficiency
$EE\mu capsule$	[%]	microcapsule encapsulation efficiency
g	[m s^{-2}]	gravity
H_e	[mm]	total emulsion height
H_s	[mm]	serum height

J_e	$[\mathrm{m\,s^{-1}}]$	emulsion transmembrane flux
J_d	$[\mathrm{m\,s^{-1}}]$	dispersed phase transmembrane flux
K_H	$[\mu\mathrm{g\ mL^{-1}min^{-0.5}}]$	Higuchi release rate
m_{p,W_1}^0	$[\mathrm{mg}]$	initial procyanidin mass in W_2
$m_{p,W_{1+2}}$	$[\mathrm{mg}]$	total procyanidin mass in both water phases
m_{p,W_2}^n	$[\mathrm{mg}]$	procyanidin mass in W_2 after n^{th} cycle
$m_{W_1}^0$	$[\mathrm{mg}]$	initial mass of W_1
m_{W_2}	$[\mathrm{mg}]$	mass of W_2 phase
$m_{W_2}^0$	$[\mathrm{mg}]$	initial mass of W_2
$m_{W_2}^n$	$[\mathrm{mg}]$	mass of W_2 after n^{th} cycle
R^2	$[\text{-}]$	coefficient of determination
R	$[\text{-}]$	procyanidin released
R_0	$[\text{-}]$	procyanidin released during production
R_f	$[\mathrm{m^{-1}}]$	membrane fouling resistance
R_m	$[\mathrm{m^{-1}}]$	clean membrane resistance
$release$	$[\%]$	release during storage
$serum$	$[\%]$	serum layer percentage
T	$[\%]$	transmission
t	$[\mathrm{days}]$	time
v	$[\mathrm{m\,s^{-1}}]$	creaming velocity
γ_{ow}	$[\mathrm{N\,m^{-1}}]$	oil-water interfacial tension
ΔP_{tm}	$[\mathrm{Pa}]$	transmembrane pressure
ϵ	$[\text{-}]$	membrane porosity
η_d	$[\mathrm{Pa\,s}]$	dispersed phase viscosity
η_e	$[\mathrm{Pa\,s}]$	emulsion viscosity inside pore
θ	$[°]$	contact angle
ξ	$[\text{-}]$	tortuosity factor of pores
$\Delta\rho$	$[\mathrm{kg\,m^{-3}}]$	density difference
$\sigma_{w,p}$	$[\mathrm{Pa}]$	wall shear stress inside pore
ϕ	$[\text{-}]$	volume fraction of dispersed phase

Abbreviations

CMC	carboxymethyl cellulose
Chi	chitosan
ESEM	environmental scanning electron microscope
GA	gum Arabic
LbL	layer-by-layer
MD	maltodextrin
ME	membrane emulsification
O–W	oil-water interface
O/W	oil-in-water emulsion
PDL	pentadecalactone
PEG	polyethylene glycol
PGPR	polyglycerol polyricinoleate
PLGA	poly(lactic-co-glycolic) acid
PVA	polyvinyl alcohol
RI	refractive index
ROS	reactive oxygen species
RU	response unit
SC	sodium caseinate
SPR	surface plasmon resonance
SPRi	surface plasmon resonance imaging
SPG	Shirasu porous glass
TBARS	thiobarbituric acid-reactive substances
W_1	inner water phase of double emulsion
W_2	outer water phase of double emulsion
W–O	water-oil interface
W/O	water-in-oil emulsion
W/O/W	water-in-oil-in-water emulsion
WPC	whey protein concentrate
WPI	whey protein isolate

Abstract

The regular intake of foods rich in bioactive compounds, such as polyphenols, has been linked to a risk reduction in cardiovascular diseases and certain types of cancer. Although their particular role on reducing risk factors requires a better understanding, *in vitro* and clinical studies show consistently their positive effects on human health. As a result, the use of commercial extracts rich in polyphenols from different sources (i.e. grapes, tea, apple, etc.) to formulate foods and beverages has become a trend in the sector. Nevertheless, the effectiveness of those extracts depends on preserving the stability, bioactivity and bioavailability of the active ingredients.

A strategy to improve the stability and bioavailability of sensitive bioactive compounds is encapsulation. In this work, we investigated two encapsulation systems to entrap a procyanidin-rich extract: double (water-in-oil-in-water, $W_1/O/W_2$) emulsions and solid microcapsules (spray dried double emulsions). Premix membrane emulsification was the methodology applied to produce emulsions because it uses low shear stresses (what reduces the release of W_1 droplets during emulsification), requires low energy input and shows a good control of droplet size distribution.

We have focused on how the type and structure of the layer at the oil-water interface, made of whey proteins and polysaccharides, affects the physical and chemical stability of emulsions, and their capacity to retain procyaninds during processing and further storage. To understand the role of the interfacial layer, the

properties of the several amphiphilic emulsifiers in aqueous solution and absorbed to plane surfaces, which mimic the O–W interfaces in real emulsions, have been determined.

Premix ME enabled to produce single and double emulsions with a droplet size close to the membrane pore size (10 μm). To stabilize emulsions, several hydrophilic emulsifiers were used to adsorb on the oil-in-water (O/W) emulsion interface: whey protein isolate (WPI), and WPI–Carboxymethyl cellulose (WPI–CMC), WPI–Gum Arabic (WPI–GA) and WPI–Chitosan (WPI–Chi) complexes. Adsorption measurements by means of Surface Plasmon Resonance (SPR) showed that WPI–polysaccharides interfaces form thicker but less dense layers than only WPI. Furthermore, WPI–CMC and WPI–GA complexes produced an interface with a negative surface charge, while WPI and WPI–Chi lead to an interfacial layer positively charged.

Initially we assessed that premix ME enabled to produce sunflower O/W emulsions stabilized by different interfacial structures made of WPI and CMC. Although SPR measurements confirmed the adsorption between the several layers, only O/W emulsions stabilized by one interfacial layer (either WPI or WPI–CMC complex) did not coalesce after preparation. Even though WPI stabilized emulsions showed a mean droplet size close to the pore membrane size (10 μm), a significant amount of much smaller droplets contributed to increase droplet dispersion. This seemed to affect emulsion stability during storage.

The oxidation rate of sunflower O/W emulsions strongly depended on the interfacial composition: TBARS (by-product of lipid oxidation) in WPI–CMC stabilized emulsions increased much faster than in emulsions with WPI. Adsorption data at a hydrophobic interface of the WPI–CMC complex suggest that it formed a thick but less dense interface than WPI. Additionally the negative surface charge measured in the O/W interface of emulsions stabilized with WPI–CMC complex indicated that this interface was able to attract any transition metal cation and promote lipid oxidation. According to these results, some strategies to improve the oxidation stability of O/W emulsions by tailoring their interface should consider multi-layer arrangements, e.g. made of WPI, or protein–polysaccharide complexes having a positive electrical charge at the emulsion conditions, among others.

In the case of procyanidin-loaded $W_1/O/W_2$ emulsions stabilized by WPI–CMC, WPI–GA, or WPI–Chi complexes, the procyanidin encapsulation was at least 70% at the end of premix ME, regardless of the hydrophilic emulsifier used. Encapsulation of procyanidin decreased with each premix ME cycle, mainly linked to the escape of the inner W_1 phase as a result of the break-up of W_1/O droplets. Even though no important differences in the procyanidin encapsulation

were observed among emulsions stabilized with WPI–polysaccharide complexes, data about the shear stress in the membrane pores would help to better determine the effect of those on the break-out of inner W_1 droplet.

Stability of $W_1/O/W_2$ emulsions, encompassing creaming rate, droplet size distribution and polyphenol release during storage, was affected by the type of WPI–polysaccharide complex used as emulsifier. In the case of creaming rate, the viscosity imposed by each WPI–polysaccharide complex to the W_2 phase was a parameter to consider. The progress of the droplet size distribution during storage, in turn, was affected by pH, due to its influence on the surface charge of emulsion droplets as well as on the interactions between WPI and each polysaccharide. Hence, different windows of pH values, in which emulsions kept droplet size distribution stable, were identified for each WPI–polysaccharide complex. Furthermore, release rate constants during 14 days of storage ranged from 5.6 to 11.3 $\mu g \, mL^{-1} min^{-0.5}$ and depended more on the type of hydrophilic emulsifier than on pH environment. When the release rate constants were related to the thickness of the interfacial layer made of WPI–polysaccharides (obtained from SPR measurements), we observed that thicker layers led to lower release rates. Further research on the relationship between the properties of tailor-made interfaces with the diffusion of entrapped bioactive compounds is required to optimize each particular application.

To obtain solid microcapsules from $W_1/O/W_2$ emulsions, a wall material (maltodextrin) was added to the freshly produced double emulsions and, subsequently, the mixture was spray dried. At the operating conditions, the emulsions stabilized with WPI or WPI–polysaccharide complexes (WPI–CMC, WPI–GA or WPI–Chi,) showed good resistance to dehydration so that they could be converted into powders, able to retain procyanidins. Even though all the spray dried double emulsions recovered the structure of $W_1/O/W_2$ emulsions after rehydration, with a clearly differentiated W_1 phase, only rehydrated microcapsules from double emulsions stabilized by WPI–CMC were able to recover the droplet size distribution of the fresh ones. In this case, emulsions were able to keep their droplet stability over the whole production process, i.e. from emulsification to spray drying. Bridge flocculation of the $W_1/O/W_2$ emulsions stabilized with WPI–GA and depletion flocculation after addition of maltodextrin to the WPI–Chi stabilized emulsions are the suggested instability mechanisms that resulted in polydisperse droplets after microcapsule rehydration.

Results on encapsulation efficiency indicated that between 72.5% and 79.9% of the procyanidins in microcapsules were entrapped in the inner W_1 droplets, regardless the hydrophilic emulsifier. It has been shown that, WPI–CMC com-

plex was able to truly stabilize the W_1/O droplets during the different stages of microcapsule production but it moderately retained the migration of procyanidins through the W_1/O interface. According to this, we observed how small changes in hydrophilic emulsifiers have large influence on microcapsules and rehydrated microcapsules. These results suggest that interfacial properties of emulsions prior and during spray drying should be studied in order to increase microcapsule quality.

For each type of encapsulation system (single emulsion, double emulsion and spray dried double emulsion) a tailor-made hydrophilic emulsifier is required to comply with the type of protection needed, the addenda used and the delivery conditions.

Resumen

El consumo regular de alimentos ricos en compuestos bioactivos, tales cómo los polifenoles, se ha asociado a una reducción en el riesgo de contraer enfermedades cardiovasculares y ciertos tipos de cáncer. Pese a que su papel en la reducción de factores de riesgo requiere un conocimiento más profundo, estudios *in vitro* y clínicos muestran de forma consistente su efecto positivo en la salud humana. Como resultado, el empleo de extractos comerciales ricos en polifenoles ha llegar a ser tendencia en el sector. Sin embargo, la efectividad de estos extractos está condicionada a que se mantenga la estabilidad, bioactividad y biodisponibilidad de los ingredientes activos.

Una estrategia para mejorar la estabilidad y biodisponibilidad de compuestos bioactivos es la encapsulación. En este trabajo, se han investigado dos sistemas para encapsular extractos ricos en procianidinas: emulsiones dobles (agua-en-aceite-en-agua, $W_1/O/W_2$) y microcápsulas sólidas (emulsiones dobles atomizadas). La emulsificación por membranas (ME) premix ha sido la metodología empleada para producir las emulsiones debido a que aplica un esfuerzo de cizalladura reducido, presenta una necesidad energética baja y muestra un buen control de la distribución del tamaño de gota.

ME premix ha permitido producir emulsiones simples y dobles con un tamaño de gota similar al del tamaño de poro de la membrana (10 μm). Para estabilizar la interfase de las emulsiones aceite-en-agua (O/W), se han empleado varios emulsificantes hidrofílicos: fracción de proteínas de suero de leche (WPI) y los com-

plejos WPI–carboximetil celulosa (WPI–CMC), WPI–goma Arábica (WPI–GA) y WPI–quitosano (WPI–Chi). Las medidas de adsorción realizadas mediante Surface Plasmon Resonance (SPR) mostraron que las interfases estabilizadas con complejos WPI–polisacáridos presentaron un mayor espesor aunque una menor densidad que las estabilizadas con WPI. Además los complejos WPI–CMC y WPI–GA dieron lugar a una interfase con una carga superficial negativa, mientras que en el caso de WPI y el complejo WPI–Chi, la interfase presentó carga positiva.

Inicialmente se ha evaluado ME premix como técnica para producir emulsiones de girasol O/W estabilizadas con distintas estructuras interfaciales de WPI y CMC. A pesar de que las medidas de SPR confirmaron la adsorción entre las distintas capas, únicamente las emulsiones O/W estabilizadas por una única capa interfacial (constituida por WPI o el complejo WPI–CMC) no presentaron coalescencia tras de la preparación. Las emulsiones estabilizadas con WPI mostraron un tamaño de gota medio próximo al del tamaño de poro de la membrana (10 μm), aunque la presencia significativa de gotas de tamaño menor contribuyó a aumentar la dispersión. Esto último afectó la estabilidad de la emulsión con el tiempo.

La velocidad de oxidación de las emulsiones O/W dependió de la composición de la interfase: los valores de TBARS (subproducto de la oxidación de lípidos) en emulsiones O/W estabilizadas con WPI–CMC aumentaron mucho más rápidamente que en las emulsiones estabilizadas con WPI. Los datos de adsorción a una interfase hidrófoba de los complejos WPI–CMC sugirieron que éstos formaron una capa de mayor espesor, pero menos densa que la formada por WPI. Por otro lado los valores negativos de la carga eléctrica superficial en emulsiones estabilizadas con WPI–CMC indicaron su capacidad para atraer iones de metales de transición y provocar la oxidación de lípidos. Según estos resultados, las estrategias para mejorar la estabilidad de las emulsiones O/W frente a la oxidación basadas en el diseño de interfases deberían incluir sistemas multi-capa, en los que se emplearan proteínas, como por ejemplo WPI, o complejos WPI–polisacárido capaces de conferir a la interfase carga positiva.

En el caso de emulsiones $W_1/O/W_2$ con procianidinas encapsuladas y que se estabilizaron con complejos WPI–CMC, WPI–GA o WPI–Chi, la eficacia de encapsulación fue al menos de un 70 % al finalizar el proceso de ME premix. La encapsulación de procianidinas disminuyó con cada ciclo de ME premix, lo que se asoció con la salida de la fase acuosa interna W_1, resultado de la ruptura de las gotas W_1/O propia del proceso. No se observaron importantes diferencias en la encapsulación de procianidinas entre emulsiones estabilizadas con diferentes complejos WPI–polisacárido, aunque datos sobre el esfuerzo de cizalladura al que son sometidas las gotas en los poros de la membrana permitirían determinar el

efecto de éstos sobre la ruptura de las gotas W_1/O.

La estabilidad de las emulsiones $W_1/O/W_2$, incluyendo velocidad de flotación, distribución del tamaño de gota y liberación de procianidinas con el tiempo, se vio afectada por el tipo de complejo WPI–polisacárido utilizado como emulsificante. En el caso de la velocidad de flotación, la viscosidad originada por cada complejo WPI–polisacárido en la fase W_2 resultó ser un factor importante a tener en cuenta. La evolución de la distribución del tamaño de gota con el tiempo, a su vez, se vio afectada por el pH, debido a su influencia en la carga superficial de las gotas de la emulsión así como en las interacciones entre WPI y cada polisacárido. A partir de estos resultados, se han identificado para cada complejo WPI–polisacárido diferentes rangos de pH en los que las emulsiones mantuvieron constante su distribución de tamaño de gota. Por otro lado, se han determinado los valores de las constantes de liberación de procianidinas durante un periodo de 14 días, con valores que oscilan entre 5,6 y 11,3 $\mu g\,mL^{-1}min^{-0,5}$. Estos valores se mostraron más dependientes del tipo de emulsificante empleado que del pH del medio. Al relacionar las constantes de velocidad de liberación con el espesor de las capas interfaciales constituidas por complejos WPI–polisacárido (obtenidos a partir de medidas de SPR), se observó que las capas de mayor espesor condujeron a menores velocidades de liberación. En este sentido y con el fin de poder optimizar cada aplicación particular, resulta necesario investigar con mayor profundidad la relación entre las propiedades de la interfase y la difusión de los compuestos bioactivos encapsulados.

Para obtener microcápsulas sólidas a partir de emulsiones $W_1/O/W_2$, se adicionó a emulsiones acabadas de preparar un material de pared (maltodextrina) y, seguidamente, la mezcla se atomizó. A las condiciones de operación empleadas, se observó que las emulsiones estabilizadas con WPI o complejos WPI–polisacárido (WPI–CMC, WPI–GA o WPI–Chi) mostraron buena resistencia frente a la deshidratación, de manera que todas ellas se convirtieron en un polvo capaz de retener procianidinas. A pesar de que todas las emulsiones dobles atomizadas recuperaron la estructura de emulsión $W_1/O/W_2$ tras la rehidratación, únicamente las microcápsulas a partir de emulsiones $W_1/O/W_2$ estabilizadas con WPI–CMC fueron capaces de recuperar la distribución de tamaño de gota de las emulsiones frescas. En este caso, las gotas mantuvieron su estabilidad durante todo el proceso de producción, es decir, desde la etapa de emulsificación hasta la atomización. La floculación por formación de puentes, en emulsiones $W_1/O/W_2$ estabilizadas con WPI–GA, y la floculación por agotamiento, después de la adición de maltodextrina a emulsiones $W_1/O/W_2$ estabilizadas con complejos WPI–Chi, se sugieren como los mecanismos responsables de la inestabilidad, que dio lugar a emulsiones

polidispersas tras la etapa de rehidratación de las microcápsulas.

Los resultados sobre eficacia de encapsulación mostraron que entre un $72{,}5\,\%$ y $79{,}9\,\%$ de las procianidinas de las microcápsulas quedaron retenidas en la fase acuosa W_1, independientemente del tipo de emulsificante empleado. Se ha observado que el complejo WPI–CMC fue capaz de estabilizar las gotas W_1/O durante las diferentes etapas de la producción de microcápsulas aunque retuvo de forma moderada la migración de procianidinas a través de la interfase W_1/O. Según esto, se observó cómo pequeños cambios en los emulsificantes hidrofílicos tuvieron una gran influencia en las propiedades de las microcápsulas y de las microcápsulas rehidratadas. Estos resultados sugieren que las propiedades interfaciales de las emulsiones antes y durante el proceso de atomización deberían de ser estudiadas con el fin de mejorar la calidad de las microcápsulas.

Para cada tipo de sistema de emulsificación (emulsión simple o doble, o emulsión doble atomizada) se necesita diseñar el emulsificante hidrofílico que permita conseguir el tipo de protección requerido, para compuestos determinados, y de liberación frente a unas condiciones establecidas.

1

Introduction & Objectives

1.1 General introduction

1.1.1 Emulsions

An emulsion is a mixture between two immiscible liquids, usually oil and water, with one of the phases dispersed as small spherical droplets into the other (McClements et al., 2007). Systems where water is dispersed in an oil phase are called water-in-oil (W/O) emulsions, while an oil-in-water (O/W) emulsion, is an oil phase dispersed in water. The liquid that forms droplets is referred to as the dispersed phase, while the liquid that contains the droplets is referred to as the continuous phase.

According to droplet size, emulsions show differences in their stability and the methods used to produce them. Emulsions (also known as macroemulsions), with droplet sizes between $0.2 - 100 \ \mu m$, are kinetically stable while thermodynamically unstable and require a substantial energy input to be produced. Nanoemulsions, with droplets of sizes below 200 nm, show higher stability than emulsions even though they are still thermodynamically unstable dispersions, thus requiring the input of some external energy to convert the separate components into a colloidal dispersion (McClements, 2012). Finally, microemulsions are thermodynamically stable, transparent isotropic solutions with particles ranging from 5 to 100 nm that arise from the spontaneous self assembly of the hydrophobic and hydrophilic parts of surfactant molecules (Flanagan and Singh, 2006). Although microemulsions, because of their enhanced long-term stability, have found applications over a wide range of areas, such as pharmaceutical or cosmetics, their application to food has been limited by the types of surfactants used to facilitate microemulsion formation and the low solubility shown by long-chain triglycerides (Flanagan and Singh, 2006).

As thermodynamically unfavorable systems that tend to break-down over time due to a variety of physicochemical mechanisms, emulsions become kinetically stable for a reasonable period of time by including substances such as emulsifiers able to stabilize the O–W interface. Emulsions are widely used in industries such as pharmaceutical, cosmetic, agricultural, petrochemical and food (Nazir et al., 2010). Typical examples of emulsions in the food industry include vinaigrettes, milk, mayonnaise and sauces.

Recently double emulsions, a more complex type of liquid-liquid dispersion, have been receiving increased interest. Double emulsions (also duplex or multiple emulsions) are emulsions of emulsions such as an oil-in-water-in-oil (O/W/O) emulsion or a water-in-oil-in-water (W/O/W) emulsion (Charcosset, 2009). In the

Chapter 1

later case water droplets (W_1) are dispersed in a larger oil droplet (O) which in turn is dispersed in a continuous aqueous phase (W_2). There are two different interfacial layers in this type of emulsion: the W_1–O interface surrounding the inner water droplets, and the O–W_2 interface surrounding the oil droplets. Consequently, two different types of emulsifier are usually needed to stabilize $W_1/O/W_2$ emulsions: an oil-soluble emulsifier for the inner water droplets and a water-soluble emulsifier for the oil droplets. Due to their increased interfacial area, these double emulsions have a lower thermodynamic stability than single emulsions. In addition, the prepared double emulsions are susceptible to break-down (to become single emulsions) during processing, among other mechanisms by the migration of water between the inner and the outer aqueous phases.

Although, double emulsions are less stable than single emulsions, they have some potential advantages. The inner water (W_1) phase can be used as a carrier of flavors, aromas, colors, preservatives, antimicrobials, vitamins, minerals, polyphenols, amino acids, bioactive proteins, enzymes, or peptides, keeping them apart from the continuous aqueous phase. Entrapment of these ingredients can:

- protect them from environmental effects

- be used as delivery system

- mask undesired sensory attributes.

Other usage of double emulsion is for reduced fat products, where the inner water droplet reduces the total volume of fat, keeping the same outer droplet size, and having a minor effect on sensory aspects.

Emulsification systems

Emulsification consists of dispersing one fluid into another non-miscible fluid by creation of an interface. The energy requirements that involve the creation of new interfacial area mainly depend on the interfacial tension between the two phases and the size of the newly created droplets. Emulsions properties (like stability and rheological properties) and their industrial uses are not only governed by variables such as temperature and composition but also by the droplet size distribution (Leal-Calderon et al., 2007).

The several methods developed for producing emulsions differentiate in how energy is applied to the two-phase system, the mechanisms of droplet disruption and, overall, in their energy efficiency to obtain a particular droplet size distribution.

Conventional emulsifier systems Conventional methods to prepare emulsions encompass stirring equipment, colloid mills, homogenizers or ultrasonics. These systems are industrially applied due to their high throughput. However, such methods utilize a strong shearing stress which may result in coalescence of the dispersed phase and subsequently in a poor control over droplet size and distribution. In addition, the high shear and extensional stresses applied to the product may cause loss of functional properties of heat and shear sensitive components. To overcome these problems, alternative methods for emulsification using microstructured systems have received increasing attention (Nazir et al., 2010, Charcosset, 2009).

Emulsification by microfluidic devices In the last few decades, new techniques have been investigated to produce emulsions with a narrow droplet size distribution, while being more energy efficient. Several of these techniques have been found to produce mono-disperse emulsions, where the geometry of the system is the main determinant of the droplet sizes. The systems can be divided into two groups:

i) shear based systems (Figure 1.1a and b), where flow of continuous and disperse phase need to be controlled:

- T-junction (Graaf et al., 2004, Thorsen et al., 2001)
- Y-junction (Kubo et al., 2006)
- microcapillary device (Utada et al., 2005, Muschiolik, 2007)
- parallelized cross-flow junctions (Nisisako and Torii, 2008)
- flow-focusing (Anna et al., 2003)
- co-flowing system (Umbanhowar et al., 2000)

ii) spontaneous droplet formation systems (Figure 1.1c), where only the flow of the dispersed phase is critical for droplet formation:

- microchannel (Sugiura et al., 2002, Muschiolik, 2007, Kobayashi et al., 2002a)
- EDGE-based droplet generation (van Dijke et al., 2010)
- hollow fiber emulsification (Hoppe and Melin, 2007, Breisig et al., 2014)

Chapter 1

These systems have been used for small scale droplet production or to study the mechanisms behind droplet formation. In addition, there is a limited number of applications in which food-grade ingredients have been used to produce emulsions with a mean droplet size in the commercial range (about some few microns). Furthermore, wetting and fouling of micro devices have often been neglected while being crucial for robust prolonged operation and cleanability. For all this, scale-up is still an issue in spite of the significant advances already made (van Dijke et al., 2010).

Membrane emulsification Membrane emulsification (ME) is an alternative technique to produce emulsions with a narrow droplet size distribution applying a low energy input compared to that required by conventional emulsification techniques. Two types of membrane emulsification are commonly used, namely direct (or cross-flow) and premix ME. The process parameters primarily controlling droplet size distribution and transmembrane flux in ME are: membrane properties, membrane wetting, transmembrane pressure, wall shear stress and phase parameters (e.g. interfacial tension, viscosity and density of continuous and disperse phases). The membrane emulsification method involves using a transmembrane pressure to force the dispersed phase (in direct ME) or the coarse pre-emulsion (in premix ME) to permeate through the membrane. Droplet formation takes place at either the membrane pore end (in direct ME) or within the membrane pores (in premix ME).

i) Membranes

A membrane is a porous structure where the pores work as a kind of channels. Droplet break-up can be compared to that occurring in the channels of microfluidic devices although pores are less precisely defined. Membrane pore size and distribution lead to different membrane resistance, and thus droplet break-up (Charcosset, 2009). The type of material determines the membrane microstructure and wettability. Various materials have been used to produce emulsions, such as:

- silicon nitride (Zhu and Barrow, 2005, Geerken et al., 2007)

- polycarbonate (Kobayashi et al., 2002b)

- ceramic aluminium oxide (α Al$_2$O$_3$) (Schröder et al., 1998)

- zirconia (Joscelyne and Trägårdh, 1999)

- polytetrafluoroethylene (PTFE) (Suzuki et al., 1998, Yamazaki et al., 2003)

- polypropylene (Sotoyama et al., 1999)

- silica glass (Fuchigami et al., 2000)

- polyamide (Giorno et al., 2003, 2005)

- silica-based monolithic (Hosoya et al., 2005)

- Shirasu porous glass (SPG) (Charcosset, 2009)

Depending on the material, different techniques, such as track-etching or chemical synthesis, are used to produce membranes which results in a wide range of membrane properties. A variety of pore sizes, with circular, square, or slit shaped pores surfaces with different area, or materials with diverse wettability (either hydrophobic or hydrophilic) can be commercially found.

Shirasu porous glass (SPG) membranes, synthesized from $CaO–Al_2O_3–B_2O_3–SiO_2$-type glass made from a Japanese volcanic ash, are the most used in ME. Their structure with uniform cylindrical interconnected pores, mean pore diameters from 0.05 to 30 μm and porosity between $50 – 60\%$ seems to facilitate droplet break-up, although the percentage of active pores is usually below 10%. The surface wettability can be changed by reaction with organic silanes, such as octadecyltrichlorosilane (Charcosset, 2009).

ii) Direct ME

In direct ME (see Figure 1.1a) the to-be-dispersed phase is pressurized through a microporous membrane into the continuous phase. To detach the droplets which are formed at the membrane surface, some shear stress is applied. Usually a flow of the continuous phase over the membrane surface provides a tangential shear that induces droplet snap-off. This flow should be not excessive to prevent further droplet break-up. Other methods to induce droplet detachment are rotation or vibration of the membrane (Charcosset, 2009).

Transmembrane pressure (ΔP_{tm}), is the pressure needed for the dispersed phase to flow through the membrane pore (by Darcy's law) and form droplets at the membrane pore end (Laplace pressure). ΔP_{tm} for direct ME is expressed by:

$$\Delta P_{tm,directME} = \eta_d J_d R_m + \frac{4\gamma_{ow}\cos\theta}{d_d} \qquad (1.1)$$

where η_d is the dispersed viscosity, J_d the dispersed phase transmembrane flux, R_m the membrane resistance, γ_{ow} the O–W interfacial tension, θ the contact

Chapter 1
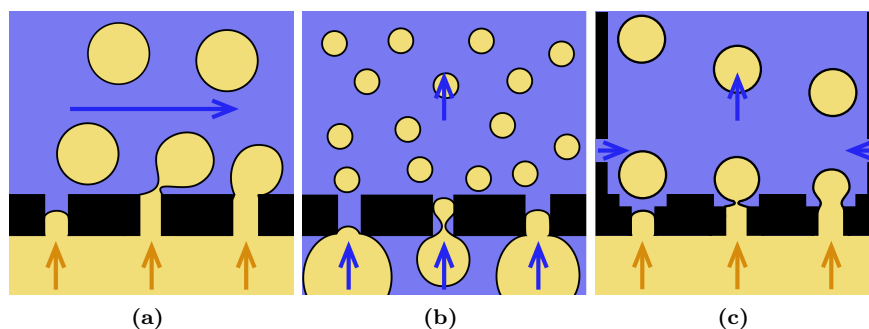
Figure 1.1: Emulsification systems: (a) direct ME, which is a shear based system, the flow of continuous and dispersed phase needs to be controlled, (b) premix ME, is a shear based system, where continuous and dispersed phase are mixed in a previous step, and (c) microchannel emulsification, which is a spontaneous droplet formation system, only the flow of the dispersed flow is critical for droplet formation.

angle of the oil droplet against the membrane surface wetted with the continuous phase and d_d the mean droplet size (Luca et al., 2004, Peng and Williams, 1998). Although process, membrane and phase parameters influence the emulsifying process, only the wetting behavior of the dispersed phase at the pore openings to the continuous phase (θ) governs the droplet formation and therefore droplet size and distribution (Fuchigami et al., 2000).

iii) Premix ME

In premix ME (see Figure 1.1b), first an emulsion with large droplet sizes (coarse emulsion) is prepared using a conventional emulsification system. Secondly this coarse emulsion is pressurized through a microporous membrane where the large emulsion droplets are broken into smaller ones. Repetitive passage of the emulsions through the membrane is needed to reduce and homogenize droplet sizes. The formation of mono-disperse emulsions in membrane pores has been suggested to occur by several phenomena (van der Zwan et al., 2006):

- snap-off due to localized shear forces

- break-up due to interfacial tension effects (Rayleigh and Laplace instabilities)

- break-up due to steric hindrance between droplets

In premix ME, in which an emulsion passes several times through the membrane, transmembrane pressure depends on droplet break-up, membrane resistance and, eventually, membrane fouling. The transmembrane pressure, is a combination of the required pressure to overcome flow resistances inside the pores and to break-up droplets. ΔP_{tm} for premix ME is expressed by:

$$\Delta P_{tm,premixME} = \eta_e J_e (R_m + R_f) + C\phi\gamma_{ow}\Big(\frac{1}{d_{d,f}} - \frac{1}{d_{d,i}}\Big) \qquad (1.2)$$

where η_e is the emulsion viscosity in the pores, J_e is the emulsion transmembrane flux, R_m the membrane resistance of a clean membrane, R_f the overall fouling resistance, C a constant, ϕ volume fraction of dispersed phase of the emulsion, $d_{d,f}$ the droplet size of the finally obtained emulsion, and $d_{d,i}$ the droplet size of the initial emulsion (Nazir et al., 2010). According to Vladisavljević et al. (2004) the extent of droplet disruption is closely related to the wall shear stress ($\sigma_{w,p}$) inside the membrane pores.

$$\sigma_{w,p} = \frac{8\eta_e J_e \xi}{\epsilon d_p} \qquad (1.3)$$

where ξ the mean tortuosity factor of the pores, ϵ the mean membrane porosity, and d_p the pore diameter. Considering the effect of transmembrane pressure on droplet break-up, three different regions can be distinguished (Vladisavljević et al., 2004):

i) at low transmembrane pressures, the large coarse emulsion droplets are insufficiently deformed to enter the membrane pores

ii) above critical pressure the large droplets enter the pores but due to small shear stresses inside the pores, droplet sizes are larger than the pore diameter

iii) at high transmembrane pressures droplets smaller than the pore diameter are formed due to higher shear stresses and droplet collisions between droplets and pore walls.

Thicker membranes give more uniform emulsions due to multiple droplet break-up inside the membrane. Wetting of the membrane with the continuous phase is of importance to lower the contact angle between the droplets and

membrane in order to produce uniform droplet sizes. Membranes that are incompletely wetted by the continuous phase often give high polydispersity and larger average droplet sizes (Nazir et al., 2010).

iv) Direct versus premix ME

Direct and premix ME production processes have both their own advantages and disadvantages that make them suitable for different applications. In direct ME, droplet sizes are typically a factor 2 – 10 times larger than the membrane pore diameter while in premix ME the droplet to pore size ratio ranges from 1.25 to 0.68 after five passes (Nazir et al., 2010, Joscelyne and Trägårdh, 2000). However, emulsions obtained by premix ME are not as mono-disperse as with direct ME. In the case of direct ME, monodispersity is mainly determined by the pore diameter distribution, while in premix ME it is mainly influenced by the wall shear stress. The main disadvantage of direct ME is the requirement of large membrane surface area to obtain high throughput at reasonable production rates, which is one or two magnitudes smaller than premix ME which is typically above 1 $m^3m^{-2}h^{-1}$. Furthermore, premix ME process is easier to control and operate than direct ME, since the driving pressure and emulsifier properties are not as critical for the successful operation as in the direct ME process. Also, from an energy cost point of view, less energy input is needed for premix ME due to the absence of continuous phase flow as in direct ME, though, in premix ME an coarse emulsion must be made before emulsifying. The main drawback of premix ME is the fouling of the membrane which may become worse depending on the emulsion formulation used (Vladisavljević and Williams, 2005).

Both direct and premix ME offer a great potential in comparison to conventional emulsification systems since less emulsifier is needed, lower shear stresses and less heat are applied. These advantages make ME suitable for producing emulsions which may contain compounds sensitive to heat or mechanical stress or for producing double emulsions.

v) Production of double emulsions

Production of double emulsions ($W_1/O/W_2$) is usually done in a two-step procedure. First, by preparing a W_1/O emulsion, where hydrophobic emulsifiers are used to stabilize the W_1–O interface. This emulsification used to be performed under high shear conditions (e.g. conventional emulsification methods) to obtain small droplets. Second, by adding the W_1/O emulsion to a W_2 phase which contains a hydrophilic emulsifier. This emulsification step should be carried out under less shear to avoid the rupture of the internal W_1/O droplets. In the sec-

ond emulsification step, ME offers a great potential in comparison to conventional emulsification systems since lower shear stresses are used, what makes ME suitable for the production of double emulsions.

Stabilization of emulsions

To make emulsions kinetically stable for a limited period of time, emulsifiers are included in their formulation. As surface active molecules that adsorb to the surface of freshly formed droplets during homogenization, emulsifiers form a protective layer that prevents droplets from coalescing. Additionally they have the ability to reduce the interfacial tension, decreasing the energy requirements during emulsification. If possible, emulsifiers should quickly adsorb to the oil-water interface during emulsification, reducing significantly the interfacial tension and preventing droplet coalescence. Emulsifiers vary widely in their ability to form and stabilize emulsions depending on their molecular and physicochemical properties (Capek, 2004).

Surfactants   Monomeric low molecular weight surfactants or simply surfactants, is a group of amphiphilic molecules which consists of a hydrophilic "head" group attached to a lipophilic "tail" group. The small molecules can rapidly coat freshly created oil-water interfaces, where the lipophilic tail group interpenetrates the oil phase and the hydrophilic head sticks in the aqueous phase, thus lowering the total free energy. Surfactants are above all very efficient in reducing the interfacial tension and keeping it constant due to possible desorption. At low concentrations in solution, surfactants exist as monomers, however, with an increase in concentration above the critical micelle concentration, they spontaneously aggregate into structures such as micelles, bilayers, vesicles, and reverse micelles. In the case of micelles in aqueous solution, the unfavorable contact of the lipophilic tail with water forces a group of surfactants to put their tails together, and thus reduce their contact with water. The type of head and the size, shape or amount of tails determines the surfactant geometry, which in turn determines the type of structure it can form or which type of emulsion it can stabilize i.e. O/W or W/O emulsions (McClements et al., 2009). For double emulsions, two type of surfactants are needed, hydrophilic ones that can stabilize the O–W_2 interface and hydrophobic ones that can stabilize the W_1–O interface. Monoglycerides, lecithins, glycolipids, fatty alcohols and fatty acids have been used as surfactants, but are gradually replaced by polymeric high molecular weight emulsifiers (Kralova and Sjöblom, 2009).

Chapter 1

Amphiphilic biopolymers   Polymeric high molecular weight emulsifiers encompass proteins and polysaccharides. Proteins are polymers of amino acids, whereas polysaccharides are polymers of monosaccharides, which can be surface active depending on their molecular characteristics. The interfacial activity of many biopolymers relies on the hydrophilic and lipophilic regions distributed along their molecular structure. When a biopolymer adsorbs to an interface, it can adopt a conformation where the non-polar groups are located in the oil phase while the polar groups are in the aqueous phase. Adsorption also reduces the contact area between the oil and water molecules at the oil-water interface, reducing interfacial tension. Even though the conformation that a biopolymer adopts at an interface depends on its molecular structure and interactions, they form interfacial layers that use to be thick and dense. In food industry, proteins are widely used to stabilize O/W emulsions because they show good surface active properties and form a viscoelastic layer at the interface that improves the encapsulation properties due to a barrier effect (Bos and van Vliet, 2001). Nevertheless, most protein stabilized emulsions are rather heat sensitive because of the protein denaturation on the O–W interface what usually leads to emulsion break-up. Due to the poor surface active properties of most polysaccharides, their application as emulsifiers is limited, with some exceptions. For all this, strategies based on the combined used of proteins and polysaccharides to stabilize emulsions have been developed.

Complex emulsifiers   Blends of proteins and polysaccharides form, under specific conditions, complexes (conjugates) with enhanced functional properties in comparison to those shown by single proteins or polysaccharides. Protein–polysaccharide complexes combine the positive properties of each of their components:

  i) proteins show good adsorption to O–W interfaces

 ii) polysaccharides enable to form a thicker stabilizing layer that is capable of protecting droplets against aggregation (Benichou et al., 2003, Dickinson, 2003, Jourdain et al., 2009).

Emulsions stabilized with protein–polysaccharide complexes are stable over a wide range of unfavorable conditions, such as thermal shock treatment, pH, mechanical agitation, chilling, freezing, drying and the presence of multivalent ions (Benichou et al., 2004, Aoki et al., 2005, McClements et al., 2007). In emulsions designed as encapsulation systems, this kind of dense and thick interfaces made of protein–polysaccharide complexes could improve protection of the encapsulated sensitive

compounds or enable their controlled release. Furthermore, these interfacial structures have been suggested to improve chemical stability against oxidation reactions, e.g., interactions between lipids and metal ions can be minimized by controlling the interfacial charge, thickness and density (see page 23).

Regarding how emulsions stabilized simultaneously by proteins and polysaccharides can be produced, two kinds of methods for interfacial layer assembly have been described:

i) electrostatic layer-by-layer (LbL) deposition (Klinkesorn et al., 2006)

ii) complex deposition

The latter has been used to produce the so-called "mixed emulsions" (Dickinson, 2009). In electrostatic LbL deposition, an oppositely charged polysaccharide is added to a "primary" emulsion stabilized only by proteins. The electrostatic interactions at the droplet surface between the adsorbed protein and the oppositely charged polysaccharide produce a "secondary" emulsion. This procedure can be repeated to form oil droplets coated by multiple layers.

In complex deposition, first a protein–polysaccharide soluble complex is formed in a water solution that is subsequently used as continuous phase. In this way, the protein–polysaccharide complex acts as emulsifier, stabilizing the oil-water interface. This type of protein–polysaccharide complexes can be formed either by covalent cross-linking or electrostatic interactions like in LbL coated emulsions (Tolstoguzov, 1991). Covalent cross-linking between a protein and a polysaccharide can be achieved in various ways, but probably the method of conjugation most widely used is based on Maillard reaction (Dickinson, 2009). The Maillard reaction is a series of non-enzymatic browning reactions, which naturally occur between an amino acid and a reducing sugar. Maillard-type complexes have been produced for several protein–polysaccharide pairs (Evans et al., 2013). Conditions, of temperature, relative humidity and reaction time are adjusted in a case-by-case basis to improve the surface active properties of the complex and thus increase emulsion stability. Another example of covalent binding, is the use of the carbodiimide, gluteraldehyde, or laccase, which are used to cross-link proteins to polysaccharides. Covalent cross-links are irreversible and very stable to pH and ionic changes (Chen et al., 2010, Cooper et al., 2005, Schmitt et al., 1998).

Protein–polysaccharide electrostatic complexes   A requirement for the formation of protein–polysaccharide electrostatic complexes is the existence of opposing charges on the reacting species. Conventionally this is achieved by the

utilization of an anionic polysaccharide in combination with a protein bearing a significant number of cationic groups. However, the conditions to form a particular protein–polysaccharide electrostatic complex in solution are very specific.

When a protein and a polysaccharide are mixed they may either form a one-phase or a two-phase system depending on the nature of the biopolymers involved, the concentration of both biopolymers in solution, the ionic strength and pH of the solution (McClements et al., 2009). In a one-phase system, the two biopolymers can exist either as individual molecules or as soluble complexes that are evenly distributed throughout the entire system. In a two-phase system, the solution separates into two distinct phases that have different biopolymer compositions. These different behaviors can be explained from the type and intensity of electrostatic interactions occurring between protein and polysaccharide.
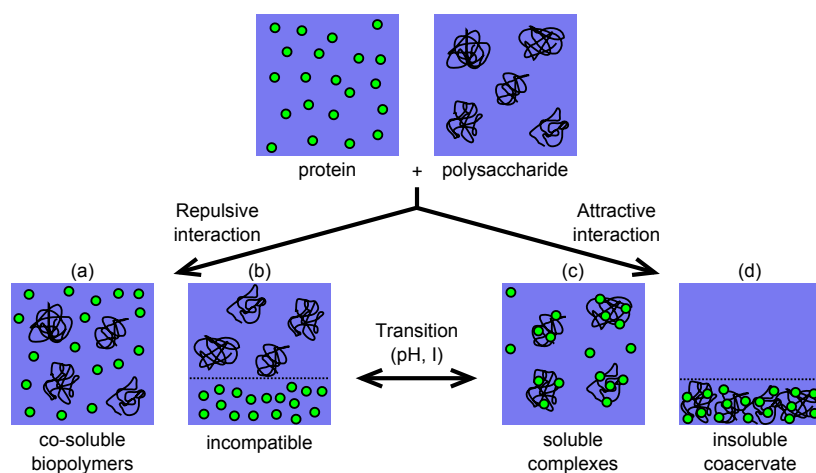
Figure 1.2: Proteins and polysaccharides may form a variety of different phases in aqueous solutions due to repulsive or attractive electrostatic interactions. Adaptation from McClements et al. (2007).

If repulsive electrostatic interactions between the two biopolymers prevail, the biopolymers are co-soluble (one-phase system) at low concentrations (Figure 1.2a) or separate in two phases at high concentrations (Figure 1.2b). This two-phase system, with one of the phases being rich in protein and depleted in polysaccharide

and the other phase vice versa, is formed due to a relatively high positive (unfavorable) free energy of mixing (Tolstoguzov, 1991). This type of phase separation occurs when one or both biopolymers are uncharged or carry similar electrical charges (McClements et al., 2009). Figure 1.3 shows a phase diagram of a protein and polysaccharide mixture controlled by repulsive electrostatic interactions where the binodal curve, with its typical shape, defines the regions of two-phase systems.
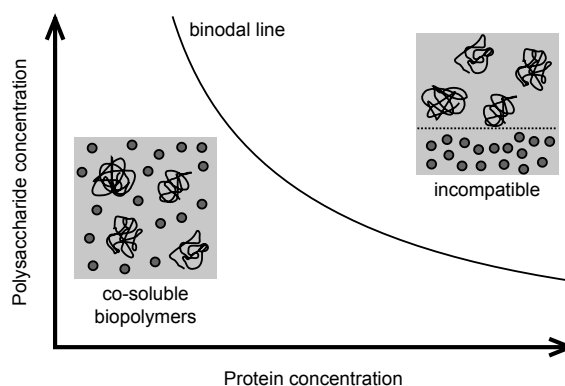
Figure 1.3: Generalized phase diagram of protein and polysaccharide at repulsive electrostatic interaction.

In the case that the electrostatic interactions between protein and polysaccharide are predominantly attractive, we can obtain a one- or a two-phase system depending on the interaction intensity. Strong electrostatic interactions, resulting from the opposite net charges of both biopolymers, cause that protein and polysaccharide associate and form coacervates which are no longer soluble. According to this, a two-phase system is made of insoluble coacervates and a surrounding solution depleted in both biopolymers (Figure 1.2d). By controlling the pH and ionic strength of the solution, the attractive electrostatic interactions between both biopolymers can be milder, and produce soluble complexes uniformly distributed over the solution (Figure 1.2c).

The state diagram of protein/polysaccharide systems in which attractive electrostatic interactions occur between both biopolymers strongly depends on pH, ionic strength and the protein to polysaccharide mass ratio of the solution. Figure 1.4 shows a simplified state diagram for a protein in solution with an anionic

Chapter 1

polysaccharide. At salt concentrations between 0 to 50 mM, pH dependency can be divided into four regions delimited by phase transition lines; pH_c, $pH_{\varphi 1}$, and $pH_{\varphi 2}$ (de Kruif et al., 2004):

Figure 1.4a) at pH values above the isoelectric point $(pH > pI)$, both protein and polysaccharides have relatively strong net negative charges. Thus, repulsive electrostatic interactions prevent complex formation.

Figure 1.4b) by reducing pH below pH_c at pH values close to the isoelectric point $(pH \approx pI)$, proteins present sufficient cationic groups $(-NH_3^+)$ on its surface to interact with a single polysaccharide molecule and produce soluble complexes.

Figure 1.4c) below $pH_{\varphi 1}$, at pH values still below the isoelectric point $(pH < pI)$, strong electrostatic interactions occur between proteins and polysaccharides what leads to the formation of non-soluble complexes or coacervates that precipitate.

Figure 1.4d) below $pH_{\varphi 2}$, at pH values far below the isoelectric point $(pH \ll pI)$, due to neutralization of the weak polyelectrolyte, the interaction between protein and polysaccharides results into one phase where both biopolymers co-exists.

The conditions required to obtain soluble complexes are applied to produce electrostatic LbL and complex deposit emulsions. In this way, the electrostatic interactions are sufficient to deposit one or multiple layers on the emulsion interface. If the environmental conditions are adjusted to increase the electrostatic attraction between the proteins and polysaccharides located at the interface, they will form insoluble coacervates unable to stabilize the interface and, as a result, emulsion will break-up. Differences in stability have been found between the electrostatic LbL and complex deposit emulsions which have been related to differences in the structure of the adsorbed layer (Jourdain et al., 2008). In general multi-layer (either electrostatic LbL or complex deposit) emulsions have been claimed to have improved stability properties over emulsions only stabilized by proteins. Due to the high number of biopolymers and combinations, tailor-made layers can be produced to have specific stability, encapsulation capacity or release properties.

Mechanisms of emulsion instability

Due to thermodynamic instability, emulsion droplets tend to grow reducing their interfacial area and thus decreasing their total free energy (Capek, 2004, Mc-
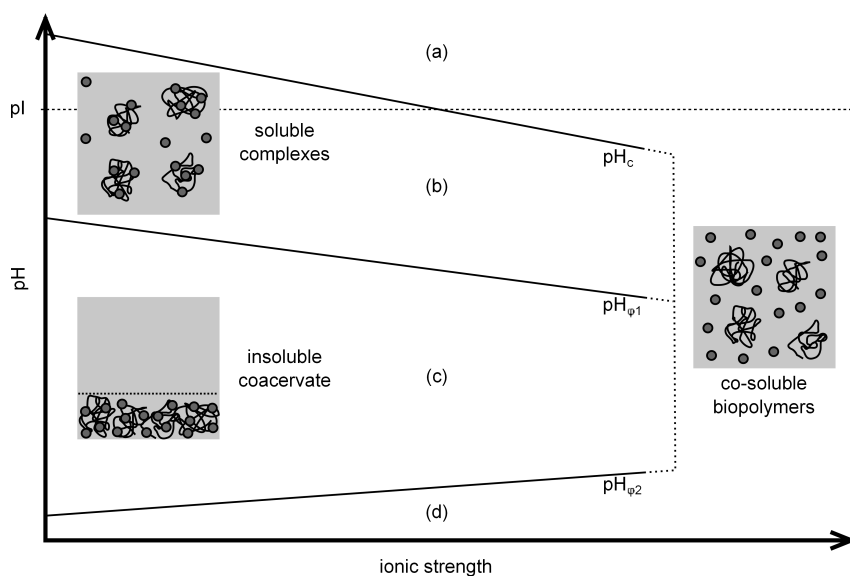
Figure 1.4: Generalized state diagram of protein–anionic polysaccharide complex formation. Adaptation from de Kruif, Weinbreck, and de Vries (2004).

Clements et al., 2007). Several physical mechanisms, such as *creaming*, *coalescence*, *Ostwald ripening* or *flocculation*, are responsible for the break-up of emulsions and their instability. In practice, two or more of these mechanisms may occur simultaneously, reason why it is important to determine the relative significance of each of them and the factors that influence them in order to develop effective strategies to control emulsion stability. Droplet size and droplet size distribution, interfacial tension, type of interface, and disperse and continuous phase properties are the main factors involved.

Gravitational separation is the result of the difference in density between disperse and continuous phases: *creaming* occurs when droplets have lower density that the continuous phase while sedimentation involves a higher density of the droplets than the surrounding liquid. The rate at which isolated droplets creams in an ideal liquid is given by Stoke's law:

Chapter 1

$$v = \frac{\Delta \rho g d_d^2}{18 \eta_c} \qquad (1.4)$$

where creaming velocity (v) is influenced by gravity (g), the emulsion droplet size (d_d) and droplet size distribution, density difference of continuous and dispersed phase ($\Delta \rho$) and the viscosity of the continuous phase (η_c). Although in real food emulsions, creaming velocity depends on some other parameters, such as disperse phase fraction, droplet size distribution or droplet electrical charge, the basic strategies to reduce this phenomenon are based on decreasing droplet sizes and droplet size dispersion, increasing viscosity or choosing similar continuous and dispersed phase densities. Among them, the most common solution against creaming is to increase the continuous phase viscosity by adding polymeric amphiphile or polymeric non-adsorbing compounds (Lutz and Aserin, 2007). Even though creaming usually is an undesired phenomenon because of its negative impact on taste and mouth feel, it can be easily reversed by shaking the emulsion what redistributes droplets over the emulsion. An additional problem is that creaming can enhance flocculation or coalescence because it causes droplets to come into close contact for extended periods.

Coalescence consists of the merging of two adjacent droplets into one larger droplet, leading to increased creaming. In general, coalescence is determined by the physical mechanisms responsible for droplet encounters (e.g., simple shear, turbulence, gravity), the nature of the forces that act on and between the droplets and the resistance of the thin film separating the droplets to rupture. A number of mechanisms is involved in the rupture of this thin film. The importance of these different mechanisms is determined by the characteristics of the continuous phase separating the droplets (e.g. viscosity, interfacial tension) and the interfacial membranes surrounding the droplets (e.g. thickness, shear modulus, and colloidal interactions). As a consequence, the most appropriate methods for controlling coalescence are based on the type of emulsifier used to stabilize the system and the environmental conditions. These have to be selected to prevent droplet contact and the rupture of the interfacial membranes surrounding the droplets (Capek, 2004). Among others, the thickness of the interfacial layer plays an important role; thicker interfacial membranes are less likely to be ruptured and provide a greater steric hindrance (see page 20) between droplets.

Another emulsion instability phenomenon is *Ostwald ripening*, which involves smaller droplets to shrink and disappear at the expense of the growth of larger droplets. This process is thermodynamically driven by the chemical potential of molecules from the dispersed phase. By molecular diffusion of emulsion droplets

through the continuous phase, a mass transfer between the droplets takes place. Smaller droplets having higher Laplace pressure, due to their radius of curvature, leads to increased solubility (Capek, 2004, Dickinson, 2009). In O/W emulsions, the solubility of the oil phase in water has a great influence on the rate of Ostwald ripening: emulsions with flavor oil (relatively water-soluble) are less stable than emulsions with vegetable oil (water insoluble). Other main parameters to control Ostwald ripening include the emulsifier type and concentration, and the properties of the interfacial layer. Micelles formed by emulsifiers in the continuous phase can entrap oil and therefore enhance Ostwald ripening. Furthermore, thickness and density of the interfacial layer significantly affect Ostwald ripening: thick layers lower Ostwald ripening, while less dense layers are supposed to be more prone to it (Lim et al., 2011, Zeeb et al., 2012).

Flocculation occurs when emulsion droplets glue together. Emulsion droplets aggregate without disruption of the stabilizing layer at the oil-water interface, whether the process is reversible depends on the strength of attraction (Dickinson, 1997). Two kinds of flocculation are distinguished: Depletion flocculation, which occurs when non-adsorbing biopolymers forces emulsion droplets together (see page 20 for details) and bridge flocculation which is the result of attractive interactions of biopolymers between neighboring droplets. Bridge flocculation occurs when a biopolymer, acting as emulsifier, has some of their non-polar residues associate with hydrophobic patches on one droplet, while others associate with hydrophobic patches on another droplet. As a result, droplets stick together. This type of bridge flocculation is observed when a biopolymer is used as an emulsifier and there is insufficient quantity present to completely cover the oil-water interface formed during emulsification. Bridge flocculation can also happen when a biopolymer in the continuous phase has an electrical charge that is opposite to that of the droplets (Dickinson, 1997). To prevent flocculation, non-adsorbed biopolymers have to be small with a similar charge as the adsorbed biopolymer, and the emulsion must be sufficiently covered by emulsifier, additionally steric hindrance (see page 20) can prevent droplets of coming into close contact.

Interactions between emulsion droplets (Colloidal interactions) Colloidal interactions determine if emulsion droplets aggregate or remain separate. As aforementioned, stability or sensory properties, among others, are determined by the degree of droplet aggregation and the characteristics of the aggregates. The overall interaction between the droplets depends on the relative magnitude and range of the attractive and repulsive forces. These interactions are mainly controlled by the properties of the interfacial layers coating the emulsion droplets.

Chapter 1

Repulsive interactions   Two repulsive interactions have been distinguished namely, *electrostatic repulsion* and *steric hindrance* (Benichou et al., 2004).

Electrostatic repulsion takes place between electrical charged surfaces which repel when equally charged. Food-grade emulsions stabilized by proteins or combinations of protein and polysaccharides show electrostatic interactions which can be controlled by changing pH or ionic strength of the aqueous solution (McClements et al., 2009). In water, dissolved ions can modify the electrostatic interactions of charged surfaces by screening the interface and forming an electrical double layer. The magnitude and range of electrostatic repulsion between two droplets decreases as the ionic strength of the solution separating them increases because of electrostatic screening. Consequently, much smaller concentrations of multivalent ions are required to promote emulsion instability (Jones, 2002).

Steric hindrance occurs when two emulsion droplets covered by adsorbed biopolymers come into a close distance where the interface layers overlap and interact with each other. At close droplet separations steric interactions are strongly repulsive and may therefore prevent emulsion droplets from aggregating. In this overlapping zone, as biopolymers become more concentrated than in the bulk solution, diffusion of water initiates, separating the emulsion droplets from one and another (Capek, 2004).

Attractive interactions   Oppositely to repulsive interactions which lead to emulsion stability, attractive interactions lead to instability via droplet aggregation (flocculation) or coalescence. Three different types of attractive interactions have been recognized.

Van der Waals interactions are attractive forces between any pair of atoms or molecules in the dispersed or continuous phase. They act between all kinds of colloidal particles, and therefore they are always occurring in emulsions. The fact that van der Waals interactions are relatively strong and long range, suggests that emulsions droplets would end up associating with each other in the absence of any other interaction. Many food emulsions are stable to droplet aggregation, which indicates that repulsive forces are strong enough to overcome the van der Waals attractions.

Unlike electrostatic repulsion, *electrostatic attraction* occurs between electrical charged surfaces oppositely charged. The strong influence that pH and ionic strength of the solution have on this type of interactions has been mentioned above.

Depletion interaction is the result of non-adsorbing colloidal particles present in the continuous phase, which is the interaction behind depletion flocculation. These non-adsorbing colloidal particles may be surfactant micelles (when the free surfac-

tant concentration exceeds some critical value), individual polymer molecules or aggregated polymers. The presence of these colloidal particles causes an attractive interaction between the droplets that is often large enough to promote emulsion instability. The origin of this interaction is the exclusion of colloidal particles when two droplets approach each other at a distance smaller than the colloidal particle sizes, a depleted zone of colloids is created. As a consequence there is an osmotic potential difference (between the depletion zone without colloids and the bulk solution rich in colloids) that enhances the movement of solvent from the depletion zone into the bulk liquid. The removal of solvent between the droplets, initiate an attractive force between them. According to this, the main parameters affecting the strength of the depletion interaction are size and concentration of non-adsorbing colloidal particles in the continuous phase (Jones, 2002).

Double emulsion instabilities Double emulsions show, besides the instabilities seen in single emulsions, additional instabilities result of their particular microstructure. As in single emulsions, double emulsions are susceptible to coalescence, Ostwald ripening and flocculation for both W/O and O/W emulsions. Double emulsions, such as $W_1/O/W_2$, require a hydrophobic emulsifier to stabilize the W_1–O interface and a hydrophilic emulsifier to stabilize the O–W_2 interface. The different interactions between the two emulsifiers located at each of both interfaces and the compounds present in W_1, O and W_2 are of great importance to maintain the microstructure of the initially produced double emulsion (Muschiolik, 2007).

Regarding the mechanisms controlling the stability of double emulsions, we can find coalescence of the outer droplets, or coalescence of the inner droplets without any change in droplet interfaces, being droplet coalescence in these cases analogous to the coalescence of single emulsions. Only in double emulsions, a mass transport through the intervening liquid film results in an exchange of material between the internal phase and the external phase. In the case of a $W_1/O/W_2$ emulsion, the water transport from W_1 to W_2 or vice versa determines the emulsion stability. Several mechanisms on the mass transfer between W_1 and W_2 have been identified (Garti, 1997): inner-outer phase coalescence, lamellae thinning, reversed micelles and hydrated surfactants.

The coalescence of the inner W_1 droplets to the outer water phase (W_2) leads to transfer of internal dispersed phase to the external continuous phase (Figure 1.5b). Since the outer droplet size is much larger than the size of the inner droplets, the attraction of small droplets to the outer interface is larger than the attraction between the small droplets. This increases the likelihood of small droplets coming

in contact with the outer interface (Pays et al., 2002). When this contact occurs without coalescence, molecules may pass from W_1 to W_2 across the very thin lamellae, made of oil and interfacial emulsifiers, by a mechanism called lamellae thinning (Figure 1.5c).
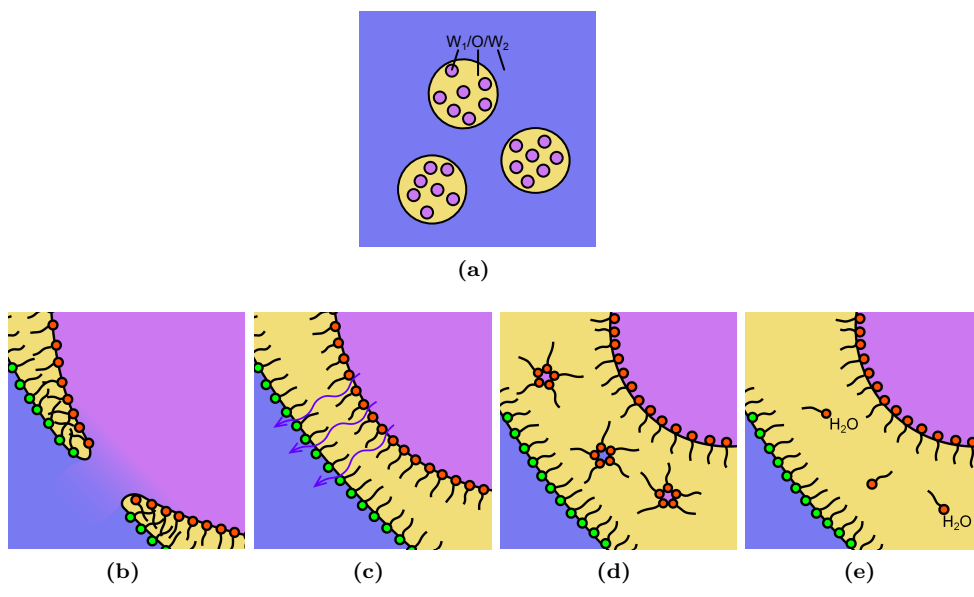
Figure 1.5: (a) microstructure of a double emulsion and its instabilities: (b) inner-outer phase coalescense, (c) lamellae thinning, (d) reversed micelle, and (e) hydrated surfactant.

Another pathway for molecular transport through the oil phase can occur by means of reversed micelles (Figure 1.5d). When the emulsifier concentration in the oil phase is higher than the critical micelle concentration, reversed micelles able to entrap water or addenda can be formed, promoting water release.

Molecular transport can also take place via hydrated surfactants (Figure 1.5e) in a way that the hydrophilic portion of the surfactant hydrates at one O–W interface and dehydrates at another O–W interface. This mechanism is osmotic driven and can work in both ways (from W_1 to W_2 or vice versa) leading droplets to shrink or swell. Considering the double (or multiple) compartment structure of

these emulsions, they can be considered as reservoirs of encapsulated substances to be released under variable conditions (see page 23). For the application as delivery systems, all those transport mechanisms can be accounted not only for the release of water but also (and especially) for the release of the addenda contained in the inner phase of the double emulsion. Research has been done on lowering the transport effects, by matching osmotic pressures in both water phases, and by equilibrating the amount of emulsifiers used, which has to be enough to stabilize the droplets but not in excess to avoid reversed micelles.

Emulsion as protection and delivery system of bioactive/sensitive compounds

The encapsulation of sensitive compounds (e.g. flavors, aromas, colors, preservatives, antimicrobials, vitamins, minerals, polyphenols, amino acids, bioactive proteins, enzymes, peptides, polyunsaturated oils and bioactive lipids) has to fulfill some of the following requirements to be used as a delivery system in the food industry (Desai and Park, 2005, Fang and Bhandari, 2010):

- to protect the addenda upon processing and storage.

- to reduce the release of addenda during production and storage.

- to tailor the release for a specific delivery or to mask off-flavors.

Protection upon processing and storage Emulsions, as encapsulation systems, have to protect the entrapped addenda over the whole production process, which may involve different kinds of food preservation treatments, such as heat, cooling, freezing, pH changes etc. In this respect, the impact of the emulsification process itself on the stability of the addenda to be encapsulated has to be considered. Finally, the ability of the emulsions to protect the entrapped compound has to cover the storage period, during which the environmental conditions can change.

As aforementioned, the production of emulsions involves heat and shear stresses and mechanical forces which may deteriorate the quality of the emulsion. Oil phase and emulsifiers are the main components which suffer under these stresses. Low shear emulsification systems, such as ME (see page 5) can efficiently encapsulate and protect addenda and may leave physicochemical and molecular properties of the biopolymers (e.g. proteins) and oil unaffected. Furthermore, these systems are able to produce mono-disperse emulsions which increase the system stability,

Chapter 1

affect taste perception (more homogeneous product), and lower bacterial growth (Charcosset, 2009). Even if emulsions are physically stable during storage, chemical stability is important to maintain the properties of the emulsion components. The encapsulation, protection and delivery of sensitive compounds are necessary to improve the quality of foods and the production of functional foods.

A major chemical degradation observed in O/W emulsions is lipid oxidation, which causes noticeable changes in their taste, texture, shelf life, appearance and nutritional value. When emulsions are used to encapsulate bioactive lipophilic molecules, such as ω-3 fatty acids, carotenoids, tocopherols, oryzanols, phytosterols etc., they can be irreversibly oxidized, reducing their specific health benefits (McClements and Decker, 2000). Lipid oxidation occurs when light, oxygen and/or free radicals are present in the oil phase. Reactive oxygen species (ROS), a type of free radical that contains an oxygen molecule, are a natural by-product of oxygen metabolism which can, in combination with oxygen, react with unsaturated lipids, converting them into lipid peroxides (Figure 1.6). Levels of ROS drastically increase upon environmental stresses such as UV or heat. Other mechanisms that accelerate lipid oxidation involve: the auto-oxidation of transition metal cations (iron, copper, etc.) which results in $\cdot$OH radicals and the decomposition of lipid hydroperoxides into new radicals induced by transition metals cations (Gutteridge, 1986).

A straightforward strategy to lower lipid oxidation, is to keep the product away from heat, light and oxygen. Additionally, reducing the content of transition metal cations in food products would also decrease lipid oxidation, although it can be either unfeasible or costly. Alternatives to withhold the transition metal cations from the O–W interface encompasses electrical repulsion (by means of positively charged surface droplets) or steric hindrance resulting from thicker and denser interfacial layers at the O–W interface.

To maintain the stability of $W_1/O/W_2$ emulsions during the emulsification process and further storage, other considerations have to be made. Particularly in the second step of the emulsification process (production of $W_1/O/W_2$ from W_1/O emulsion), inner water phase easily escapes upon disruption of the outer oil droplets. To effectively keep the W_1 and its addenda within the oil droplets, less energy should be introduced in the second than in the first step of the process (production of W_1/O emulsion). Other factors, such as the W_1 droplet size and the oil fraction should be adjusted to reduce W_1 loss during emulsification.

Regarding the chemical stability of $W_1/O/W_2$ emulsions, they present some advantages as encapsulation system of hydrophilic compounds in the W_1 phase. The oil droplet acts as a barrier, protecting them from the chemical degradation
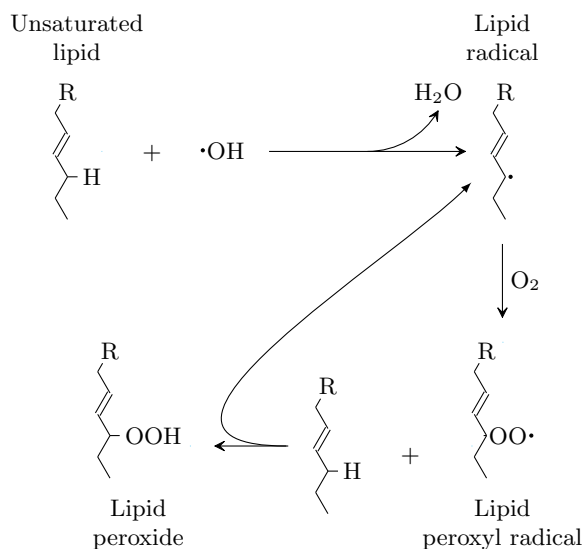
Figure 1.6: Mechanism of lipid peroxidation by a free radical, $\cdot$OH in this example.

that the environmental or compositional conditions in the external W_2 could cause. For both single and double emulsions, interfacial structures made of biopolymers, such as proteins in combination with polysaccharides, result in an enhanced physical stability against environmental stresses (pH, salt, temperature, dehydration, and mechanical agitation). Additionally, they can improve the chemical stability against lipid oxidation induced by transition metal ions through control of charge, thickness and/or density of the interfacial layer (McClements et al., 2009).

Controlled Release When designing emulsions, either single or double, as encapsulation systems of bioactive compounds, a major concern is to increase their bioavailability. To do so each bioactive compound should be delivered in a specific site of the gastrointestinal tract. In addition, emulsions have to be stable and efficiently able to retain the entrapped addenda, from the production process until they are ingested after storage. Depending on the desired delivery site, emulsions

should be able to endure or release their content upon mastication, presence of enzymes, salts and acids in mouth, stomach, small intestine and colon. In the case that encapsulation is required to mask off-tastes, (astringent, bitter or fishy flavors) the addenda has to be retained within the emulsion while passing the mouth.

For triggering the release of bioactive compounds, emulsion instability used to be induced by a response to a change in a particular environmental parameter (Cooper et al., 2005). Multi-layered emulsions can become unstable when losing their electrical charge induced by dilution, pH change or change of ionic strengh (McClements et al., 2009). Properties of electrostatic behavior of two biopolymers on O–W interfaces is closely related to the behavior in aqueous solutions (Jourdain et al., 2008). Study of the state diagram (Figure 1.4) is helpful to understand the stability of emulsions prepared through electrostatic LbL or complex deposition, which enables to predict release of addenda.

1.1.2 Microcapsules

Emulsions (single or multiple) enable to encapsulate a bioactive/sensitive compound in a liquid system, however, there is also a demand for encapsulation in solid state. Microcapsules, dry particles with sizes between $1 - 1000$ μm, protect a bioactive/sensitive compound by packing it in another material. The to-be protected compound can be pure or a mixture, that in turn can be a solid, or liquid material, and is usually refered to as the core material. Numerous techniques for encapsulation have been developed to meet the specific properties of:

- the core material,
  such as the type of compound, applications, mechanisms of release

- the final microcapsules,
  that is, particle size, final physical form, and overal cost (Desai and Park, 2005)

These techniques, widely described in several review articles by (Augustin and Hemar, 2009, Fang and Bhandari, 2010, Gibbs et al., 1999, Gouin, 2004, Madene et al., 2006), encompass: coacervation, cocrystalization, molecular inclusion, nanoparticles, encapsulation with supercritical fluids, spray drying, spray chilling or spray cooling, fluidized bed coating, freeze drying, yeast encapsulation, extrusion, spinning disk and centrifugal coextrusion. Encapsulation technologies

to produce solid microcapsules are used in multiple industries such as pharmaceutical, chemical, cosmetic, foods and printing (Madene et al., 2006). The encapsulation of foods or food ingredients (e.g. flavors, aromas, colors, preservatives, antimicrobials, vitamins, minerals, polyphenols, amino acids, bioactive proteins, enzymes, peptides, polyunsaturated oils and bioactive lipids) can be required for several reasons (Desai and Park, 2005, Fang and Bhandari, 2010):

i) to protect the core material upon processing and storage.

ii) to diminish the release of core material during production and storage.

iii) to tailor the release for a specific delivery or to mask off-flavors.

iv) to improve handling by modification of the physical characteristics

v) to enhance the protection of sensitive compounds by diminishing the surrounding environmental effects

vi) to apply core material in dry products.

vii) to achieve uniform dispersion of core material in host material

Spray drying

Spray drying is the most commonly used encapsulation method since it is flexible, continuous in operation, produces particles of good quality, and is less expensive than the other techniques. For over 50 years the technique has been widely used in the food industry to encapsulate flavors, volatiles and to convert liquids into powders (Desai and Park, 2005, Fang and Bhandari, 2010).

To spray dry, a liquid containing the active ingredient is added to the coating agent (wall material) and fed to the spray dryer (Figure 1.7). Feed flow is controlled by a peristaltic pump and compressed gas is used to atomize the feed with a nozzle into the drying chamber. A temperature controlled hot air enters in a co-current or counter-current flow which, in contact to the atomized material, evaporates the liquid fraction. The dry microcapsules are then transported into the cyclone to separate them from humid air and to obtain the dry powder microcapsules in the recovery chamber.

Final characteristics of the microcapsule are influenced by the chemical and physical properties of core and wall material. Furthermore, processing properties of the spray dryer, such as feed flow, air inlet temperature, compressed gas flow

Chapter 1
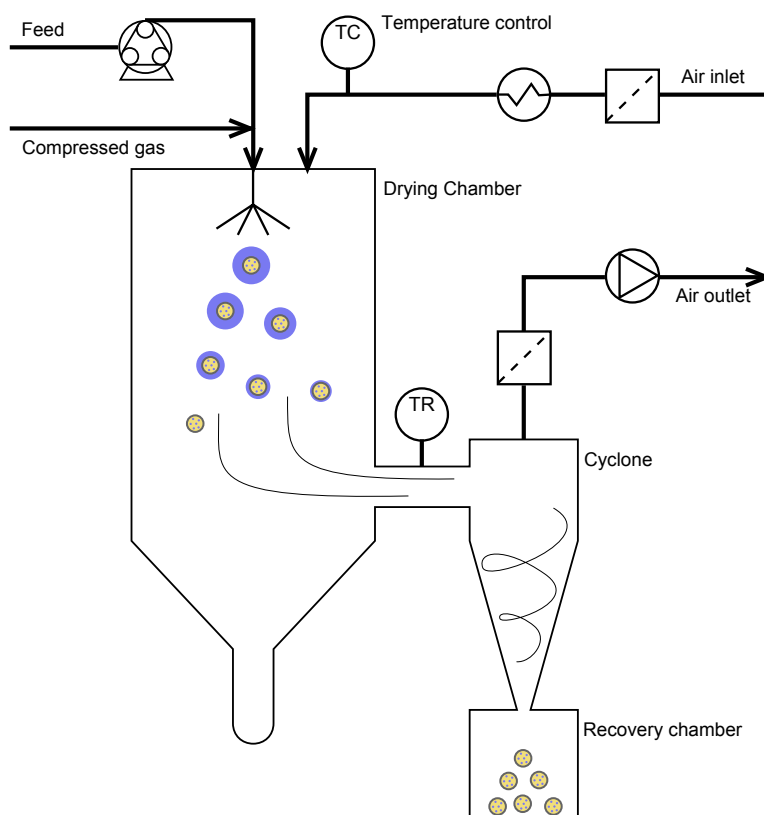
Figure 1.7: Spray dryer setup. Double emulsion mixed with wall material is fed by peristaltic pump and sprayed with compressed gass. Dry hot air takes the droplets in a co-current flow to the cyclone where wet air and microcapsules are separated and leaves the microcapsules in the recovery chamber.

and air outlet flow have a large influence on the characteristics of the microcapsules (Madene et al., 2006).

The type of core material determines partly the morphology of the produced microcapsule (Figure 1.8). A hydrophilic core material directly mixed to the wall material, forms a microcapsule where the core material is dispersed over the wall material matrix (Figure 1.8a). Otherwise, a hydrophobic core material is usually dispersed in an oil phase, and an emulsion is produced prior to spray drying. This emulsion can be stabilized by emulsifiers to improve droplet stability during spray drying. Emulsion viscosity, droplet size and dispersion have significant effects on the microencapsulation process. Depending on the dimensions of the initial emulsion and the spray dryer nozzle, the morphology will either be a simple (Figure 1.8b) or a multi-core microcapsule (Figure 1.8c).

Figure 1.8: Morphology of different type of spray dried microcapsules: (a) matrix, (b) simple, (c) multi-core, (d) multi-wall, and (e) double.

Typical materials used as microcapsule wall include maltodextrins, gum Arabic, and hydrophobically modified starch. Other wall materials, such as proteins (whey proteins, soy proteins, and sodium caseinate) and polysaccharides (alginate, carboxymethyl cellulose, and guar gum), have higher encapsulation efficiencies, however their low solubility in water makes them non suitable. A strategy to improve the encapsulation efficiency is to use mixtures of different wall materials. A recent approach involves to spray dry multi-layer emulsions (Figure 1.8d) (Serfert et al., 2013, Gharsallaoui et al., 2010, Klinkesorn et al., 2006), which has some advantages, such as a higher physical and/or oxidative stability than simple microcapsules. Overall, several factors have to be considered when selecting a wall material: molecular weight, solubility in water, viscosity at high concentration, glass/melting transition, crystallinity, diffusibility, film forming and emulsifying properties (Gharsallaoui et al., 2007, Madene et al., 2006).

Chapter 1

Table 1.1: Spray dried double emulsion studies for food aplications. marker (m), emulsifier (e), wall material (w), first (W_1/O) emulsification (1), second ($W_1/O/W_2$) emulsification (2), and ($\star$) best combination according to authors.

$W_1/O/W_2$ phase fractions [%]	W_1 phase characteristics	oil phase characteristics
6 / 16 / 78	0.04% 1,3,6,8-pyrenetetrasulfonic acid tetrasodium salt (m)	10% hexaglycerin polyricinoleate (e) in olive oil
10 / 15 / 75	55% glycerin, 0.25% 3-methylbutyraldehyde (m),	5% span 80 (e) in rape seed oil
2.5 / 7.5 / 90	0.25% orange oil with Sudan III red dye (m) dispersed in 3.375% SC (e), 6.3% lactose (e), methylene blue dye (m) aqueous solution	50% PGPR (e) in rape seed oil
2 / 11 / 87, or 2 / 8 / 91, or 4 / 19 / 77, or 3 / 14 / 83	1 or 1.5% Chi, 2.5 or 10% promethazine (m), 0.5% acetic acid	1 or 4% ethylcellulose (e) in ethyl acetate
8 / 32 / 60	0.6% gelatin, 1.68% salt, 0.16% mango seed kernel extract (m)	2.33% PGPR (e) in soybean oil
3 / 14 / 83	0.5% gellan gum, 7.9% hydrophilic emulsifier, 0.8% saponified oleoresin from Aztec marigold petals (m)	7.9% hydrophobic emulsifier (e), 1.1% oleoresin from red chilies in a blend of sunflower-canola-cartamum oils

W_2 phase characteristics	1st emulsification (1), 2nd emulsification (2)	spray dry conditions	Reference
0.2% soybean lecithin (e), 7.14% MD or GA (w)	rotor-stator at 17,000 rpm for 2 min (1), rotor-stator at 10,000 rpm for 1 min, high-pressure at 34 MPa (2)	T_{input}=200°C, T_{output}=100°C, feed flux=50 mL min^{-1}	Adachi et al. (2004)
32% WPC, or 14% SC, or 44% skim milk powder, or 49% soy protein, or 39% modified starch, or 44% MD, or 28% GA (e/w)	centrifugal ball mill at 500 rpm for 10 min (1), centrifugal ball mill at 500 rpm for 10 min (2)	T_{input}=190°C, T_{output}=85°C, feed flux=11 mL min^{-1}	Brückner et al. (2007)
5.6% SC (e/w), 7.8% lactose monohydrate (e/w)	overhead stirrer for 15 min (1), magnetic stirrer for 15 min (2)	T_{input}=180°C, T_{output}=79 – 80°C, feed flux=10 mL min^{-1}	Edris and Bergnståhl (2001)
0.5 or 1% Chi microspheres (w)	sonification (1), magnetic stirrer at 900 rpm (2)	T_{input}=135°C, T_{output}=85°C, feed flux=4.2 mL min^{-1}	Hafner et al. (2007)
5.95% GA (e), 0.11% alginate (e), 26.9% MD (w)	2× high-pressure at 20.7 MPa (1), rotor-stator at 10,000 rpm for 2 min (2)	T_{input}=180°C, T_{output}=90°C, feed flux=30 – 35 mL min^{-1}	Maisuthisakul and Gordon (2012)⋆
17% GA (e/w), 66% mesquite gum (e/w), 17% MD (e)	rotor-stator at 5800 rpm for 5 min (1), rotor-stator at 5200 rpm for 10 min (2)	T_{input}=165-175°C, T_{output}=77 – 83°C, feed flux=20 mL min^{-1}	Rodríguez-Huezo et al. (2004)

Table 1.2: Spray dried double emulsion studies for pharmaceutical applications. marker/medicine (m), emulsifier (e), wall material (w), first (W_1/O) emulsification (1), second ($W_1/O/W_2$) emulsification (2), and ($\star$) best combination according to authors.

$W_1/O/W_2$ phase fractions [%]	W_1 phase characteristics	oil phase characteristics
	isoniazid (m), phosphate buffered saline	rifampicin (m), PLGA 50:50 in ethyl acetate
3 / 14 / 83	2% gelatin, 2% cimetidine (m)	0.8% ethylcellulose (e) in dichloromethane
3 / 5 / 92	1% human IgG, 1% sorbitol (m)	0.625% 1,2-dipalmitoyl-sn-glycerol-3-phosphocholine (e), 5% PLGA in dichloromethane
	0.1% DNA (m), tris-edetate buffer	1% PLGA in dichloromethane
0.7 / 2.3 / 97	0 or 8% salbutamol sulphate (m)	0 or 2.67% beclometasone dipropionate (m), 0.67% span 80 (e), 0.67% PLGA 50:50 (s) in chloroform
15 / 35 / 50	10^{-4}M 1,3,6,8-pyrenetetrasulfonic acid tetrasodium salt (m), 0.35% insulin, Hanks' balanced salt solution	1-10% hexaglycerin polyricinoleate (e), 0.1% 1-monolinoleoyl-rac-glycerol or 0.2% 1,3-dilinoleoyl- rac-glycerol or 0.1% linoleic acid in Octanoic acid triacylglycerol or soybean oil

W_2 phase characteristics	1st emulsification (1), 2nd emulsification (2)	spray dry conditions	Reference
0.375% PVA (e), 1.25% lactose (e), 0.075% Chi, 0.125% PEG (w)	rotor-stator at 3000 – 5000 rpm (1), rotor-stator 8000 rpm (2)	T_{input}=95 – 110°C	Booysen et al. (2013)
0.3% Chi (w), glutaraldehyde	rotor-stator at 12,600 rpm for 1 min, sonification (1), dropwise, rotor-stator at 11,000 rpm for 1 min (2)	T_{input}=150°C, feed flux=6 mL min^{-1}	He et al. (1999)
0.43% lactose (e), 0 or 1% leucine, 0 or 1% magnesium stearate	rotor-stator at 24,000 rpm for 2 min (1), rotor-stator at 10,000 rpm for 10 min (2)	T_{input}=90 – 100°C, T_{output}=55°C, feed flux=2 mL min^{-1}	Kaye et al. (2009)
1% PVA (e)	dispersed (1), rotor-stator (2)	T_{input}=78 – 79°C, feed flux=10%	Lane et al. (2005)
0 or 0.064% salbutamol sulphate (m), 0.8% Chi, 0.6% acetic acid, 0.416 – 0.544% leucine, Synperonic PE/L101 (e) , 80% ethanol	vortex-mixing (1), homogenized (2)	T_{input}=180°C, T_{output}=87 – 96°C, feed flux=3.2 mL min^{-1}	Learoyd et al. (2010)
2, 5 or 10% decaglycerol monolaurate (e), Hanks' balanced salt solution, fructooligosaccharides (w)	rotor-stator at 22,000 rpm for 2 min (1), rotor-stator at 10,000 rpm for 1 min, membrane filter 0.8 μm, or membrane filter 0.44 μm, 0.2 μm (2)	T_{input}=200°C, T_{output}=100°C, feed flux=50 mL min^{-1}	Shima et al. (2006)

(continued on next page)

Chapter 1

Table 1.2 (continued): Spray dried double emulsion studies for pharmaceutical applications. marker/medicine (m), emulsifier (e), wall material (w), first (W_1/O) emulsification (1), second (W_1/O/W_2) emulsification (2), and ($\star$) best combination according to authors.

W_1/O/W_2 phase fractions [%]	W_1 phase characteristics	oil phase characteristics
	diclofenac sodium (m)	Eudragit RS PO (s), polyethylene glycol stearate, sorbitan mono-oleate (e), $0 - 75\%$ acetone or methyl ethyl ketone or n-propanol or n-butyl acetate in dichloromethane
3 / 15 / 82, or 3 / 17 / 81, or 3 / 21 / 76	5% diphtheria toxoid (m), 5.6% PVA	5% polycaprolactone (s), 10, 20 or 40% tocopheryl polyethylene glycol succinate (e) in dichloromethane
1 / 9 / 90	0.3% sodium fluorescein (m)	3% PGA-co-PDL (s/e) in dichloromethane
1 / 9 / 90	DNase I or 0.3% Native enzyme (α-chymotrypsin) (m), 1% Pluronic F68	3% PEG-co-(PGA-co-PDL) (s/e) in chloroform
	2% PVA, lamivudine (m)	1.25% polycaprolactone (s/e) in ethyl acetate

W_2 phase characteristics	1st emulsification (1), 2nd emulsification (2)	spray dry conditions	Reference
PVA (w), polyoxyethylene 20 sorbitan mono-oleate (e)		T_{input}=140°C, T_{output}=95 − 108°C, feed flux=2.1 mL min^{-1}	Sipos et al. (2008)
2.5% PVA (e)	rotor-stator at 24,000 rpm for 2 min (1), rotor-stator 10,000 rpm 5 min (2)	T_{input}=38-42°C, T_{output}=24 − 28°C, feed flux=5 mL min^{-1}	Somavarapu et al. (2005)
0.5, 1 or 1.5% L-leucine or L-arginine, 1% PVA (e)	rotor-stator at 8000 rpm for 3 min (1), rotor-stator at 2000 rpm (2)	T_{input}=100°C, T_{output}=47°C, feed flux=5 − 7 mL min^{-1}	Tawfeek et al. (2011)
1% PVA (e), 1.5% L-leucine	rotor-stator at 8000 rpm for 1 min (1), rotor-stator at 2000 rpm (2)	T_{input}=100°C, T_{output}=47°C, feed flux=5 − 7 mL min^{-1}	Tawfeek et al. (2013)*
2% PVA (e/w), 0.5% PEG, 5% lactose (e), 0.3% Chi	rotor-stator at 5000 rpm (1), rotor-stator at 8000 rpm for 5 min (2)	T_{input}=96°C, T_{output}=65 − 70°C	Tshweu et al. (2013)*

Chapter 1

Spray dried double emulsion A recent development is to produce double emulsions in powder form (Figure 1.8e). Spray drying of W/O/W emulsions has been suggested as an approach to encapsulate hydrophilic bioactive compounds due to several benefits (Adachi et al., 2004, Augustin and Hemar, 2009, Fang and Bhandari, 2010, Learoyd et al., 2010, Maisuthisakul and Gordon, 2012):

i) to increase storage stability as W_1/O droplets are immobilized in a solid continuous matrix and therefore, droplet coalescence and release of the entrapped compounds are limited

ii) to gain the convenience of powdered ingredients

iii) to encapsulate both hydrophilic as hydrophobic ingredients in one capsule

A possible disadvantage of this system is the low concentration of core material retained in the microcapsule, however the unique protection might compensate for this (Gouin, 2004). Tables 1.1 and 1.2 summarize some of the few examples of microcapsules obtained by spray drying of double emulsions found in literature, which are mainly food and pharmaceutical applications. In the case of pharmaceutical applications, the main compounds/solvents used as oil phase are dichloromethane, chloroform, and ethyl acetate. Their low boiling points, 39.6, 61.2, and 77.1°C, for dichloromethane, chloroform, and ethyl acetate, respectively, make them easy to evaporate.

Poly lactide-co-glycolide (PLGA) has been recently used as oil phase because it easily evaporated during spray drying while the remaining oil phase solidifies. At those conditions, the final solid microcapsules present a rigid/semisolid oil phase which retains more efficiently the inner water phase.

For food applications (Table 1.1), the main drawback is the limited number of food-grade ingredients available for formulating these complex microcapsules obtained by spray drying double emulsions. The effects of the formulation on the properties of the final microcapsule (e.g. composition, retention of inner water phase, and size) are still in an initial stage of research.

1.2   Aim of the thesis

The main objectives of this work were to encapsulate sensitive bioactive compounds in emulsion-based systems using emulsification with microstructured systems, in particular premix membrane emulsification, and to determine how protein–polysaccharide complexes, used as hydrophilic emulsifiers, affect the retention and stability of the entrapped compounds. Crude sunflower oil and procyanidin-rich extracts from grape seed were encapsulated in some of the following systems: single (O/W) and double (W_1/O/W_2) emulsions and spray dried double emulsions (solid microcapsules). The main goals could be achieved by fulfilling secondary objectives:

- To produce O/W emulsions stabilized with complex interfacial structures made of whey protein isolate and carboxymethyl cellulose using premix ME.

- To determine the effect of the microstructure (density and thickness) and electrical charge of the interfacial structures made of WPI and CMC on the droplet and oxidation stability of O/W emulsions.

- To assess premix ME to produce W_1/O/W_2 emulsions entrapping a procyanidin-rich extract in the inner water phase, using whey protein isolate–polysaccharide complexes as hydrophilic emulsifiers

- To analyze the influence of three whey protein isolate–polysaccharide complexes, WPI–carboxymethyl cellulose, WPI–gum Arabic and WPI–chitosan, used as hydrophilic emulsifiers of W_1/O/W_2 emulsions, on the emulsion stability and procyanidin release during storage.

- To encapsulate a procyanidin rich extract in spray dried emulsions obtained by premix ME and stabilized by whey protein isolate and several whey protein isolate–polysaccharide complexes, such as WPI–carboxymethyl cellulose, WPI–gum Arabic and WPI–chitosan.

- To determine how the properties of the W_1/O/W_2 emulsions, in particular the interfacial properties of the O–W_2 interface, affect the characteristics of the final microcapsules, in terms of particle size distribution and encapsulation of procyanidins.

2

Oil-in-water emulsions stabilized with whey protein and carboxymethyl cellulose

Abstract

Premix Membrane Emulsification (ME) with Shirasu Porous Glass membranes of 10 μm pore size enabled to produce oil-in-water (O/W) emulsions with different interfacial structures made of whey protein isolate (WPI) and carboxymethyl cellulose (CMC). Emulsions were stabilized by one interfacial layer, made of WPI or 0.5%wt WPI − 0.25%wt CMC complex, or by two interfacial layers: one layer made of WPI and the second made of CMC (WPI + CMC) or WPI–CMC complex (WPI + WPI–CMC). Although the adsorption between the several layers was confirmed by Surface Plasmon Resonance (SPR), only O/W emulsions stabilized by one interfacial layer did not coalescence after homogenization. WPI and WPI–CMC emulsions were stable after emulsification with a 8.7 μm and 14.4 μm mean droplet size respectively, although a significant amount of much smaller droplets contributed to increase droplet dispersion giving span values of 1.8 and 3.2 for WPI and WPI–CMC emulsions respectively.

Regarding oxidation rate, TBARS in WPI–CMC emulsions increased much faster than in WPI emulsions. Adsorption data at a hydrophobic interface and the electrical charge of the WPI–CMC complex suggested that it formed a thick (2.2 nm) but less dense (1.40 $\mathrm{g\,cm^{-3}}$) interface than WPI (2.59 $\mathrm{g\,cm^{-3}}$) with a negative charge able to attract any transition metal ion and promote lipid oxidation. Premix ME should be further optimized to obtain multi-layered interfaces with an external positive layer, e.g. made of WPI.

2.1 Introduction

The use of emulsions is common in food industry, many products we daily consume are in fact oil-in-water (O/W) emulsions. Some typical examples are milk, cream, salad dressings, mayonnaise, soups and sauces.

In food emulsions, stability, quality and the ability to deliver functional compounds are of great importance (Guzey and McClements, 2006). Emulsions are kinetically unstable and tend to spontaneously coalesce minimizing the interfacial area (Capek, 2004). Average droplet size and droplet size dispersion are two properties which determine the physical stability of the emulsion. To prevent emulsion breakage, surfactants are added to provide a layer which lowers the interfacial tension between the oil and water phases (Kralova and Sjöblom, 2009).

Food emulsions are traditionally produced by colloid mills, rotor-stator systems and high pressure homogenizers, these produce emulsions with small droplet size but with a relatively high droplet size dispersion. Furthermore, they require a high energy input and high shear forces to produce emulsions. Membrane emulsification (ME) is a low energy technique that requires fewer surfactants, produces emulsions with low polydispersity and reduces damage to emulsifiers sensitive to shear stress, in contrary to the traditional methods (Joscelyne and Trägårdh, 1999, Nazir et al., 2010, Silva et al., 2012, Vladisavljević et al., 2006a).

There are different methods to operate membrane emulsification (ME): direct (or cross-flow) ME and premix ME. In direct ME, the dispersed phase is forced, using low pressure, to permeate through a membrane into the continuous phase. In premix ME, emulsions are produced in a two-step process:

  i) production of a coarse emulsion

 ii) the entire coarse emulsion passes through the pore structure of the membrane.

Premix ME has some advantages over direct ME: the optimal transmembrane fluxes, with regard to droplet size uniformity, are one or two orders of magnitude higher than those of direct ME. The experimental set-up is generally simpler and easier to control and operate than in direct ME (Nazir et al., 2010, Vladisavljević et al., 2006a).

In food industry, whey proteins have been widely used to stabilize O/W emulsions because they show good surface active properties and form a viscoelastic layer at the interface (Bos and van Vliet, 2001) that improves the encapsulation properties due to a barrier effect. Nevertheless, whey protein-stabilized emulsions are rather heat sensitive when whey protein denaturates on the O–W interface; the protein unfolds and can form irreversible aggregates between emulsion droplets

Chapter 2

(Dickinson and Parkinson, 2004). A strategy to improve interfacial properties has been the use of protein–polysaccharide complexes which combines the positive properties of each of them:

- proteins show good adsorption to O–W interfaces

- polysaccharides enable to form a thicker stabilizing layer that is capable of protecting droplets against aggregation over a wide range of unfavorable conditions, such as thermal shock treatment and the addition of calcium salts (Chanamai and McClements, 2002).

In addition, emulsions stabilized by complex interfaces made of protein and polysaccharides have been suggested to improve chemical stability against oxidation reactions, e.g., interactions between lipids and metal ions can be minimized by controlling the interfacial charge, thickness and density (Dickinson, 2008, 2011a, Grigoriev and Miller, 2009, Katsuda et al., 2008, McClements and Decker, 2000, Rodríguez Patino and Pilosof, 2011).

The formation of protein–polysaccharide electrostatic complexes and coacervates mainly depends on pH, ionic strength and protein to polysaccharide ratio (Schmitt and Turgeon, 2011, Semenova, 2007). In the food industry, applications of these complexes are: to form and stabilize emulsions possibly in combination with the design of multi-layered structures, micro- and nano-encapsulation processes, to form gels and to recover proteins from industrial by-products (Turgeon et al., 2007).

In this study we used whey protein isolate (WPI) which is a by-product in cheese-making and has excellent emulsifying properties (Dybowska, 2011), and carboxymethyl cellulose (CMC) which is widely used in food for its physical properties and its low cost. In addition, CMC can form electrostatic complexes with WPI over a range of pH and ionic strength (Hansen et al., 1971).

The aim of this Chapter was to produce O/W emulsions with complex interfacial structures made of WPI and CMC using premix ME, and determine droplet and oxidation stability of those emulsions. To do so, we determined the state diagram of the WPI/CMC system and set the conditions (WPI to CMC ratio, pH and ionic strength) required to form WPI–CMC complexes. The adsorption properties of the different interfacial structures made of WPI and CMC were measured by Surface Plasmon Resonance. Moreover premix ME was applied to produce O/W emulsions stabilized by the different interfacial structures. To the author's knowledge no application of premix membrane emulsification to obtain single emulsions stabilized by protein–polysaccharide complexes has been previously reported in

literature. To determine to what extent the several interfacial structures affected the physical and oxidative stability of O/W emulsions, we monitored during 2 weeks droplet size distribution and the oxidative degradation of the oil phase.

2.2 Materials and Methods

2.2.1 Materials

Whey protein isolate (BiPRO) lot no. JE 034–7–440–6 (Davisco Foods International. Inc., Le Sueur, MN), with a reported protein content of 98.1% on dry basis, was dissolved in distilled water to obtain a 2.0%wt solution, stirred for 2 h at room temperature, and kept overnight at 7°C. Carboxymethyl cellulose, sodium salt (Acros Organics), with a M_w of 250,000 and a degree of substitution of 0.7, was dissolved in distilled water to obtain a 2.0%wt solution and stirred for 2 h at room temperature. Acetic acid 96% (Panreac) together with sodium azide (Sigma-Aldrich), were dissolved in distilled water to obtain 0.02 M acetic acid and 0.04%wt sodium azide (NaN_3). WPI and CMC solutions were mixed with the acetic acid solution to obtain 1.0%wt WPI, 0.25%wt CMC and 0.5%wt WPI – 0.25%wt CMC in 0.01 M acetic acid and 0.02%wt NaN_3. The solution pH was adjusted to 3.8 with 1 M HCl (Panreac) or 1 M NaOH (Sigma-Aldrich). All distilled water used in this research had an electrical conductivity of 2 $\mu S\,cm^{-1}$. Crude sunflower oil was kindly provided by Cargill S.L.U. Reus, Spain.

2.2.2 Methods

WPI/CMC state diagram

Aqueous solutions containing 0.5%wt of WPI and different concentrations of CMC were prepared to obtain a final ratio of 1:0, 1:1, 2:1, 3:1 and 4:1, respectively. All mixtures contained 0.01 M acetic acid, 0.02%wt NaN_3 and the pH was adjusted from 6 to 3 with 1 M HCl or 1 M NaOH solutions. Turbidity and pH of each mixture was measured right after preparation to identify a clear solution, a cloudy solution or the formation of a precipitate. Turbidity was quantitatively measured from the Transmission (T) profiles obtained with a Turbiscan Lab™ Expert (Formulaction, France).

ζ-potential measurement

Laser Doppler micro-electrophoresis was used to measure ζ-potential of WPI, CMC and a WPI–CMC complex by means of a Zetasizer Nano ZS (Malvern Instruments). Particles were detected at a measurement position of 2 mm using a 633 nm laser at 25°C. Solutions of 1%wt WPI, 0.25%wt CMC and 0.5%wt WPI–0.25%wt CMC in 0.01 M acetic acid, 0.02%wt NaN$_3$ at a pH of 3.8 were prepared and centrifuged at 1000 G for 30 min to remove impurities. After that, the ζ-potential distribution of each of them was measured. The reported ζ-potential values are an average of six measurements and calculated by the Smoluchowski equation. All measured ζ-potential distributions gave a monomodal distribution.

Surface plasmon resonance measurements

Surface plasmon resonance is an optical measurement technique highly sensitive to localized refractive index changes occurring at the surface of a metal-dielectric interface. A typical set-up includes shining a monochromatic light beam through a high refractive index glass prism coated with a 50 nm thick gold layer. Under total internal reflectance conditions, the evanescent wave created at a specific incident angle will result in a plasmonic wave seen as a sharp decrease in intensity of the reflected beam. The position of the incident angle is strongly dependent on the refractive index changes occurring at the metal surface making surface plasmon resonance an ideal tool for studying the adsorption of biomolecules and biopolymers at surfaces (Gopinath, 2010, Fang et al., 2009, Jung et al., 1998).

Surface plasmon resonance (SPR)

A Biacore 3000 (GE Healthcare, Uppsala, Sweden) was used to study the surface adsorption of the various biopolymers to a gold sensor chip. The microfluidic cell divided the bare gold sensor chip in four flow cells (each of them with a surface area of 1.2 mm^2) used in series at a flow rate of 40 μL min^{-1}. Baseline was acquired by flowing 0.01 M acetic acid (pH 3.8) with 0.02%wt NaN$_3$ (running buffer) over the chip till the system was stabilized, with temperature control at 20°C.

Each biopolymer layer was obtained by the successive injection of a biopolymer solution over the chip for 8 min followed by the injection of the running buffer solution over the chip for 8 min to remove the non-adsorbed biopolymer. This sequence was repeated to obtain multi-layer arrangements. The aqueous solutions of biopolymers were: 0.1%wt WPI, 0.05%wt CMC and 0.1%wt WPI–0.05%wt CMC all in 0.01 M acetic acid at pH 3.8 containing 0.02%wt NaN$_3$. Finally the gold surface was cleaned using 0.5%wt/vol sodium dodecyl sulphate and glycine-

```
UNIVERSITAT ROVIRA I VIRGILI
ENCAPSULATION OF PROCYANIDINS IN DOUBLE EMULSIONS STABILIZED BY PROTEIN-POLYSACCHARIDE COMPLEXES
Rikkert Berendsen
Dipòsit Legal: T 1926-2014
```

Oil-in-water emulsions stabilized with whey protein and carboxymethyl cellulose

HCl pH 1.7 until initial baseline was re-established.

The output signal of the Biacore 3000 was measured in Response Units (RU), where 1 RU corresponds to a sensor surface coverage of 0.1 $ng\,cm^{-2}$ (Fivash et al., 1998). All experiments were run in duplicate and the error in the surface coverage of each layer was below 15%.

Surface plasmon resonance imaging (SPRi)

To measure thickness and density of the interfacial biopolymer structure, a different SPR arrangement was selected. An SPRi-PlexII™ (Genoptics-Horiba Scientific, Orsay, France) was used to record the entire SPR curves over larger sensing area and the comparison of the curves recorded before and after exposure to the biopolymers used to estimate the thickness of the adsorbed layer using the Fresnel equations (Winspall 3.02, WINSPALL-Material Science Group-MPI-P Mainz). The sensor chips were initially pre-treated with Piranha solution (70%wt H_2SO_4 : 30%wt H_2O_2) for 5 min, rinsed with distilled water three times and immersed overnight in a 1 mM solution of cystamine prepared in ethanol. Thereafter the biochip was rinsed with distilled water three times, kept in distilled water, sonicated for 30 s, and finally dried in a stream of nitrogen, providing the sensor chip a hydrophobic layer similar to an oil interface (Tsukruk and Bliznyuk, 1998).

The system was left to equilibrate in a 50 $\mu L\,min^{-1}$ flow of 0.01 M acetic acid pH 3.8 containing 0.02%wt NaN_3 (running buffer) till the signal stabilized, with temperature control at 25°C. The optimal incident angle was set and the initial SPR angles recorded at 10 different locations 988 μm in diameter across the modified sensor chip. The sensor chip was exposed to the biopolymer solution and the flow stopped after 1 min. Adsorption of the biopolymer onto the sensor chip was carried out over a 10 min period, after which the buffer was flowed over the sensor surface for an additional 10 min at a flow rate of 50 $\mu L\,min^{-1}$. The adsorption experiment was stopped and plasmonic curves for the ten spots recorded. The reflectivity after 10 min of desorption was taken and expressed in $ng\,cm^{-2}$, where 1% reflectivity corresponds to 200 $pg\,mm^{-2}$.

Emulsification process

To produce O/W emulsions stabilized with WPI or WPI–CMC complex a two-step emulsification was applied. First 40 g of crude sunflower oil and 160 g of acidified WPI or WPI–CMC solution were mixed by a rotor-stator homogenizer (Ultra Turrax, IKA® T18 basic) at 7000 rpm for 10 min. Secondly, the coarse emulsion

45

Chapter 2

(cycle 0) was loaded into a High-speed mini kit (SPG Technology Co., Japan) equipped with a hydrophilic Shirasu porous glass (SPG) membrane of 10 μm pore size (membrane dimensions were 125 mm × 10 mm × 0.8 mm) (SPG Technology Co., Japan). The coarse emulsion was forced through the membrane by nitrogen gas, 175 ± 25 kPa and 750 ± 50 kPa was used for WPI and WPI–CMC respectively. This procedure was performed up to 4 times, from cycle 1 to 4, to progressively reduce the mean droplet size. After use, the SPG membrane was successively cleaned by sonication in acetone for 15 min and kept in acetone for several days, subsequently the membrane was dried in an oven at 500°C for 30 min. Before reuse, the membrane was washed again with distilled water while sonicating for 15 min.

Fresh emulsions were washed to reduce the amount of free emulsifier and reduce the effect of the water phase composition during the final step of the emulsification process. To do so, emulsions were centrifuged (Biocen 22R, rotor RT 223, Orto Alresa) at 16 G, supernatant was removed and was refilled with 0.01 M acetic acid solution at pH 3.8. After each washing step a sample of the supernatant was kept for protein quantification; this showed that after each washing step the WPI concentration was lowered leading to final concentrations below 0.3%wt WPI. Protein quantification was done with Coomassie Brilliant Blue protein assay by spectrophotometric measurements (DR 5000 Hach Lange) at 595 nm (Bradford, 1976).

To produce O/W emulsions with a second interfacial layer, such as, a CMC covering a WPI layer (WPI + CMC) and a WPI–CMC complex layer covering a WPI layer (WPI + WPI–CMC), interfacial components were added to the WPI stabilized O/W emulsion in the final step. To add the second interfacial layer, the WPI stabilized emulsion was centrifuged at 16 G for 10 min, supernatant was removed and the cream was resuspended in the same volume of acidified CMC or WPI–CMC solution at pH 3.8 while stirring for 30 min. Table 2.1 shows the final step of the emulsification process including the interfacial components added to form the first and second layer and the washing steps performed.

To assess the effect of several washing steps used in the process on emulsion stability:

i) all emulsions were washed twice (Table 2.1)

ii) a sample of WPI and WPI–CMC emulsions were not washed and used as a blank.

Oil-in-water emulsions stabilized with whey protein and carboxymethyl cellulose

Table 2.1: Final step of the emulsification process including the interfacial components of the first and second layer and the washing steps.

Interfacial structure	First layer	washing	Second layer	washing
WPI	WPI	2×		
WPI–CMC	WPI–CMC	2×		
WPI + CMC	WPI	1×	CMC	1×
WPI + WPI–CMC	WPI	1×	WPI–CMC	1×

Droplet size distribution measurement

The droplet size distribution of O/W emulsions was measured, after every emulsification step and at day 0, 3, 7, 10 and 14 for the washed emulsions and at day 0 and 14 for non-washed emulsions, by laser light scattering (Mastersizer 2000, Malvern Instruments). Distilled water was used as continuous phase, stirring speed was set at 1400 rpm, and laser obscuration was between 10 – 15%. Refractive index (RI) of both phases was measured by a refractometer (Digital Abbe Refractometer-WYA–1S, 315). RI of distilled water and crude sunflower oil were 1.3324 and 1.4724, respectively, at 25°C. From the droplet size distributions, mean droplet size and droplet size dispersion can be calculated, which were expressed as the volume-weighted mean diameter $d_{4,3}$ and the relative span factor respectively. The volume-weighted mean diameter (De Brouckere) is calculated as:

$$d_{4,3} = \frac{\sum_i n_i d_{n,i}^4}{\sum_i n_i d_{n,i}^3} \quad (2.1)$$

where d_d is the droplet size of a single droplet and n is the amount of droplets with equal size. The relative span factor (from this point on, span) is a dimensionless parameter indicative of the uniformity of the droplet size dispersion defined as:

$$span = \frac{d_{90} - d_{10}}{d_{50}} \quad (2.2)$$

where d_{10}, d_{50} and d_{90}, are the representative diameters where 10%, 50% and

90% respectively of the total volume are made up of droplets with diameter smaller or equal to these values.

Kinetics of lipid oxidation

To determine the kinetics of lipid oxidation, emulsions were stored in transparent glass beakers covered with glass Petri-dish in a closed box at 7°C. The box had a UV-light (Philips TL 8W/108 ultraviolet) attached to the lit to promote the oxidation process. Emulsion oxidation was monitored for 2 weeks and representative samples were analyzed after 0, 3, 7, 10 and 14 days of storage. Before taking a sample, the emulsions were homogenized by stirring. Lipid oxidation was determined by thiobarbituric acid-reactive substances (TBARS) assay (Bernheim et al., 1948). A TBA reagent was prepared by 0.375%wt 2-thiobarbituric acid ($\geq 98\%$, sigma-aldrich), 15%wt trichloroacetic acid (99+%, acros organics) in 0.25 M HCl. 3 mL of emulsion was mixed with 6 mL TBA reagent thereafter, the oil and water phase were separated by centrifuge (Biocen 22R, rotor RT 223, Orto Alresa) at 1000 G. 3 mL of aqueous phase was heated for 15 min in a water bath at 100°C, cooled down to room temperature and centrifuged (rotor 222) at 10,000 G. Absorbance was measured by photospectrometry (DR 5000 Hach Lange) at 532 nm. A calibration curve was prepared with 1,1,3,3 tetra ethoxypropane ($\geq 96\%$, Aldrich chemistry).

Creaming stability measurement

Oil droplets in O/W emulsions are subjected to buoyancy forces and depending on the size of the droplet and the viscosity of the aqueous phase are bound to cream (Stokes' law). Creaming of emulsions can be expressed by the vertical velocity of the front of the emulsion droplets and the aqueous phase, expressed in $\mathrm{mm\,h^{-1}}$. To measure the creaming velocity front, a Turbiscan Lab™ Expert (Formulaction, France) was used. The Turbiscan Lab™ Expert transmits light (880 nm) and measures the amount of light which passes through (transmission) and which is reflected (backscattering) over the full height of a glass tube. Backscattering (BS) profiles were taken from approximately 20 mL of freshly prepared emulsion every 5 min for 4 h.

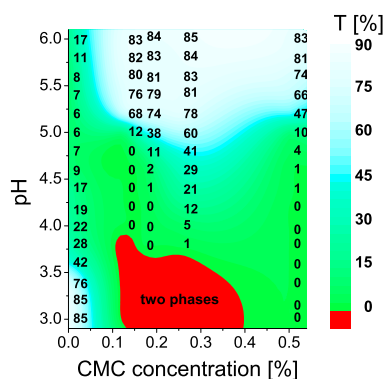Oil-in-water emulsions stabilized with whey protein and carboxymethyl cellulose

Figure 2.1: State diagram of the WPI/CMC system in aqueous solution at a constant WPI concentration of 0.5%wt (dissolved in $0.01M$ acetic acid). Values show transmission (T [%]) through the liquid phase, accentuated by the color shading. The two phase region is delimited by the (■) area.

2.3 Results and discussion

2.3.1 Complex formation

To investigate WPI and CMC multi-layers formation on O–W interfaces, interaction between WPI and CMC was studied in aqueous solutions. Transmission data of the pure WPI and CMC components was compared to mixtures at different pH and ratio. To investigate WPI and CMC multi-layers formation on O–W interfaces, interaction between WPI and CMC was studied in aqueous solutions. Transmission data of the pure WPI and CMC components was compared to mixtures at different pH and ratio.

Figure 2.1 shows the state diagram of aqueous solutions of 0.5%wt WPI with CMC at concentrations ranging from 0 to 0.5%wt in 0.01 M acetic acid and 0.02%wt NaN$_3$. The influence of pH and the WPI to CMC mass ratio on turbidity, expressed in terms of transmission data enabled to identify a liquid phase region and a two-phase region, made of an insoluble precipitate and a clear liquid phase.
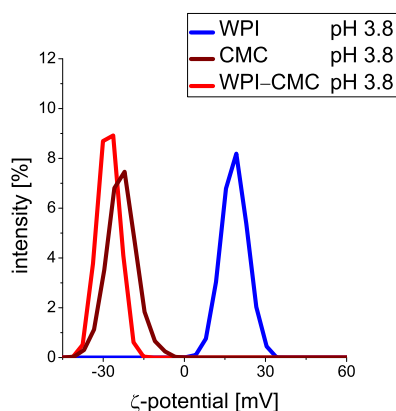
Figure 2.2: ζ-potential measurement of 0.5%wt WPI (━), 0.25%wt CMC (━), and 0.5%wt WPI−0.25%wt CMC (━) dissolved in 0.01 M acetic acid at pH 3.8.

At pH values above 5.5, transparent solutions with high transmission values ($> 80\%$) can be seen after mixing WPI and CMC. By decreasing pH, the turbidity of the liquid phase increased and transmission values significantly decreased. At pH between 4 and 4.6, a milky solution, with no precipitate but low transmission values of $0 - 30\%$ were detected in the whole range of WPI:CMC ratio. The aqueous solution of 0.5%wt WPI showed lowest transmission data at a pH of 5.2 which is the isoelectric point of the protein where maximum aggregate sizes occur (Ju and Kilara, 1998). Simultaneously, we checked the turbidity of a solution containing 0.25%wt of CMC: a clear solution ($> 88\%$) was found over the whole pH range. At conditions of low pH, soluble WPI–CMC complexes are formed as a result of the negative protein surface charge and by a pH value close to the pK of the polysaccharide. A further pH decrease (< 3.6) leads to a two-phase region, made of the precipitated WPI–CMC complex and a clear liquid phase. These results are in agreement with those reported by (Koupantsis and Kiosseoglou, 2009) for a similar system.

At low transmissions, interactions between WPI and CMC are stronger and should form a thick dense layer on O–W interfaces (Dickinson, 2008). Therefore, considering the state diagram, a soluble complex of WPI:CMC ratio of 2:1 (0.5%wt

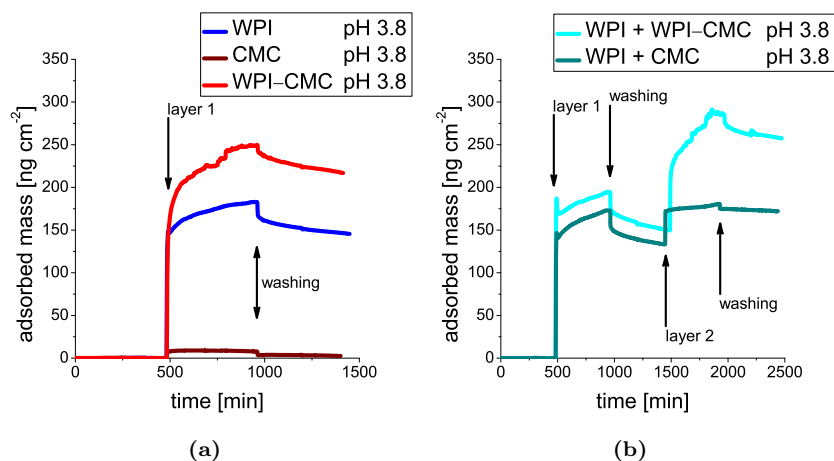Oil-in-water emulsions stabilized with whey protein and carboxymethyl cellulose

Figure 2.3: Progress of the adsorbed amount of biopolymer measured by SPR after applying one and/or two layers. (a) One layer interface: WPI (—), WPI–CMC (—), and CMC (—). (b) Two layer interface: WPI + WPI–CMC (—), and WPI + CMC (—).

WPI – 0.25%wt CMC complex) at pH 3.8 was chosen for further experiments. To confirm complex formation ζ-potential measurements were conducted. Figure 2.2 shows the ζ-potential distributions of WPI, CMC and 0.5%wt WPI – 0.25%wt CMC complex. A monomodal disperion for each of them indicates that, at the chosen pH, WPI (+18.5 mV) and CMC (– 23.3 mV) had a positive and negative ζ-potential, respectively, while the WPI–CMC complex was truly formed given a ζ-potential of – 28.1 mV. Although, one would expect for WPI–CMC a ζ-potential between the values of WPI and CMC, the real value is even lower than that of CMC. Considering that ζ-potential measures the electrical surface charge of the hydrocolloid, a displacement of the positive electrical patches inwards, away from the WPI–CMC complex surface, during the complex formation may explain this result.

Table 2.2: Mass adsorption of interfacial structures to a gold surface by SPR.

layer one		layer two		total
compound	mass [ng cm^{-2}]	compound	mass [ng cm^{-2}]	total mass [ng cm^{-2}]
WPI	150			150
WPI–CMC	220			220
WPI	150	+ WPI–CMC	110	260
WPI	130	+ CMC	40	170
CMC	0			0

2.3.2 Adsorption of WPI, CMC and WPI–CMC complex

Surface plasmon resonance was used to study the mass adsorption and thickness of several interfacial structures of WPI and CMC to surfaces. A gold layer (by SPR) and a hydrophobic layer (by SPRi) were used to mimic the O–W interface.

SPR

We first measured the amount of WPI, WPI–CMC complex and CMC adsorbed to a gold surface at the same conditions of pH and ionic strength as those used for obtaining the WPI–CMC complex. Figure 2.3a shows the progress of the adsorbed amount of one layer of biopolymer over time. As expected, only WPI and WPI–CMC complex extensively adsorbed to the gold surface, reaching an adsorption of 150 and 220 ng cm^{-2}, respectively (Table 2.2).

In the case of interfacial structures made of two layers, we measured the amount of WPI–CMC complex and CMC adsorbed to a first WPI layer to characterize the WPI + WPI–CMC and WPI + CMC interfacial structures, respectively (Figure 2.3b). Both WPI–CMC complex and CMC were significantly adsorbed to the WPI layer at the conditions considered, with a final amount of mass adsorbed of 260 and 170 ng cm^{-2}, respectively. Therefore, the surface mass adsorption of CMC can only be efficiently obtained in combination with WPI. Figure 2.3 shows that when applying only one layer, the WPI–CMC layer yields a higher mass adsorption than a WPI. In case of two layers, the WPI + WPI–CMC layer yields a higher mass adsorption than the WPI + CMC.

According to these results, any of the complex interfacial structures considered,
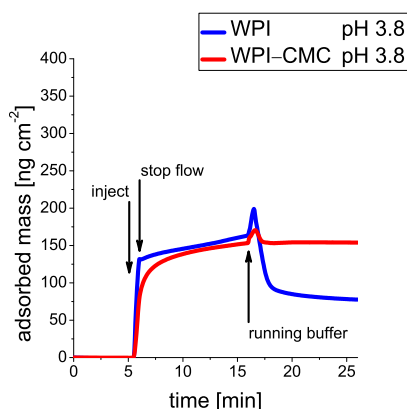
Figure 2.4: Progress of the adsorbed amount of biopolymer measured by SPRi after applying one layer: WPI (—) and WPI–CMC (—) complex.

WPI–CMC, WPI + WPI–CMC and WPI + CMC, formed a stable layer at the studied conditions, providing suitable alternatives to produce multi-layered O/W emulsions. All of these complex interfacial structures were used to produce O/W emulsions.

SPRi

Additional adsorption experiments were conducted to investigate the mass adsorption, the adsorbed layer thickness, and density of 1%wt WPI and 0.5%wt WPI $-$ 0.25%wt CMC complex to a hydrophobic surface that mimics an O–W interface in a real emulsion. Figure 2.4 shows the progress of mass adsorption and mass desorption of biopolymers over time.

After injection, both WPI and WPI–CMC directly adsorbs to a large extend to the hydrophobic surface. At desorption both curves show a peak in adsorbed mass, due to the remains of the biopolymer solution in the tubes which start to flow over the prism. In case of WPI, the adsorbed mass decreases drastically during desorption, while the adsorbed mass for WPI–CMC is maintained.

Figure 2.5 shows the reflection of the prism surface at varying laser incident angles, for both WPI and WPI–CMC before and after its adsorption. The angle

shift after adsorption provides information about the thickness of the adsorbed layer: a small angle shift indicates a thin layer, while a larger angle shift indicates a thicker layer. For both biopolymers, Figure 2.5a and b, an angle shift was observed, Table 2.3 shows the mass, thickness and density of the WPI and WPI–CMC layers.

Even though the adsorbed mass of WPI–CMC complex was higher than that of WPI, the interfacial structure of WPI was significantly denser than that of the WPI–CMC complex.

Comparing the results obtained with SPR and SPRi, we observed that the measured mass adsorbed of WPI was the same by any of both techniques, regardless of the surface hydrophobicity (gold versus cystamine). In the case of the WPI–CMC complex, the mass adsorbed to the gold surface was significantly lower than that adsorbed to the hydrophobic surface.

2.3.3 Premix membrane emulsification

Coarse O/W emulsions (cycle 0) stabilized by 1.0%wt WPI and 0.5%wt WPI–0.25%wt CMC complex were pressurized through SPG membranes to obtain one-layer emulsions. After premix emulsification a final step was preformed where all samples were washed and a second layer was added to form WPI + WPI–CMC and WPI + CMC emulsions.

Figure 2.6 shows the typical progress of the droplet size distribution of the emulsions during premix ME for the first layer, as shown by other authors (Vladisavljević et al., 2006a). After the rotor-stator step, the droplet size distribution shows a broad, flat peak in the region of 10 μm and a higher peak around 70 μm. After the first cycle of emulsification, two narrow peaks were obtained (bimodal dispersion): a narrow peak around 10 μm and a flat peak in the region of 0.1 μm. From cycles 2 to 4, a slight reduction in droplet size was observed.

Table 2.3: Mass adsorption, thickness and density of two interfacial structures to a hydrophobic surface by SPRi.

compound	mass [ng cm^{-2}]	thickness [nm]	density [g cm^{-3}]
WPI	155	0.6	2.59
WPI–CMC	308	2.2	1.40

Oil-in-water emulsions stabilized with whey protein and carboxymethyl cellulose
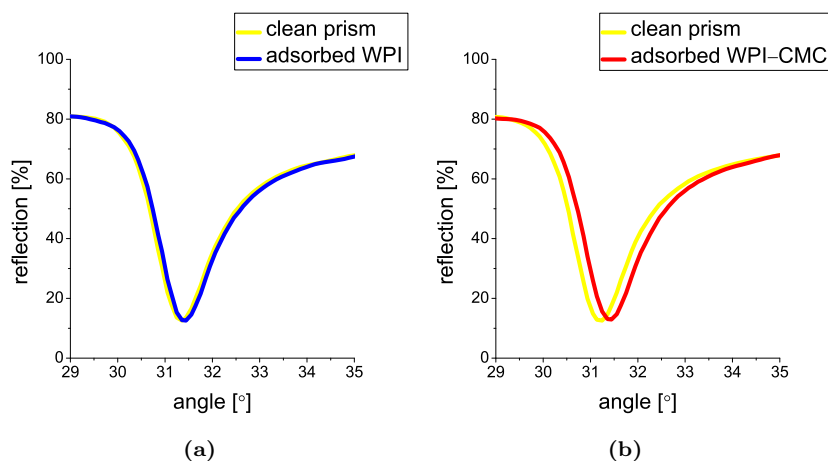

Figure 2.5: Reflectivity of the prism measured at varying incident angles for the clean prism (—) and after adsorption of (a) 1%wt WPI (—) and (b) 0.5%wt WPI–0.25%wt CMC (—).

Figure 2.7 shows how the number of cycles of premix ME affect the $d_{4,3}$ and span of the O/W emulsions stabilized with the several interfacial structures, and the effect of the final step. Regardless of the composition of the first layer (WPI or WPI–CMC complex), it is clear that droplet break-up occurs predominantly during the first emulsification cycle: mean values of $d_{4,3}$ reduced from, relatively large droplets in the coarse emulsion, approximately 70 μm to 15 μm after the first cycle. Increasing the number of emulsification cycles, a slight further reduction in the droplet size diameter was observed, even though this reduction was much smaller than for the first cycle. The final $d_{4,3}$ was, in all cases, very close to the mean pore size of the SPG membrane (approximately 10 μm), reported as one of the key parameters controlling droplet size (Nazir et al., 2010).

Regarding the droplet size dispersion of the emulsions obtained in the present work, the span values (Figure 2.7b) showed a significant increase after the first emulsification cycle. A significant amount of much smaller droplets (from 0.1 to 1 μm) than the membrane pore size (Figure 2.6) were formed already in the first premix cycle, increasing the droplet size dispersion. This behaviour, reported by
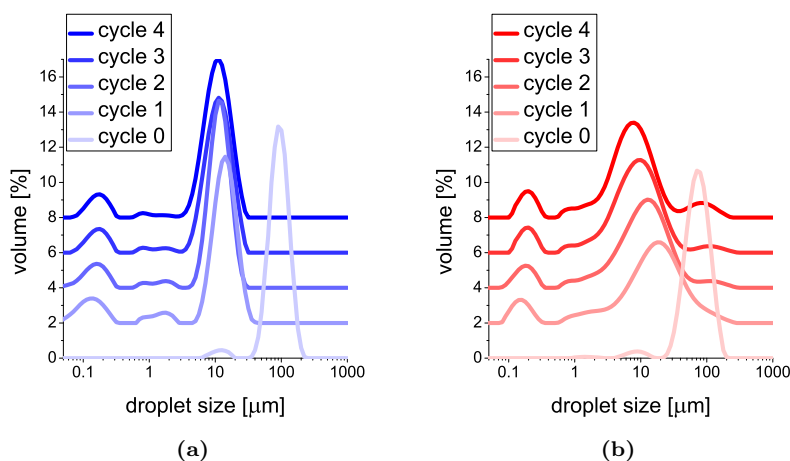
Chapter 2

Figure 2.6: Progress of droplet size distribution during premix membrane emulsifica-
tion of O/W emulsions stabilized by (a) 1.0%wt WPI and (b) 0.5%wt
WPI−0.25%wt CMC: coarse emulsion (cycle 0) (▬, ▬), cycle 1 (▬,
▬), cycle 2 (▬, ▬), cycle 3 (▬, ▬), and cycle 4 (▬, ▬).

other authors (Driessen and Jeurissen, 2011, van der Zwan et al., 2006), indicates
elongation as one of the mechanisms controlling droplet break-up during droplet
passage through the membrane pores. Their effect on emulsion stability during
storage will be discussed in the following section (2.3.4).

After cycle 4, all emulsions were washed and, subsequently, the second layer was
added to the O/W emulsions (WPI + WPI–CMC and WPI + CMC emulsions).
This final step had an unequal effect: $d_{4,3}$ of WPI and WPI–CMC emulsions kept
almost constant while WPI + WPI–CMC and WPI + CMC emulsions showed a
tremendous increase in droplet size. Coalescence of the emulsion occurred upon
addition of the second layer. Apparently, the O–W interface was left less protected,
therefore, coalescence could occur. At addition of the second layer the biopolymer
might be interacting with the adsorbed WPI in such a way that it takes away
the WPI from the surface, which leaves the emulsion less protected. Due to the
instability of both WPI + WPI–CMC and WPI + CMC emulsions (Figure 2.7a),
these emulsions were not further monitored during the storage conditions.

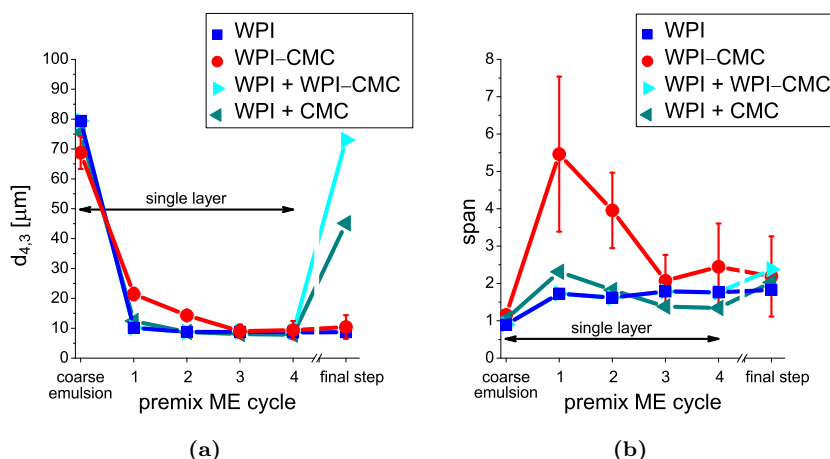Oil-in-water emulsions stabilized with whey protein and carboxymethyl cellulose

Figure 2.7: (a) Droplet sizes ($d_{4,3}$) and (b) droplet size dispersion (span); for WPI (■), WPI–CMC (●), WPI + WPI–CMC (▶), and WPI + CMC (◀) emulsions, during the emulsification process from cycle 0 (coarse emulsion) to 4. And the final step existed of washing for WPI and WPI–CMC emulsion, and washing and addition of second layer for WPI + WPI–CMC and WPI + CMC emulsions.

As a first measure of the physical stability of the several O/W emulsions obtained, we determined the creaming velocity, that is, the vertical velocity of the droplet/aqueous phase front for the first 4 hours after the emulsification process. According to these results, WPI and WPI–CMC emulsions had a creaming front velocity of 5.17 and 5.18 mm h^{-1} respectively.

2.3.4 Emulsion stability

The emulsion stability regarding droplet size and lipid oxidation of WPI and WPI–CMC O/W emulsions was monitored for two weeks during storage under UV-light at 7°C. Additionally, and to examine the effect of the final washing step on emulsion stability, the droplet size dispersion for WPI and WPI–CMC O/W emulsions that were not washed was determined after two weeks of storage at 7°C (from here on,
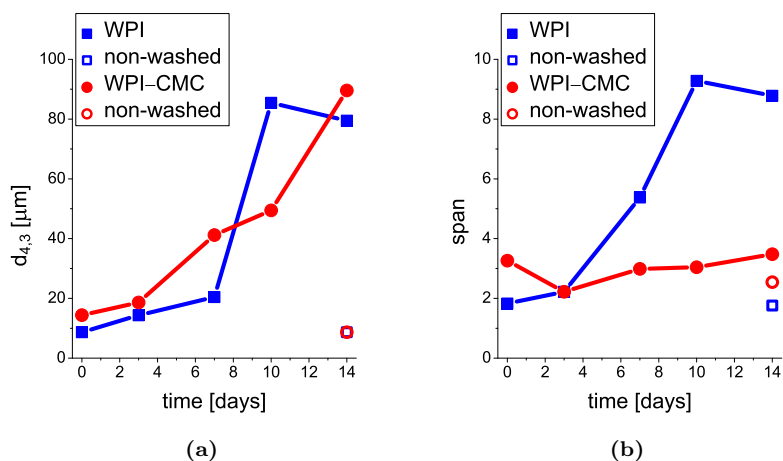
Chapter 2

Figure 2.8: (a) Droplet sizes ($d_{4,3}$) and (b) droplet size dispersion (span); stability measurements over time of WPI (■), WPI–CMC (●), non-washed WPI (□), and non-washed WPI–CMC (○) emulsions.

non-washed emulsion).

Figure 2.8a shows a significant increase in droplet size already during the first week of storage for WPI and WPI–CMC. After two weeks of storage values between 6 and 9 times the initial $d_{4,3}$ were observed. Although both emulsions presented a poor stability, the progress of span over time showed differences between them: the span (Figure 2.8b) of the WPI emulsions increased abruptly after one week of storage, while the span of the WPI–CMC layer kept almost constant over time. After 14 storage days, individual droplets of both emulsions were significantly larger in size than the initial droplets, suggesting that coalescence or Ostwald ripening (also disproportionation) was responsible for the observed droplet growth.

The evolution of the droplet size distribution of the WPI and WPI–CMC O/W emulsions is plotted in Figure 2.9. The complex emulsions initially had a bimodal droplet size dispersion, but over time the small droplets disappeared and the larger ones grew leading to a monomodal dispersion after 7 storage days, which slowly moved up the droplet size axis over time. These results are consistent with Ostwald ripening, in which oil droplets diffuse through the aqueous phase and join larger

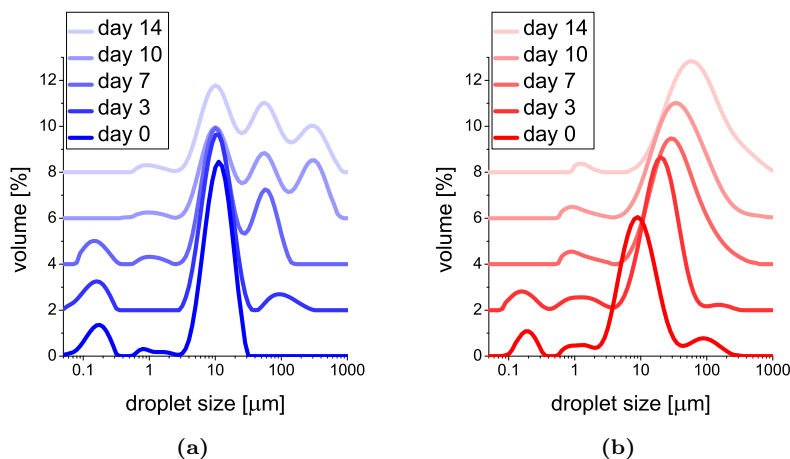Oil-in-water emulsions stabilized with whey protein and carboxymethyl cellulose

Figure 2.9: Droplet size distribution during storage of emulsions (a) WPI and (b) WPI–CMC: day 0 (━, ━), day 3 (━, ━), day 7 (━, ━), day 10 (━, ━), and day 14 (━, ━).

droplets, which may be responsible for the observed droplet growth in WPI–CMC complex emulsions (Lim et al., 2011). Although the solubility of the lipid in the aqueous phase has been reported as the most important factor affecting the rate of Ostwald ripening, interfacial properties and droplet size dispersion can also cause this instability (Zeeb et al., 2012). In the case of WPI emulsions the droplet size distribution progressed in a different way than WPI–CMC emulsion: the initial bimodal dispersion shifted to a three modal dispersion after one week of storage. The peaks of small droplets decreased while a third peak of bigger droplets appeared. This suggests, not only one mechanism may control the stability of mono-layer emulsions, as this different pattern of droplet growth suggest.

Additionally Figure 2.8 shows a much higher stability for the non-washed emulsions regardless of the type of interfacial structure. These results suggest that the washing process, centrifugation followed by replacement of the water phase, induced a major destabilization on the O–W interfaces. A redistribution of the WPI and WPI–CMC complex at the droplet interface may be the reason of the much lower stability observed in WPI–CMC and WPI emulsions.

Chapter 2
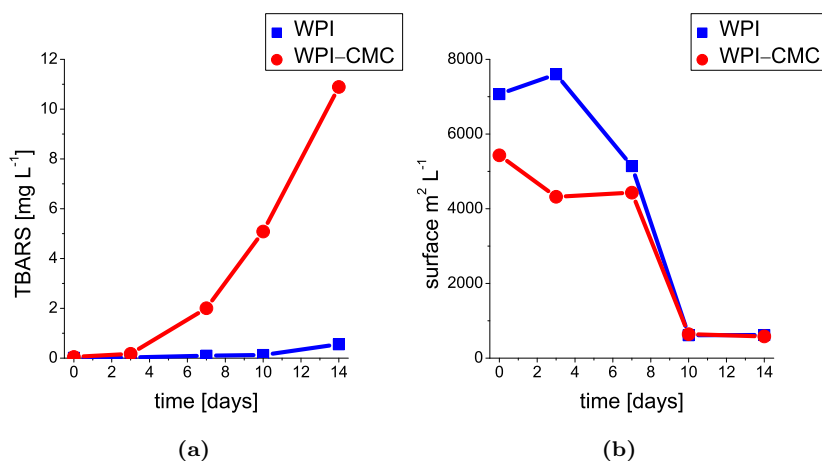
Figure 2.10: (a) oxidation measurement by TBARS assay and (b) surface evolution in time, of emulsions stabilized by WPI (■), and WPI–CMC (●) emulsions.

Figure 2.10 shows the progress of TBARS and droplet surface of WPI–CMC and WPI O/W emulsions during storage at 7°C. From three days of storage, the oxidation rate of WPI–CMC emulsions was much higher than that of WPI emulsions, even though the interfacial surface area of the WPI O/W emulsion was greater. Considering this, the rate of oxidation clearly depended on the biopolymer type at the interface.

The interfacial properties of emulsions seem to have a strong effect on the oxidative stability of the oil phase. Therefore the formation of a thicker and denser interfacial film that act as a physical barrier, separating lipids from pro-oxidants in the water phase, has been suggested as a strategy to reduce lipid oxidation in emulsions (McClements and Decker, 2000). In addition, other interfacial properties, such as the electrical charge at the droplet interface plays a key role on lipid oxidation: the greater the surface charge density on an emulsion droplet, the greater the ability to attract oppositely charges counter-ions, some of them capable of promoting lipid oxidation.

Considering this, the oxidative stability of the WPI and WPI–CMC O/W emul-

sions should be related to their properties at the interface. Since it was not possible to measure those properties at the real droplet interface, the adsorption behavior of WPI and WPI–CMC complex to interfaces of different hydrophobicity and the ζ-potential of WPI and WPI–CMC complex in solution were used to interpret the lipid oxidation progress of WPI and WPI–CMC emulsions. In this sense, SPR determinations showed that WPI formed a significantly denser interfacial structure than the WPI–CMC complex (Table 2.3). According to the oxidation rate shown by WPI and WPI–CMC emulsions, the denser interfacial coating formed by WPI would better reduce the diffusion of any transition metal present in the system than the thicker but more openly packed layer made of WPI–CMC complex.

Values of ζ-potential of WPI and WPI–CMC complex at the same conditions as those used in the emulsions were +18.5 and -28.1 mV, respectively. Considering this, the negatively charged lipid droplets of the complex emulsion could attract positively charged transition metals to their surfaces, thereby bringing the pro-oxidant into close proximity to the lipid substrate and increasing the oxidation rate.

The role of the interfacial composition, in particular electrical charge, on the oxidation rate has been reported by other authors. Charoen et al. (2012) observed that the oxidation rate of O/W emulsions stabilized with gum Arabic was much higher than that of emulsions stabilized with modified starch or WPI. These differences were particularly great at pH 3, at which the ζ-potential of droplets stabilized with gum Arabic was negative (-13 mV) while the ζ-potential of those stabilized with WPI was positive (+37 mV).

2.4   Conclusions

Premix ME enables to produce O/W emulsions with interfacial structures made of WPI and a WPI–CMC complex. Although the adsorption between the several layers was confirmed by SPR, the stability of the final O/W emulsions was different according to the composition and number of interfacial layers. Even though WPI emulsions showed a mean droplet size close to the pore membrane (10 μm), a significant amount of much smaller droplets contribute to increase droplet dispersion. This seemed to affect emulsion stability during storage. Non-washed emulsions were much more stable than their washed counterpart, this suggest that reducing the non-adsorbed WPI in the water solution (either as a complex or isolated) by centrifugation did contribute to droplet flocculation and further coalescence. A redistribution of the WPI and WPI–CMC complex at the droplet interface may

be the reason of the much lower stability.

The oxidation rate of emulsions strongly depended on the interfacial composition. Adsorption data at hydrophobic interface and the electrical charge of the WPI–CMC complex suggest that it formed a thick but less dense interface than WPI with a negative charge able to attract any transition metal ion and promote lipid oxidation. This research suggests that the strategies to improve the oxidation stability of O/W emulsions by tailoring their interface should consider multi-layer arrangements, e.g. made of WPI, or protein–polysaccharide complexes having a positive electrical charge at the emulsion conditions, among others. The use of pre-mix ME to obtain stable emulsions with multi-layer interfaces should be further investigated.

3

Water-in-oil-in-water emulsions encapsulating a procyanidin-rich extract

Abstract

Premix membrane emulsification (ME) enabled us to produce procyanidin-loaded $W_1/O/W_2$ emulsions with narrow droplet size distributions. The emulsion interface of the outer droplets were stabilized with several hydrophilic emulsifiers (whey protein (WPI), WPI–Carboxymethyl cellulose, WPI–Gum Arabic, and WPI–Chitosan) and their effect on procyanidin encapsulation, droplet stabilization, and creaming stability in different pH environments was determined.

Although premix ME produced emulsions with a narrow droplet size distribution for all hydrophilic emulsifiers with sizes around 10 μm, droplet coalescence was observed at high (pH 7) or low pH (pH 3) environments depending on the hydrophilic emulsifier. A certain range of pH was found for each hydrophilic emulsifier at which double emulsions were stable up to 14 days. The procyanidin release of $W_1/O/W_2$ emulsions stabilized with the several WPI–polysaccharides was measured during 14 days and depended on the interfacial thickness of the adsorbed hydrophilic emulsifier. WPI–Chi stabilized $W_1/O/W_2$ emulsions showed the highest stability in droplet size distribution and the lowest procyanidin release at a narrow pH range. A thicker interfacial WPI–Chi layer (4.2 nm versus 2.2 and 3.9 nm for WPI–CMC and WPI–GA, respectively) resulted in a lower procyanidin release.

3.1 Introduction

Procyanidins, oligomers of (–)-epicatechin and (+)-catechin, are secondary metabolites of plants that can be found in a number of plant-based foods and beverages (Hammerstone et al., 2000). Regular intake of foods rich in procyanidins has been linked to a reduction of risk in cardiovascular diseases (Yamakoshi et al., 1999), diabetes (Pinent et al., 2004), and certain types of cancer (Santos-Buelga and Scalbert, 2000). Although the particular role of procyanidins on reducing risk factors or acting on different parameters related to vascular diseases and cancer requires a better understanding, in vitro and clinical studies show consistently their positive effects on human health (Williamson and Manach, 2005).

One of the main problems of procyanidins consumed through our diet is that they show low bioavailability (Gonthier et al., 2003). Only a small proportion of procyanidins is bioavailable after oral administration, due to insufficient gastric residence time, low permeability or solubility in the gut or degradation at the environmental conditions of the gastrointestinal tract (pH, enzymes, presence of other nutrients). Besides, procyanidins found in food can be damaged by high temperature or exposure to oxygen during processing or storage. In terms of sensory properties, procyanidins are mainly characterized by bitterness and astringency what may additionally limit their use in formulating food products (Lesschaeve and Noble, 2005).

Procyanidin encapsulation overcomes the drawbacks of sensitivity to high temperature, chemical degradation and limited bioavailability. By choosing the adequate encapsulation technology, procyanidins can be protected from undesired degradation due to environmental effects or can be released at a controlled rate in the mouth, stomach, or small intestine (Fang and Bhandari, 2010, McClements et al., 2009). Among the existing encapsulation technologies, production of double emulsions has been reported to provide advantages for a number of industrial applications (van der Graaf et al., 2005). Water-in-oil-in-water ($W_1/O/W_2$) emulsions consist of small water droplets contained within larger oil droplets that are dispersed in an aqueous continuous phase. The structure of $W_1/O/W_2$ emulsions make them suitable as delivery systems of water soluble bioactive molecules, presenting some advantages over W/O single emulsions, such as their lower viscosity. Procyanidins, water soluble components, can be dispersed into the inner water phase to be protected from chemical degradation and to prevent their undesirable sensory qualities to be perceived during mastication (Benichou et al., 2004). Double emulsions are normally produced using a two-step procedure:

i) a W_1/O emulsion is produced by homogenizing water, oil and a hydrophobic

Chapter 3

emulsifier

ii) a $W_1/O/W_2$ emulsion is then produced by homogenizing the W_1/O emulsion in water containing a hydrophilic emulsifier.

The same kind of homogenization devices used to produced single emulsions can be used to prepare double emulsions (e.g., rotor-stator system, high pressure homogenizers, colloid mills, ultrasonic homogenizers), although the secondary homogenization step is usually carried out using a lower energy intensity than the primary step so as not to break the initial W_1/O emulsion (Charcosset, 2009).

Membrane emulsification (ME) has received increasing attention over the last years because of the low energy consumption, the better control of droplet size distribution and the mildness of the process. The use of low-shear stresses makes membrane emulsification a suitable technology for producing double emulsions, overcoming the limitations of conventional homogenization. In premix ME, first a coarse emulsion is made and successively pushed through a membrane. Passing the coarse emulsion through the membrane, the droplets break-up into smaller ones (van der Graaf et al., 2005). Generally more than one pass through the membrane is required to decrease droplet size and dispersion. The mild conditions of premix ME are especially useful for the second emulsification step in order to prevent the rupture of the emulsion structure, which might end up into a single O/W emulsion. In contrary to conventional emulsification methods, it becomes possible to produce small and monodisperse droplets without using high-shear stresses that cause escape of the internal droplets.

Several authors (Kawashima et al., 1991, Vladisavljević et al., 2004) have produced $W_1/O/W_2$ emulsions using premix ME. Shirasu porous glass (SPG) and polymeric microfiltration membranes of cellulose acetate and polycarbonate, have been used to obtain $W_1/O/W_2$ emulsions entrapping a water soluble compound in the inner water droplets. According to Vladisavljević et al. (2006b), premix ME enables a controlled production of $W_1/O/W_2$ emulsions with high encapsulation efficiency and at high production rates. Operating conditions that have a strong influence on the droplet size distribution, transmembrane flux and encapsulation efficiency are membrane pore size, number of passes through the membrane (cycles) and transmembrane pressure. These conditions have to be adjusted to each particular formulation since the content of inner droplets, the viscosity of the continuous phase or the emulsifier properties (interfacial tension and adsorption rate at newly formed interfaces) strongly determine the characteristics of the $W_1/O/W_2$ emulsions produced by premix ME.

The thermodynamic stability of double emulsions is lower than in single emul-

sions due to their higher interfacial area. Several mechanisms control the stability of double emulsions and are known to occur simultaneously during production and storage. To increase the stability of $W_1/O/W_2$ emulsions, different types of emulsifiers at varying concentrations have been formulated in the oil and external water (W_2) phases. Polymeric emulsifiers, such as proteins, successfully stabilize oil-water interfaces because of their ability to reduce the interfacial tension and simultaneously form an interfacial nanolayer able to prevent coalescence. Recent research suggests the use of proteins in combination with polysaccharides as hydrophilic emulsifiers for improving the stability and functionality of emulsions (Dickinson, 2011b, Turgeon et al., 2007). In particular, soluble protein–polysaccharide complexes, result of electrostatic interactions between oppositely charged macromolecules at certain conditions of pH and ionic strength, can be advantageously used to stabilize oil-in-water interfaces (Benichou et al., 2004, Dickinson, 2008, Guzey and McClements, 2006). The interfacial coatings made of protein–polysaccharide complexes increase the physical stability of oil-in-water emulsions against stresses such as temperature, mechanical agitation, pH and the presence of multivalent ions (Guzey and McClements, 2006, Ogawa et al., 2003). In addition, the interfacial structures made of protein complexes may improve the retention of any bioactive compound encapsulated. This kind of interfacial coating can be denser and thicker, hindering the diffusion of any encapsulated bioactive compound.

Whey protein isolate (WPI) complexed with different polysaccharides have surface active properties able to stabilize O/W emulsions. Some of those polysaccharides include: carboxymethyl cellulose (Girard et al., 2002), gum Arabic (Jiménez-Alvarado et al., 2009), chitosan (Laplante et al., 2005a), pectins (Neirynck et al., 2004) and dextran (Frank et al., 2012). In some cases, O/W emulsions stabilized with WPI–polysaccharide complexes showed higher stability than those stabilized with WPI. Damianou and Kiosseoglou (2006) investigated the effect of pH to the surface coverage of WPI–carboxymethyl cellulose complex to O/W emulsions. They found that carboxymethyl cellulose is increasingly adsorbed to the O–W interface when lowering the pH. Laplante et al. (2005b) found that O/W emulsions stabilized with WPI–chitosan were more stable at high pH and WPI to chitosan ratios. Jiménez-Alvarado et al. (2009) encapsulated ferrous bisglycinate in $W_1/O/W_2$ emulsions using WPC–gum Arabic, WPC–low methyl pectin, and WPC–mesquite gum complexes as hydrophilic emulsifiers and linked the encapsulation and the protection against oxidation of ferrous bisglycinate to the type of polysaccharide used in the complex, where they suggested that a thicker layer leads to better protection. Neirynck et al. (2004) stabilized O/W emulsions using

WPI–low methoxyl pectin Maillard type complex, which lead to improved stability near the isoelectric point of whey protein (pH 5.5). Frank et al. (2012) produced $W_1/O/W_2$ emulsions using WPI–dextran complex as a hydrophilic emulsifier and observed that their droplet size distribution changed during gastric incubation, with a significant increase of W_1/O droplet size.

In this Chapter, we assessed premix ME to produce $W_1/O/W_2$ emulsions entrapping procyanidins in the inner water phase, using WPI–polysaccharide complexes as hydrophilic emulsifiers. The influence of three WPI–polysaccharide complexes, WPI–carboxymethyl cellulose, WPI–gum Arabic and WPI–chitosan on the emulsion stability and procyanidin release during storage was investigated. To do so, the adsorption properties of the four different interfacial structures, made of WPI and each WPI–polysaccharide complex, together with the surface charge of the droplets were investigated. For producing the $W_1/O/W_2$ emulsions, firstly the conditions for WPI–polysaccharide complexation were verified for each system. Secondly, double emulsions were produced with each selected complex by setting the operating conditions (transmembrane pressure) during premix ME using Shirasu porous glass (SPG) membranes. Emulsion properties, such as droplet size distribution, creaming stability and release of procyanidins were determined over time at different pH environments. Surface Plasmon Resonance measurements were performed to determine the thickness and density of the adsorbed layer, while ζ-potential measurements provided information on the charges of the different hydrophilic emulsifiers and at the droplet surface of $W_1/O/W_2$ emulsions.

3.2   Materials and Methods

3.2.1   Materials

Vitaflavan Pur'expert (DRT, France), a water soluble commercial grape seed extract, with a reported total polyphenol content above 96% of which 22% are monomers, 19% are dimers and 56% are trimers up to pentamers, was the source of procyanidins encapsulated in the W_1 phase of the double emulsions. Vitaflavan was kindly provided by Quimidroga, S.A. Barcelona, Spain. The oil phase of the emulsions (O) was composed of crude sunflower oil, kindly provided by Cargill S.L.U. (Reus, Spain), and a 4%wt of polyglycerol polyricinoleate (PGPR), a very effective hydrophobic emulsifier.

To obtain the several WPI–polysaccharide complexes that were used as hydrophilic emulsifiers in the W_2 phase, 2.0%wt solutions were prepared by dissolving in distilled water and stirring for 2 h the following compounds: whey protein

isolate (WPI) with a reported protein content of 98.1% on dry basis (BiPRO, lot no. JE 034-7-440-6, Davisco Foods International. Inc., Le Sueur, MN) and carboxymethyl cellulose sodium salt (CMC) (Acros Organics), with a M_w of 250,000 and a degree of substitution (DS) of 0.7, and gum Arabic (GA) from acacia tree (Sigma-Aldrich Quimica, S.L.), solutions were kept overnight at 7°C.

A solution of 0.4%wt chitosan (Chi) of low molecular weight with a M_w of 150,000 (Sigma-Aldrich) was obtained after dissolving and stirring, for 2 h at room temperature, in acetic acid solution. Osmolality was adjusted by preparing all solutions in 0.01 M acetic acid (acetic acid 96%, Panreac) and 0.02%wt sodium azide (NaN$_3$, Sigma-Aldrich), from here on called acetic solution.

3.2.2 Methods

State diagram of hydrophilic emulsifiers

We obtained the state diagram of WPI–GA and WPI–Chi to determine at which conditions (pH and WPI to polysaccharide mass ratio) the soluble electrostatic complexes are formed. Aqueous solutions containing 0.5%wt of WPI were combined with either GA or Chi solutions. Different concentrations were prepared to obtain a final ratio of 1:0, 1:1, 2:1, 3:1 and 4:1, for GA and a final ratio of 1:0, 5:1, 10:1, 20:1 and 40:1, for Chi. All mixtures were made in acetic solution and the pH was adjusted to 6 or 3 with 1 M HCl or 1 M NaOH solutions. Turbidity and pH of each mixture was measured right after preparation to identify a clear solution, a cloudy solution or the formation of a precipitate. Turbidity was quantitatively measured from the transmission (T) profiles obtained with a Turbiscan Lab$^{\text{TM}}$ Expert (Formulaction, France).

From these experiments an adequate WPI–polysaccharide ratio and pH were chosen to obtain a hydrophilic emulsifier that, afterward, was used to stabilize the O–W$_2$ interface. WPI–CMC complex, which was verified in Chapter 2, and (non-complexed) WPI were the other hydrophilic emulsifiers employed. Table 3.1 summarizes the composition of each hydrophilic emulsifier and the conditions of pH and transmembrane pressure (ΔP_{tm}), at which the double emulsions were produced.

Determination of osmolality

Osmotic pressure was measured by a vapor pressure osmometer (K-7000, KNAUER) at 30°C. Calibration was done with a NaCl solution of 100 mOsm kg^{-1}. The osmotic pressure of W$_1$ and W$_2$ (see composition in Tables 3.1 and 3.2) were

Table 3.1: Premix ME conditions during the production of $W_1/O/W_2$ emulsions stabilized by different hydrophilic emulsifiers

hydrophilic emulsifier	pH	ΔP_{tm} [kPa]
1.0%wt WPI	3.8	175 ± 25
0.5%wt WPI – 0.25%wt CMC	3.8	750 ± 50
0.5%wt WPI – 0.50%wt GA	4.8	250 ± 50
0.5%wt WPI – 0.05%wt Chi	5.4	300 ± 50

measured in comparison to distilled water. Measurements were monitored, until stable values of vapor pressure were detected. Each experiment was repeated ten times.

Table 3.2: Phase fractions of double $W_1/O/W_2$ emulsion and concentrations of compounds in W_1, Oil and W_2, with acetic solution containing 0.01 M acetic acid and 0.02%wt sodium azide.

fraction	phase	compound	medium
6%wt	W_1	10%wt vitaflavan	acetic solution
14%wt	O	4%wt PGPR	sunflower oil
80%wt	W_2	hydrophilic emulsifier	acetic solution

Surface plasmon resonance measurements

To measure thickness and density of the interfacial structure built up by each hydrophilic emulsifier, a SPRi-PlexII™ (Genoptics-Horiba Scientific, Orsay, France) was used to record the entire Surface Plasmon Resonance (SPR) curves. The comparison of the curves recorded before and after exposure to the hydrophilic emulsifier was used to estimate the thickness of the adsorbed layer using the Fresnel equations (Winspall 3.02, WINSPALL-Material Science Group-MPI-P Mainz). For providing the sensor chips with a hydrophobic layer similar to oil, they were initially pre-treated with Piranha solution (70%wt $H_2SO_4 : 30$%wt H_2O_2) for 5 min, rinsed with distilled water three times and immersed overnight in a 1 mM solution of cystamine prepared in ethanol. Thereafter the sensor chip was rinsed with

distilled water three times, kept in distilled water, sonicated for 30 s, and finally dried in a stream of nitrogen (Tsukruk and Bliznyuk, 1998).

The system was left to equilibrate in a 50 μL min^{-1} flow of 0.01 M acetic acid pH 4.8 or 5.4 containing 0.02%wt NaN$_3$ (running buffer) till the signal stabilized, with temperature control at 25°C. The optimal incident angle was set and the initial SPR angles recorded at 10 different locations 988 μm in diameter across the modified sensor chip. The sensor chip was exposed to the WPI–polysaccharide solution and the flow stopped after 1 min. Adsorption of the WPI–polysaccharide onto the sensor chip was carried out over a 10 min period, after which the buffer was flowed over the sensor surface for an additional 10 min at a flow rate of 50 μL min^{-1}. The adsorption experiment was stopped and plasmonic curves for the ten spots were recorded. The reflectivity after 10 min of desorption was taken and expressed in ng cm^{-2}, where 1% reflectivity corresponds to 200 pg mm^{-2}.

ζ-potential measurement

Laser Doppler micro-electrophoresis, Zetasizer Nano ZS (Malvern Instruments), was used to:

  i) confirm WPI–polysaccharide complex formation

  ii) determine the charge at the oil droplet surface in the $W_1/O/W_2$ emulsions

To determine the ζ-potential of WPI, GA, Chi and WPI–CMC, WPI–GA, WPI–Chi complexes in solution, pH was adjusted to different values (Table 3.1) and samples were centrifuged at 1000 G for 30 min to remove impurities. After that, the ζ-potential distribution of each of them was measured.

For measuring the ζ-potential of double emulsions, freshly prepared emulsions were diluted ten times with acetic solution, keeping the emulsion pH constant. Each emulsion was divided into four aliquots and the pH of the W_2-phase of three of them was gradually changed; from the original emulsion pH to pH values of 3, 5 and 7. One aliquot was kept at its original pH. After that, the ζ-potential distribution of each of them was measured. All reported ζ-potential values are an average of six measurements and were calculated by the Smoluchowski equation. All measured ζ-potential distributions were monomodal.

Production of double emulsions by premix ME

Table 3.2 shows the composition of the $W_1/O/W_2$ emulsions. To produce the $W_1/O/W_2$ emulsions, first a single W_1/O emulsion was produced by adding 15 g

of W_1 into 35 g of oil and emulsifying it with a rotor-stator homogenizer (Ultra Turrax, IKA® T18 basic) at 11,000 rpm for 5 min. At these conditions we obtained a monodisperse W_1/O emulsion with a $d_{4,3}$ of 2.6 μm and 1.0 of span factor.

Double $W_1/O/W_2$ emulsions were produced by a two-step emulsification. First 40 g of W_1/O was added to 160 g of W_2, containing one of the four hydrophilic emulsifiers (Table 3.1), and were mixed by a magnetic stirrer at 1600 rpm for 5 min. Secondly, the coarse emulsion (cycle 0) was loaded into a High-speed mini kit (SPG Technology Co., Japan) equipped with a hydrophilic Shirasu porous glass (SPG) membrane of 10 μm pore size (membrane dimensions were 125 mm × 10 mm × 0.8 mm) (SPG Technology Co., Japan). The coarse emulsion was forced through the membrane with nitrogen gas and the applied transmembrane pressure (ΔP_{tm}) was adjusted for each emulsion (see Table 3.1). This procedure was performed up to 3 times, from cycle 1 to 3, to progressively reduce the mean droplet size and droplet dispersion. After use, SPG membranes were successively cleaned by sonication in acetone for 15 min and kept in acetone for several days, subsequently the membrane was dried in an oven at 500°C for 30 min. Before reuse, the membrane was washed again with distilled water while sonicating for 15 min.

After emulsification, each emulsion was divided into four aliquots and the pH of the W_2-phase of three of them was gradually changed, from the original emulsion pH to pH values of 3, 5 and 7. One aliquot was kept at its original pH, from here on called double emulsion original pH. All four emulsions were prepared in duplicate.

Creaming rate and serum layer thickness

Creaming stability measurements of $W_1/O/W_2$ emulsions were carried out using a Turbiscan Lab™ Expert (Formulaction, France). The Turbiscan Lab™ Expert transmits light (880 nm) and measures the amount of light which passes through (transmission) and which is reflected (backscattering) over the full height of a glass tube. Backscattering (BS) profiles were taken from approximately 20 mL every 5 min for 6 – 72 h of at least two freshly prepared double emulsions. Creaming rate, defined as the vertical velocity of the emulsion droplets front, was calculated from the BS profiles and expressed in mm h^{-1}. The serum layer thickness was the second parameter related to creaming stability that was measured. From the initial upward movement of the W_1/O droplets, emulsions separated into an optically opaque "cream" layer at the top and a transparent (or turbid) "serum" layer at the bottom. After the creaming velocity was zero according to Turbiscan measure-

ments, the height of serum and emulsion layers was measured from backscattering, at these conditions the serum layer percentage was calculated as:

$$serum = \frac{H_s}{H_e} \times 100 \qquad (3.1)$$

where H_s is the height of the serum layer and H_e is the total height of the emulsion (Surh et al., 2007). Each determination was performed in duplicate.

Droplet size distribution of emulsions

The droplet size distribution of $W_1/O/W_2$ emulsions was measured after every emulsification step and after 0, 3, 7, 10 and 14 days of storage at several pH environments: 3, 5, 7 and the original pH of each emulsion. Measurements were done by laser light scattering (Mastersizer 2000, Malvern Instruments). Distilled water was used as continuous phase, stirring speed was set at 1400 rpm, and laser obscuration was between 10 and 15%. The refractive indices applied were 1.33 for distilled water and 1.46 for the W_1/O droplets, at 25°C. The angular scattering intensity data was then analyzed, using the Mie theory of light scattering, to calculate the size of the droplets responsible for creating the scattering pattern. Mean droplet size and droplet dispersion were calculated as the volume-weighted mean diameter ($d_{4,3}$) and the relative span factor (span). Each determination was performed in triplicate.

Emulsion structure

Optical microscopy (Leica DM 2500) was used to visualize the structure of the $W_1/O/W_2$ emulsions at day 0 and after 14 days of storage at their original pH.

Determination of total procyanidin content at outer water phase

Procyanidin content in the W_2-phase was determined spectroscopically with the Folin-Ciocalteu's method (Singleton and Rossi, 1965). A 1.5 mL aliquot was centrifuged (Biocen 22R, rotor RT 223, Orto Alresa) at 15 G to separate W_2 phase from W_1/O phase and 50 μL of W_2 phase was diluted in 25 mL of distilled water. Centrifugation conditions were setup to minimize coalescence and the further escape of W_1. A sample of 1.5 mL was mixed with 20 μL of Folin-Ciocalteu's reagent and 20 μL of 30% NaOH solution. After 5 min, absorbance was measured spectroscopically (DR 5000 Hach Lange) at 660 nm. Concentration of procyanidins

was determined from a calibration curve with Gallic Acid 1-hydrate (Panreac) as standard. Each determination was performed in triplicate.

Encapsulation of procyanidins at production

Encapsulation of procyanidins during production was expressed as the mass of procyanidins that remained encapsulated within the W_1 droplets over the total mass of procyanidins initially introduced in the inner water phase. It was assumed that, during the production of the double emulsions, the procyanidins mainly escape through the loss of inner water droplets (Vladisavljević et al., 2006b). Therefore encapsulation can be expressed as:

$$\frac{EEemulsion}{100} = \frac{m^0_{p,W_1} - m^n_{p,W_2}}{m^0_{p,W_1}} = \frac{m^0_{W_1} + m^0_{W_2} - m^n_{W_2}}{m^0_{W_1}} \quad (3.2)$$

where m^0_{p,W_1} is the initial procyanidin mass in the inner water phase, m^n_{p,W_2} the procyanidin mass in the outer water phase after n^{th} cycle of premix ME, $m^0_{W_1}$ the initial mass of the inner water phase, $m^0_{W_2}$ the initial mass of the outer water phase, and $m^n_{W_2}$ the mass of the outer water phase after n^{th} cycle. The concentration of procyanidins that is measured in the outer water phase can be calculated as:

$$m^n_{p,W_2} = C^n_{p,W_2}\left(m^0_{W_1}\left(1 - \frac{EEemulsion}{100}\right) + m^0_{W_2}\right) \quad (3.3)$$

where C^n_{p,W_2} is the concentration of procyanidins in the outer water phase which was determined by Folin-Ciocalteu's reagent. Substitution of Equation 3.3 into 3.2 gives:

$$EEemulsion = \frac{m^0_{p,W_1} - C^n_{p,W_2}\left(m^0_{W_1} + m^0_{W_2}\right)}{m^0_{p,W_1} - C^n_{p,W_2}m^0_{W_1}} \times 100 \quad (3.4)$$

Kinetics of procyanidin release

Release of procyanidins was determined in freshly produced emulsions and during storage for 14 days at several pH environments: 3, 5, 7 and the original pH. Through storage, a different mechanism is assumed to control procyanidin release than during production. While during production, procyanidin mainly escapes through losses of W_1, release of the inner water phase W_1 can be considered

negligible during storage (results shown in section 3.3.4 confirm this assumption). Therefore release of procyanidins during storage was expressed as:

$$R = \frac{C_{p,W_2}^t \times m_{W_2}}{m_{p,W_{1+2}}} \tag{3.5}$$

where C_{p,W_2}^t is the concentration of procyanidins at time t, m_{W_2} is the mass of the W_2 phase, and $m_{p,W_{1+2}}$ is the total mass of procyanidins in both water phases. In the remainder of this study, we express fraction R as percentage released after production:

$$release = \frac{R - R_0}{1 - R_0} \times 100 \tag{3.6}$$

where R_0 is the procyanidin fraction already released at day 0 due to the production of the double emulsion. The model proposed by Higuchi (1961) and used by other authors to model the release of entrapped compounds in double emulsions (Jiménez-Alvarado et al., 2009, Lutz et al., 2009) was applied to the procyanidin release at different environmental pH. The progress of procyanidin concentration over storage time was fitted to Higuchi's model:

$$C_{p,W_2}^t = K_H t^{0.5} \tag{3.7}$$

where K_H ($\mu g \, mL^{-1} min^{-0.5}$) is the release rate constant of the procyanidin from the double emulsion. The obtained kinetic parameters were analyzed using one-way analysis of variance (ANOVA) followed by protected Fisher's LSD method to establish the significance of differences among the mean values at $p < 0.05$.

3.3 Results and discussion

3.3.1 Hydrophilic emulsifiers to stabilize the oil-water interface

WPI and soluble WPI–polysaccharide complexes were used to stabilize the O–W_2 interface of double emulsions. The ability of WPI–polysaccharide complexes to form thicker and, possibly, denser nanolayers than WPI at the O–W_2 interface would increase the encapsulation efficiency of emulsions entrapping a bioactive compound in the disperse phase. Prior to use those complexes, the conditions (mainly pH and WPI to polysaccharide mass ratio) at which WPI together with gum Arabic (GA) or chitosan (Chi) form soluble electrostatic complexes were set
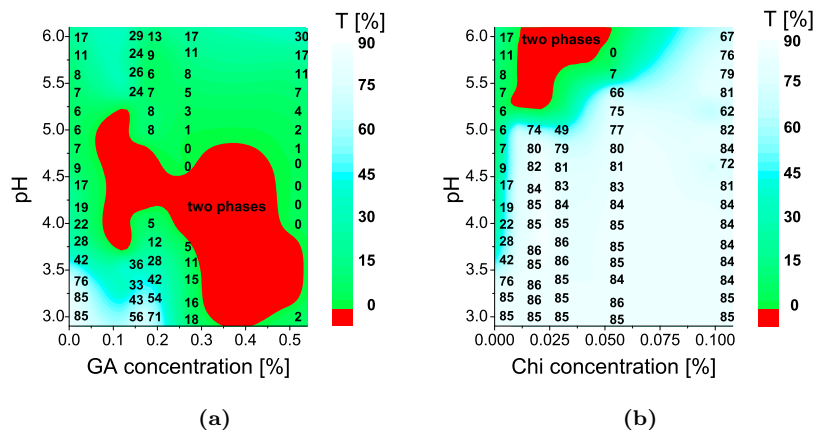
Chapter 3

Figure 3.1: State diagram of (a) WPI/GA and (b) WPI/Chi system in aqueous solution at a constant WPI concentration of 0.5%wt. Values show light transmission (T [%]) through the liquid phase. Color shading indicate transmission, the two phase region is delimited by the (■) area.

from the state diagram of each WPI–polysaccharide system. Figure 3.1 shows the state diagrams of WPI/GA and WPI/Chi in acetic solution at 0.5%wt WPI. In each state diagram it was possible to identify a liquid phase region (containing co-soluble polymers and soluble complexes) and a two-phase region made of an insoluble precipitate and a clear liquid phase (Dickinson, 2008, Sperber et al., 2009). By measuring the turbidity of the liquid phase region in terms of transmission data, the ranges of pH and WPI:polysaccharide ratio that lead to the formation of soluble complexes were identified. At those conditions milky solutions with low transmission values (0 – 30%) indicated formation of soluble complexes. The WPI:polysaccharide ratio and pH value of WPI–GA and WPI–Chi soluble complexes used as hydrophilic emulsifiers in the $W_1/O/W_2$ emulsions are summarized in Table 3.1. Regarding WPI–CMC complex, the conditions for complex formulation were obtained from Chapter 2. Furthermore, we checked the transmission of the polysaccharide in acetic solution over pH range 3 – 6, where GA gave a transmission $> 88\%$ and Chi a transmission $> 81\%$.

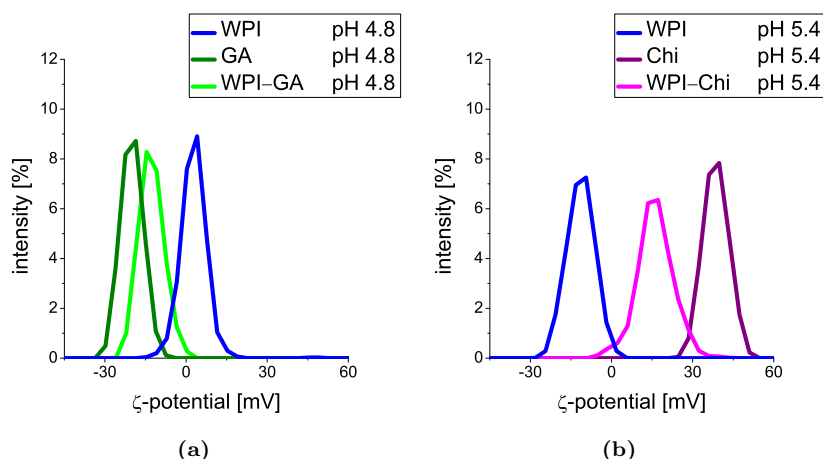Water-in-oil-in-water emulsions encapsulating a procyanidin-rich extract

Figure 3.2: ζ-potential measurement of (a) 0.5%wt WPI (——), 0.5%wt GA (——), and 0.5%wt WPI – 0.5%wt GA (——) dissolved in acetic solution at pH 4.8, and (b) 0.5%wt WPI (——), 0.05%wt Chi (——), and 0.5%wt WPI – 0.05%wt Chi (——) dissolved in acetic solution at pH 5.4.

To confirm complex formation, ζ-potential measurements were conducted. Figure 3.2 shows the ζ-potential distribution of solutions containing WPI, GA, Chi and their corresponding complexes: 0.5%wt WPI – 0.5%wt GA and 0.5%wt WPI – 0.05%wt Chi. The values of pH and ionic strength in all solutions were the same as those used in W_2 to stabilize $W_1/O/W_2$ emulsions (Table 3.1). The monomodal dispersions obtained with both complexes indicate that they were truly formed, showing ζ-potential values of WPI–GA at pH 4.8 and WPI–Chi at pH 5.4 of -13.2 mV and $+16.2$ mV, respectively. In both cases the ζ-potential value of the complex was in between that of WPI and the corresponding polysaccharide.

Surface Plasmon Resonance imaging (SPRi) was used to study the mass and interfacial thickness of WPI–GA and WPI–Chi adsorbed to a hydrophobic interface that mimics an O–W interface in a real emulsion. Hydrophilic emulsifiers studied were 0.5%wt WPI – 0.5%wt GA at pH 4.8 and 0.5%wt WPI – 0.05%wt Chi at pH 5.4 (Table 3.2). Figure 3.3 shows the progress of mass adsorption and mass desorption of the hydrophilic emulsifiers over time. After injection, both WPI–
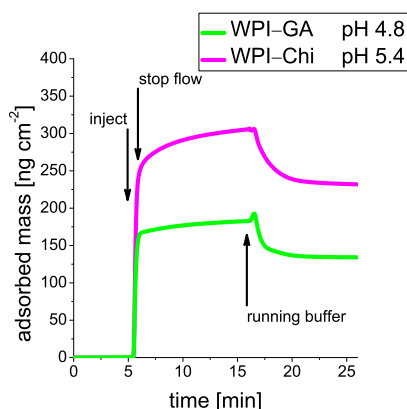
Chapter 3

Figure 3.3: Progress of the adsorbed amount of hydrophilic emulsifier measured by SPRi after applying 0.5%wt WPI−0.5% GA (—) and 0.5%wt WPI−0.05% Chi (—).

GA and WPI–Chi directly adsorbs to a large extend to the hydrophobic interface. During desorption, non-adsorbed hydrophilic emulsifier is removed by acetic solution (running buffer). The final adsorbed mass of WPI–GA and WPI–Chi was 268 and 464 $ng\,cm^{-2}$, respectively. Data on the thickness of the adsorbed WPI–GA and WPI–Chi was obtained from the difference of reflection of the prism surface at varying laser incident angles before and after adsorption, as in Chapter 2. Interfacial thickness of WPI–GA and WPI–Chi was 3.9 and 4.2 nm, respectively. Table 3.3 shows the mass, thickness and density of the WPI and WPI–CMC layers, as found in Chapter 2 and of the WPI–GA and WPI–Chi layers. According to these results, WPI–polysaccharide complexes were able to build up a thicker but less dense interfacial structure than WPI.

3.3.2 Emulsion properties during premix ME

To produce the $W_1/O/W_2$ emulsions, single W_1/O emulsions with a $d_{4,3}$ of 2.6 μm and span factor of 1.0 were dispersed in the continuous W_2 phase, first by mechanical stirring and second by repeated premix ME. The reduction in size and span of the outer droplets with the number of premix cycles can be seen in Figures 3.4a

Table 3.3: Mass adsorption, thickness and density of four interfacial structures to a hydrophobic surface by SPRi. Where 0.5%wt WPI and 0.5%wt WPI−0.25%wt CMC were measured in Chapter 2 under the same conditions.

hydrophilic emulsifier	pH [-]	mass [ng cm^{-2}]	thickness [nm]	density [g cm^{-3}]
0.5%wt WPI	3.8	155	0.6	2.59
0.5%wt WPI−0.25%wt CMC	3.8	308	2.2	1.40
0.5%wt WPI−0.50%wt GA	4.8	268	3.9	0.69
0.5%wt WPI−0.05%wt Chi	5.4	464	4.2	1.10

and 3.4b. Regardless of the hydrophilic emulsifier considered, a very drastic decrease in $d_{4,3}$ was observed in the first cycle, from about 240 μm to 10 – 25 μm. From cycle 1, all emulsions showed a slight but significant reduction in $d_{4,3}$ with each emulsification cycle, except for those stabilized with WPI–Chi that kept a constant droplet size from the first pass and showed a small decrease in span with each cycle. Regarding WPI–CMC stabilized emulsions, we observed high span values after the first cycle that drastically reduced from cycle two. They may be caused by fluctuations in pressure during the premix ME that can lead to high droplet size dispersion due to different extent of droplet break-up. High pressures as the ones required by WPI–CMC stabilized emulsions (Table 3.1) are more prone to fluctuations. Repeated premix ME reduces this effect and leads to narrow droplet size distributions. Although final values of $d_{4,3}$ and span (Table 3.4) did not show major differences between emulsions stabilized with WPI and those stabilized with WPI–polysaccharide complexes, with droplet sizes around 10 μm, lower dispersion in droplet size was found in emulsions with WPI–Chi. In addition, emulsions stabilized with WPI–GA were more polydisperse than WPI stabilized emulsions.

In terms of encapsulation of procyanidins (Figure 3.4c), we observed that it was reduced from 88 – 96% in coarse emulsions (cycle 0) to 70 – 83% after 3 cycles of premix although most of this reduction occurred during the first cycle. Besides the clear effect of droplet size reduction on encapsulation of procyanidins, the mean size of the outer droplets decreased in much higher extent than the encapsulation did. Droplet size decreased from approximately 240 to 8.2, 9.0, 9.7 and 11.8 μm for emulsions stabilized with WPI–CMC, WPI–Chi, WPI and WPI–GA, respectively. Nevertheless a reduction of 16% was observed in the encapsulation of procyanidins

Chapter 3

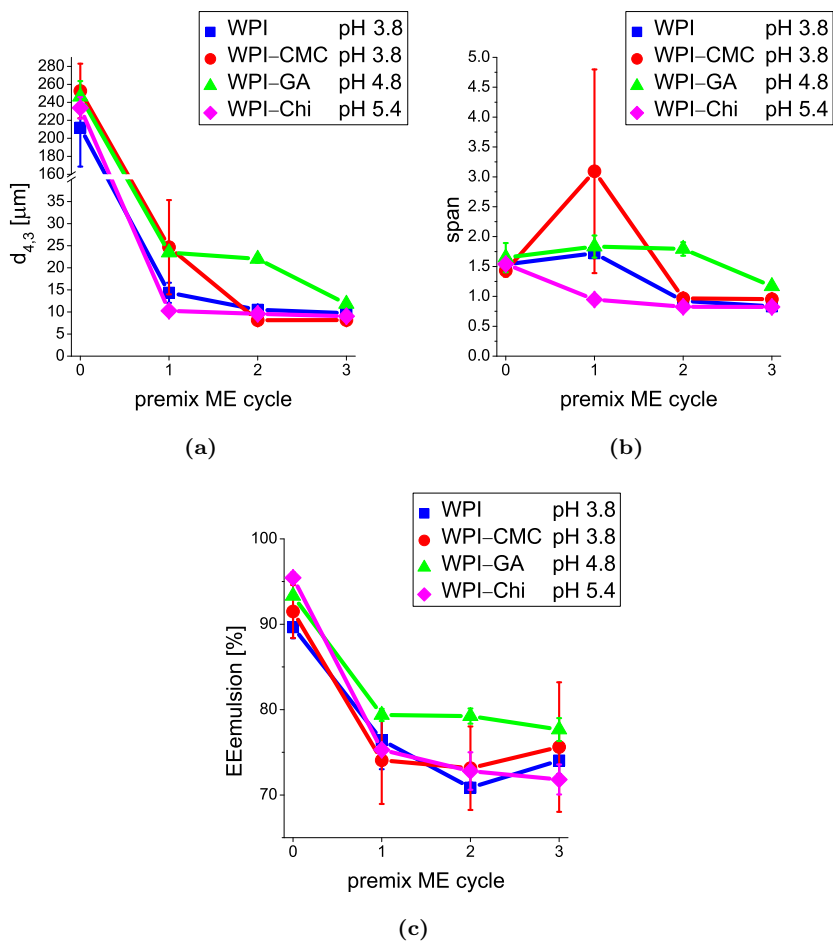**Figure 3.4:** (a) Droplet sizes ($d_{4,3}$), (b) droplet size dispersion (span) and (c) procyanidin encapsulation; for WPI (■), WPI–CMC (●), WPI–GA (▲), and WPI–Chi (◆) emulsions, during the emulsification process from cycle 0 (coarse emulsion) to cycle 3.

during premix ME (from cycle $0-3$) of emulsions stabilized with WPI, WPI–CMC and WPI–GA while those stabilized with WPI–Chi showed a higher reduction of 24%. Similar results were reported by Vladisavljević et al. (2006b) who suggested the volume fractions of inner and outer droplets, viscosity of the continuous phase, transmembrane pressure and the ratio of membrane pore size to inner droplet size determine the final stability of $W_1/O/W_2$ emulsions. According to this, an inner droplet fraction of 0.3 and a membrane pore size (10 μm) more than twice the diameter of the inner droplets (2.6 μm) are feasible operating conditions that would lead to stable emulsions with an encapsulation efficiency in the range of that obtained by Vladisavljević et al. (2006b).

Comparing the results obtained with WPI and the three WPI–polysaccharide complexes, no important differences in encapsulation of procyanidins were observed among them. The interfacial tension of O–W_2 and the continuous phase (W_2) viscosity were determined by the type and concentration of the hydrophilic emulsifier. In the case of WPI–CMC, it significantly increased the W_2 phase viscosity, requiring a much higher transmembrane pressure during premix ME (Table 3.1).

Table 3.4: Properties of freshly produced double emulsions encapsulating procyanidins, stabilized by various hydrophilic emulsifiers at original pH after premix ME (cycle 3). Mean and standard deviation of droplet size distribution, encapsulation efficiency and creaming stability measurements.

	$d_{4,3}$ [μm]	span [–]	Encapsulation [%]	serum thickness [%]	creaming rate [mm h^{-1}]
WPI	9.7 ± 0.0	0.8 ± 0.0	74 ± 2	54 ± 1	1.9 ± 0.1
WPI–CMC	8.2 ± 0.2	1.0 ± 0.0	80 ± 7	45 ± 3	0.4 ± 0.1
WPI–GA	11.8 ± 0.3	1.2 ± 0.0	78 ± 1	45 ± 0	22.6 ± 2.7
WPI–Chi	9.0 ± 0.0	0.8 ± 0.0	72 ± 2	44 ± 3	0.8 ± 0.0

3.3.3 Stability of freshly produced emulsions

To study how the composition of the O–W_2 interface affects the physical stability of fresh $W_1/O/W_2$ emulsions, creaming of the emulsions was monitored during $6-72$ hours after the emulsification process. Table 3.4 shows that the creaming rate of emulsions stabilized with WPI–CMC and WPI–Chi was much lower than those

Chapter 3

of WPI stabilized emulsions while an exceptionally high creaming rate was found for double emulsions stabilized by WPI–GA. Creaming depends on the viscosity of the emulsion, difference in phase densities and the radii of the droplets (r^5) according to Stoke's law for polydisperse systems (Lutz and Aserin, 2007). The viscosity of double emulsions, in turn is governed by the nature and behavior of the biopolymers in the continuous phase solutions, the arrangement of biopolymers at the interface and the water concentration in the continuous phase solution. In our case, the similar microstructure and $d_{4,3}$ of $W_1/O/W_2$ emulsions at day 0 and after 14 days of storage (Figures 3.4 and 3.8) seem to indicate that no significant water transport between inner and outer phases occurred, meaning that W_1 and W_2 concentrations kept constant in all the emulsions. According to this, the lower creaming velocities found in emulsions stabilized with WPI–CMC and WPI–Chi can be explained by differences in the W_2 viscosity. Although we do not have values of continuous phase viscosity, CMC imposed a significant increase that resulted in higher transmembrane pressures to make the $W_1/O/W_2$ emulsions flow through the SPG membrane (Table 3.1).

To better understand the differences in creaming rate observed among the several emulsions, we determined the ζ-potential of freshly produced emulsions (Figure 3.5a). At the original pH, the absolute values of ζ-potential were above 15 mV, with droplets positively charged when stabilized with WPI or WPI–Chi, while negatively charged in WPI–CMC and WPI–GA stabilized emulsions. Although those surface charges and the interfacial thickness (Table 3.3) suggest that electrostatic repulsion and steric hindrance should be able to keep the emulsion stable, it was not the case for WPI–GA emulsions. Probably, droplet interface was not totally covered by the oppositely charged polymer (McClements, 2005, Yuan et al., 2013) and, by bridge flocculation, droplets stuck together, increasing the effective size and accelerating creaming.

Regarding the serum layer, Table 3.4 shows that the layer formed by double emulsions stabilized by WPI was thicker (54%) than that of the double emulsions stabilized with a WPI–polysaccharide complex (44 – 45%). To explain these results, not only the higher viscosity of the emulsions stabilized by WPI–polysaccharide complexes but also their capacity to retain more water between the O–W_2 droplet interfaces, should be considered. SPRi results confirm that the interfacial layer made of WPI–polysaccharide complexes was much thicker than that of WPI.

Figure 3.5a shows how the environmental pH influences the surface charges of the droplets according to the interfacial composition in double emulsions freshly prepared. Double emulsions stabilized with WPI–CMC and WPI–GA at pH 3, and

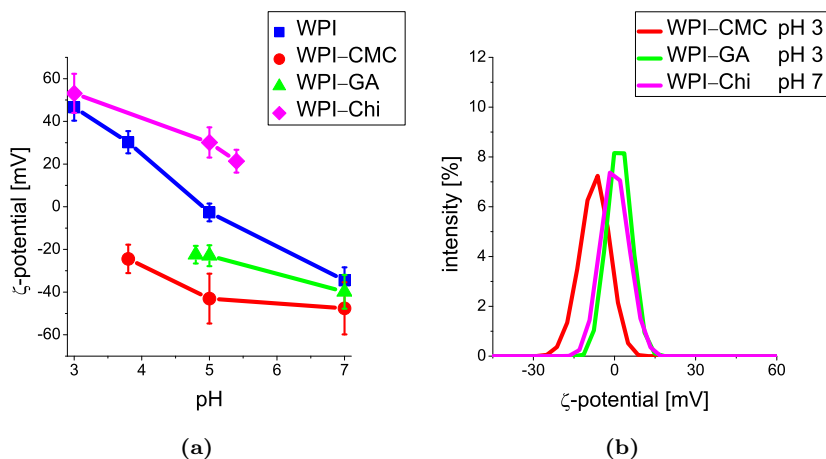Water-in-oil-in-water emulsions encapsulating a procyanidin-rich extract

Figure 3.5: ζ-potential measurements of (a) double emulsions stable at $t = 0$, stabilized by 1%wt WPI (■), 0.5% WPI – 0.25% CMC (●), 0.5% WPI – 0.5% GA (▲), and 0.5% WPI – 0.05% Chi (◆) at various pH (b) complexes of 0.5%wt WPI – 0.25%wt CMC (—), 0.5%wt WPI – 0.5%wt GA (—), and 0.5%wt WPI – 0.05%wt Chi (—) dissolved in acetic acid solution for conditions where double emulsions are unstable at $t = 0$.

with WPI–Chi at pH 7 showed droplet coalescence right after preparation and later phase separation. Measurements of the ζ-potential of these WPI–polysaccharide complexes in solution at each particular pH (Figure 3.5b) showed values close to zero. At these conditions, low repulsive forces between the interface of neighboring emulsions droplets lead to droplet aggregation and subsequently to instabilities such as coalescence.

3.3.4   Emulsion stability during storage

Figure 3.6 shows the progress of $d_{4,3}$ and span factor during 14 days of storage at several pH environments, that is, 3, 5, 7 and the original pH (see Table 3.1). At original pH, all $W_1/O/W_2$ emulsions were stable over time except those stabilized with WPI–GA, which showed a higher increase in droplet size and dispersion dur-
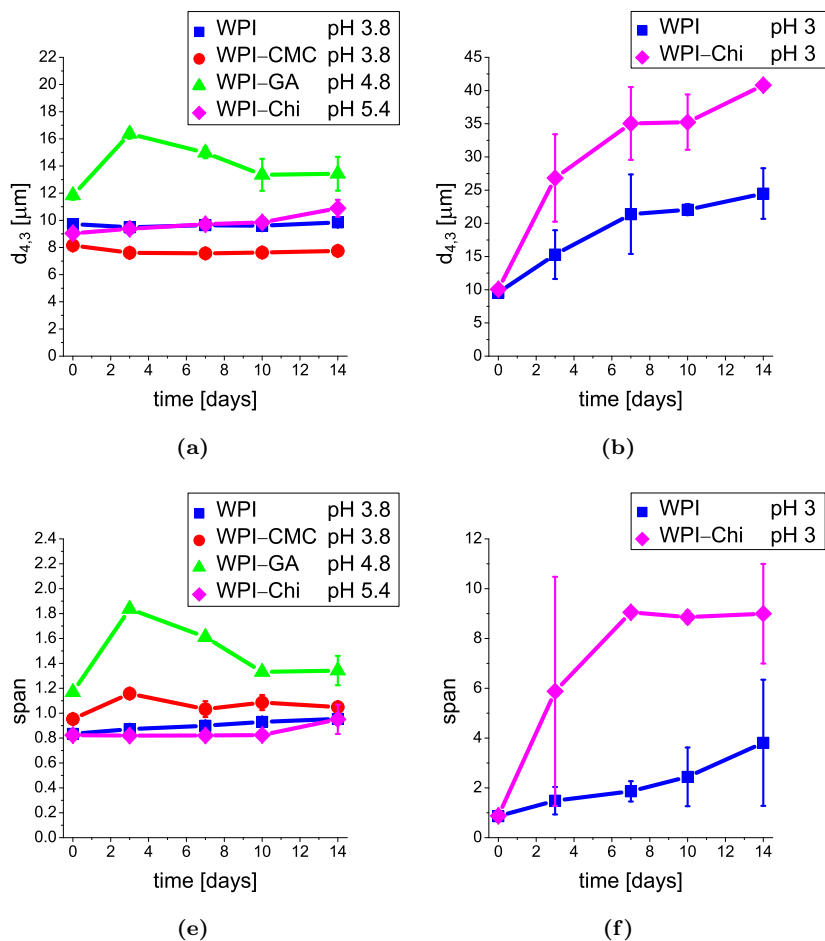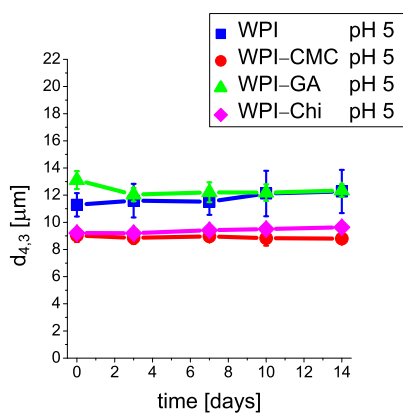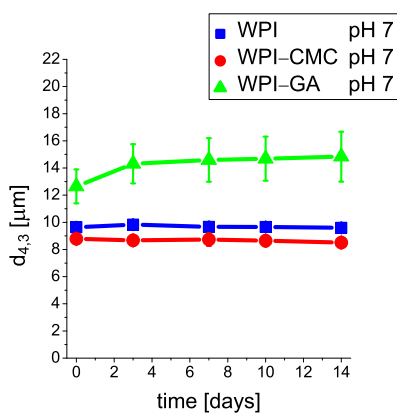
Figure 3.6: Droplet size $(d_{4,3})$ (a–d) and droplet dispersion (span) (e–h) measurements over time at (a,e) original pH, (b,f) pH 3, (c,g) pH 5, and (d,h) pH 7; of WPI (■), WPI-CMC (●), WPI-GA (▲), and WPI-Chi (◆) stabilized double emulsions.
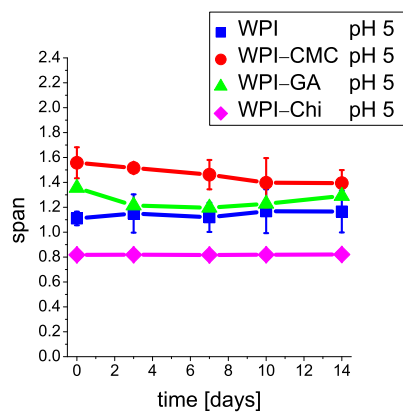
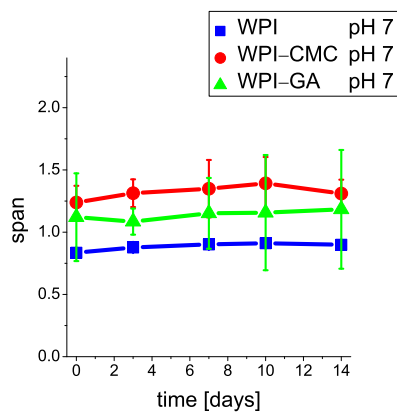Water-in-oil-in-water emulsions encapsulating a procyanidin-rich extract

(c)   **(d)**

(g)   **(h)**

ing storage. As aforementioned, bridge flocculation would explain the instability of WPI–GA stabilized emulsions, already observed in freshly produced emulsions which showed a very high creaming rate. When using WPI complexed to anionic polysaccharides (CMC and GA), $d_{4,3}$ and span did not significantly change during storage at pH values of 5 and 7. Emulsions stabilized by WPI–CMC and WPI–GA at pH 3 directly broke up at day 0, showing phase separation after few days, this instability can be explained by the low repulsive forces between the droplets as ζ-potential of the hydrophilic emulsifier is near zero (Figure 3.5b). Furthermore, the state diagram of WPI–GA (Figure 3.1a) shows that when reducing the pH from 4.8 to 3, the solution goes through the 2 phase region where WPI and GA form an insoluble complex with poor properties as emulsifier. At those conditions, droplet interactions are expected to take place through bridging, due to simultaneous interactions of polysaccharide molecules with the surface of two or more neighboring droplets. At higher pH values, the electrostatic interactions responsible for WPI–GA complex seem not to be substantially modified by the increase in the negative charge of WPI, as the minor changes in droplet size distribution show.

A different behavior was observed in $W_1/O/W_2$ emulsions stabilized with WPI–Chi complex, in which Chi is a cationic polymer: at pH 7 emulsions directly broke up at day 0, showing phase separation after few days. The neutral interfacial charge of the hydrophilic emulsifier (Figure 3.5b) appears to be the cause of emulsion instability. Furthermore, the state diagram of WPI–Chi (Figure 3.1b) shows that when increasing the pH from 5.4 to 7, the solution goes through the 2 phase region where WPI and Chi form an insoluble complex with poor emulsifier properties. At pH 5, the monodisperse WPI–Chi emulsions (span factor about 0.8) kept their properties over time, while a decrease of pH to 3 led to a fast increase in $d_{4,3}$ and span during storage. The emulsion instability at pH < 5 would be caused by a net repulsive effect between adsorbed WPI and Chi from aqueous phase, both having a net positive charge. According to Figure 3.1b no soluble complexes are formed (Transmission $> 81\%$), consequently, non-adsorbed Chi would favor depletion flocculation leading to a decrease in stability during storage (Laplante et al., 2005b). At pH values between 5 and 5.4 the higher emulsion stability is explained by the predominance of electro-attractive forces (electrostatic complexation) between adsorbed WPI proteins (negatively charged at a pH value above the isoelectric point) and Chi (positively charged) that lead to the complex formation. In addition, emulsion droplets were positively charged, with ζ-potential values of $+30$ and $+22$ mV at pH of 5 and 5.4, respectively, suggesting electrostatic repulsion as a mechanism for emulsion stabilization.

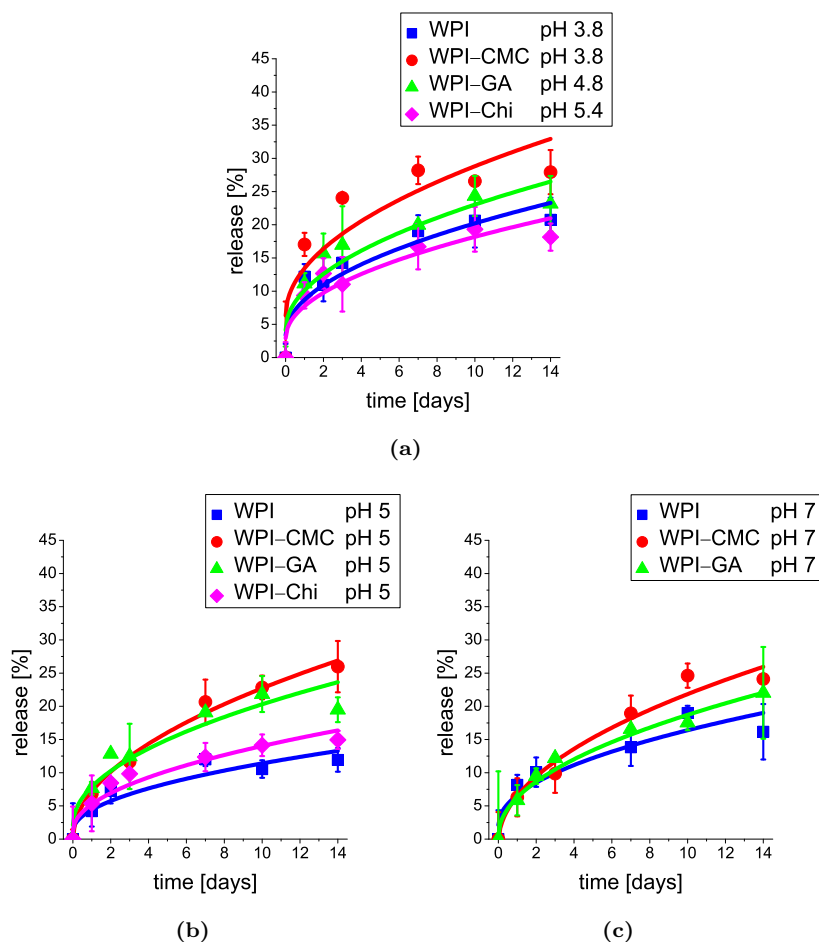Water-in-oil-in-water emulsions encapsulating a procyanidin-rich extract

Figure 3.7: procyanidin release over time (release [%]) fitted with Higuchi's model $(K_H t^{0.5})$ measurements over time at (a) original pH, (b) pH 5, and (c) pH 7; of WPI (■), WPI-CMC (●), WPI-GA (▲), and WPI-Chi (◆) stabilized double emulsions.

Chapter 3

3.3.5 Kinetics of procyanidin release

To determine how the type of hydrophilic emulsifier affected the encapsulating capacity of $W_1/O/W_2$ emulsions, we determined procyanidin release during 14 days of storage at different pH conditions (Figure 3.7). To minimize the contribution of the osmotic imbalance to procyanidin release and water transport, we adjusted the composition of W_1 and W_2 (Table 3.2). The osmotic pressure values of W_1 and W_2 were 121 ± 8 and 21 ± 8 mOsm kg^{-1}, respectively. Considering a minor effect of the Laplace pressure from the curvature of the droplets, the osmotic pressure gradient between W_1 and W_2 was 100 ± 11 mOsm kg^{-1}. According to previous studies about the role of the osmotic gradient in water transport and release of entrapped compounds (Bjerregaard et al., 1999, Wen and Papadopoulos, 2001), significant changes in droplet size distribution and rate of drug release occurred at osmotic pressure gradients one order of magnitude higher than those measured in the emulsions considered in the present work. Additionally, the emulsion microstructure after 14 days of storage (Figure 3.8) with no significant changes on W_1 droplets supports a negligible impact of the low osmotic imbalance on water transport.

The release of entrapped compounds from the inner phase of double emulsions is known to occur by three different mechanisms (Lutz et al., 2009):

i) rupture or 'break-down' of the double emulsion by swelling or under shear and the resulting leaking of the inner phase content into the outer phase

ii) 'thinning the liquid film' between the internal droplets and the outer interface followed by its rupture

iii) 'diffusion', through which the double emulsions remain intact but the entrapped compounds cross a very thin lamella either by diffusion of the emulsifier or by reverse micelle transport.

If the mechanisms of 'break-down' or 'thinning the liquid film' were involved, a decrease in the outer droplet size would be expected that had to be reflected also in the microscopic images showing empty droplets. In Figure 3.8, it can be seen how all $W_1/O/W_2$ emulsions show visible inner water droplets after 14 days of storage, while $d_{4,3}$ of the outer droplets did not decrease nor increase substantially over time for any of the emulsions investigated (Figure 3.6). Based on these results, we concluded that the procyanidin release is diffusion controlled and, therefore, used Higuchi's model to describe procyanidin release. The progress of procyanidin content in W_2 was fitted to Equation 3.7 and the release rate constant was calculated for each emulsion and storage pH (Table 3.5).

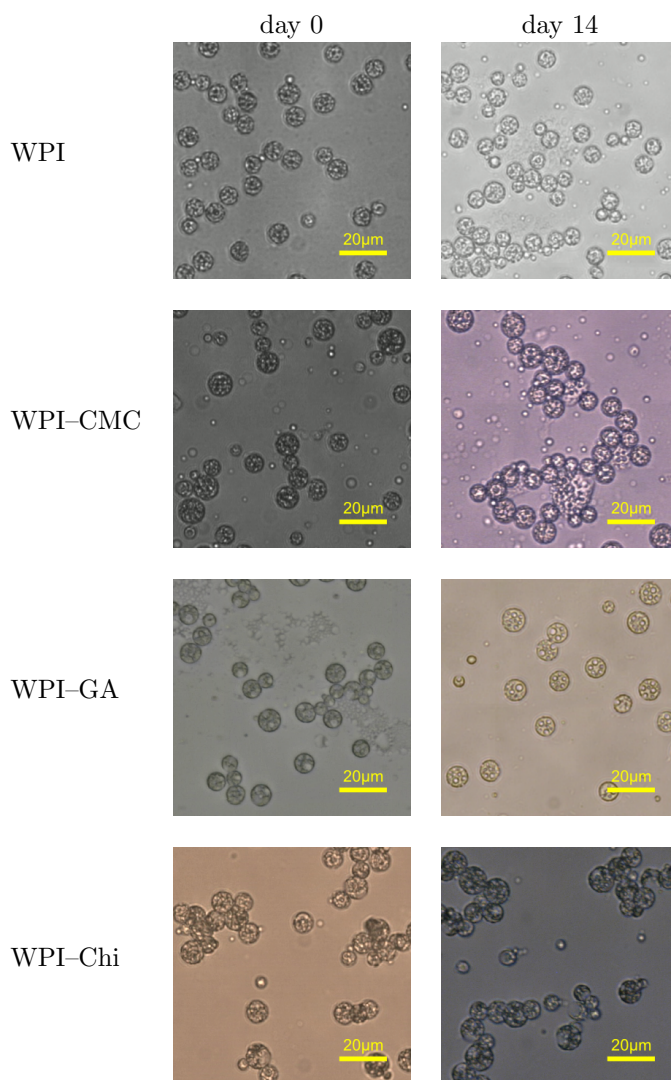Water-in-oil-in-water emulsions encapsulating a procyanidin-rich extract

Figure 3.8: Microscopic images of double emulsions at day 0 and after 14 days of storage for the 4 different hydrophilic emulsifiers.

Chapter 3

Table 3.5: Release rate constants (K_H mean and standard deviation in [μg mL^{-1}min$^{-0.5}$]) of double emulsions stabilized with WPI, WPI–CMC, WPI–GA, and WPI–Chi obtained from release data over 14 days of storage at original pH, pH 5, and pH 7, fitted with Higuchi's model ($K_H t^{0.5}$). Values with a different letter (a–d) with the same pH are significantly different (p < 0.05). Values with a different letter (x–z) with the same hydrophilic emulsifier are significantly different (p < 0.05).

	original pH			pH 5		pH 7	
	K_H	R^2	pH	K_H	R^2	K_H	R^2
WPI	7.8 ± 1.0^{az}	0.8	3.8	5.0 ± 1.0^{ax}	0.6	6.3 ± 1.0^{ay}	0.7
WPI–CMC	11.3 ± 2.0^{bx}	0.7	3.8	10.5 ± 0.8^{bx}	0.9	10.6 ± 1.0^{bx}	0.9
WPI–GA	9.2 ± 1.4^{cx}	0.7	4.8	8.8 ± 1.0^{cx}	0.8	8.5 ± 1.6^{cx}	0.7
WPI–Chi	6.9 ± 0.8^{dy}	0.7	5.4	5.6 ± 0.7^{dx}	0.7		

Although relatively low correlation coefficients (R^2 values between 0.6 and 0.9) have been found mainly because of the dispersion in experimental data, Higuchi's model seemed to describe well the release of procyanidins. To support this, we should take into account that emulsions stabilized with a particular emulsifier, i.e. WPI–CMC or WPI–GA, showed no significant differences in the release rate constants regardless of the storage pH. Contrary, significant differences in the release rate constants were found among emulsions stabilized by the three WPI–polysaccharide emulsifiers (WPI stabilized double emulsions will be discussed later). WPI–CMC, independently of pH, gave significantly the highest release rate constant with values from 10.5 to 11.3 μg mL^{-1}min$^{-0.5}$, followed by WPI–GA with a release rate constant between 8.5 and 9.2 μg mL^{-1}min$^{-0.5}$. WPI–Chi stabilized double emulsions showed the lowest release rate constants, 5.6 and 6.9 μg mL^{-1}min$^{-0.5}$. Jiménez-Alvarado et al. (2009) used the same model to study the release of ferrous bisglycinate from double emulsions stabilized with whey protein concentrate complexed to gum Arabic, mesquite gum, and low methyl pectin. They found release rate constants between 90 and 450 μg mL^{-1}min$^{-0.5}$, that is one or two order of magnitude higher than those found in the present emulsions. Release rate clearly depends, among other factors, on the encapsulated addenda: small molecules (such as ferrous bisglycinate) show higher diffusion coefficients than larger molecules (such as the trimers up to pentamers mainly present in the

encapsulated procyanidin extract). Furthermore, droplet sizes and dispersion play a large role, large droplets have lower surface area and thus lower release rates.

In the case of emulsions stabilized with WPI–polysaccharide complexes, the obtained release rate constants correlate with the thickness of the interfacial layer determined in SPRi measurements (Table 3.3): thicker interfacial layers led to lower release rate constants. These results support the assumption that diffusion is the main mechanism controlling procyanidin release, and confirm the use of WPI–polysaccharide complexes to obtain thicker interfacial layers as an effective strategy to better retain hydrophilic compounds in the inner water phase of $W_1/O/W_2$ emulsions. Among the different WPI–polysaccharide complexes investigated, WPI–Chi stabilized double emulsions showed the best performance in terms of emulsion stability and their capacity to reduce the release rate of procyanidins at a certain pH range.

The release rate of double emulsions stabilized with single WPI at pH 3.8. followed a different pattern: they show a relatively low value of the release rate constant ($5.0 - 7.8$ $\mu g \, mL^{-1} min^{-0.5}$), while having the thinnest layer compared to WPI–polysaccharides. For these emulsions, interactions between the entrapped procyanidins and WPI of the interfacial layer could explain their capacity to entrap procyanidins with a thinner interface. According to several authors, procyanidins spontaneously bind different kind of globular proteins, such as α-lactalbumin, lysozyme, bovine serum albumin, lysozyme, and WPI (Prigent et al., 2009, Liang et al., 2013, Thongkaew et al., 2014). Polysaccharides like GA and pectin, in contrast, have been found to prevent the association of proteins with procyanidins, what would suggest that interfaces made of WPI–polysaccharides would not bind procyanidins at the same extent as single WPI interfaces could do (Liang et al., 2013, Thongkaew et al., 2014). Further research on how the interfacial properties influence the kinetics of procyanidins release should be investigated in order to design systems of encapsulation adapted to each particular application.

3.4   Conclusions

Premix membrane emulsification enabled to produce procyanidin-loaded $W_1/O/W_2$ emulsions with narrow droplet size distributions, stabilized with several WPI–polysaccharide soluble complexes, such as, WPI–CMC, WPI–GA and WPI–Chi. The encapsulation of procyanidins was at least 70% at the end of the emulsification process for all the systems considered. This encapsulation decreased with each premix ME cycle, mainly linked to the escape of the inner W_1 phase

as a result of the break-up of W_1/O droplets. Even though no important differences in the procyanidin encapsulation were observed among emulsions stabilized with WPI–polysaccharide complexes, data about the shear stress in the membrane pores would help to better determine the effect of those on the break-out of inner W_1 droplet.

Stability of $W_1/O/W_2$ emulsions, encompassing creaming rate, droplet size distribution and procyanidin release during storage, was affected by the type of WPI–polysaccharide complex used as emulsifier. In the case of creaming rate, the viscosity imposed by each WPI–polysaccharide complex to the W_2 phase was a parameter to consider. The progress of the droplet size distribution during storage, in turn, was affected by pH, due to its influence on the surface charge of emulsion droplets as well as on the interactions between WPI and each polysaccharide. Hence, different windows of pH values, in which emulsions kept droplet size distribution stable, were identified for each WPI–polysaccharide complex. Furthermore, release rate constants during 14 days of storage ranged from 5.6 to 11.3 $\mu g\,mL^{-1}min^{-0.5}$ and depended more on the type of hydrophilic emulsifier than on pH environment. When the release rate constants were related to the thickness of the interfacial layer made of WPI–polysaccharides obtained by SPRi measurements, we observed that thicker layers led to lower release rates. Further research on the relationship between the properties of tailor-made interfaces with the diffusion of entrapped bioactive compounds is required to optimize each particular application of $W_1/O/W_2$ emulsions as encapsulating systems.

4

Spray dried water-in-oil-in-water emulsions containing procyanidin-rich extracts

Abstract

Spray drying of procyanidin-loaded $W_1/O/W_2$ emulsions produced by premix membrane emulsification (ME) enabled to produce microcapsules containing procyanidins. The interface of the emulsion droplets prior to spray drying was stabilized with several hydrophilic emulsifiers (whey protein (WPI), WPI–Carboxylmethyl cellulose, WPI–Gum Arabic, and WPI–Chitosan). Their effect on procyanidin encapsulation efficiency, water activity, moisture and oil content, and microcapsule size distribution was investigated. Furthermore, the microstructure and droplet size distribution of redispersed microcapsules were analyzed.

Although premix ME produced $W_1/O/W_2$ emulsions with a narrow droplet size distribution regardless the hydrophilic emulsifier (mean droplet size around 9 μm), microcapsules after spray drying and double emulsions after redispersion showed profound differences in sizes depending on the interfacial composition. WPI–CMC stabilized capsules not only showed the highest procyanidin content but also gave the narrowest particle size distribution with the lowest particle size for both microcapsules and the corresponding emulsions after rehydration. WPI–CMC complex was able to truly stabilize the W_1/O droplets during the different stages of microcapsule production but it moderately retained the migration of procyanidins through the O–W_2 interface. The interfacial properties of $W_1/O/W_2$ emulsions strongly affected the particle size distribution of both microcapsules and double emulsions after rehydration.

4.1   Introduction

Commercializing extracts rich in polyphenols from different sources such as grapes, tea, apple, berries, pomegranate and so on, has become a trend in the food sector. Water soluble grape seed extracts from grape, rich in procyanidins, i.e. oligomers of (−)-epicatechin and (+)-catechin, are available as food ingredients. The numerous scientific reports about the health benefits of a regular intake of foods rich in procyanidins support the formulation of these ingredients in foods and beverages (Shahidi and Naczk, 2003). Nevertheless, the effectiveness of those extracts depends on preserving the stability, bioactivity, and bioavailability of the active ingredients.

Entrapping a sensitive bioactive compound inside another material by microencapsulation is a strategy to improve the stability of phenolic compounds (Fang and Bhandari, 2010). The use of encapsulated polyphenols instead of their free form can protect them from environmental factors such as temperature, oxygen, light and pH and mask their off-flavors, such as astringent or bitter tastes. Water-in-oil-in-water ($W_1/O/W_2$) emulsions are used as a carrier for hydrophilic bioactive compounds by loading them in the inner water phase (W_1). Frank et al. (2012) and Hemar et al. (2010) have encapsulated anthocyanins and resveratrol from grapes in double emulsions, respectively. However, the use of $W_1/O/W_2$ emulsions is not yet widespread because of their low stability during storage compared to single emulsions (O/W or W/O). Spray drying of double emulsions has been suggested as an approach to improve the encapsulation of hydrophilic bioactive compounds by:

- increasing storage stability as W_1/O droplets are immobilized in a solid continuous matrix and, therefore, droplet coalescence and the release of the entrapped compound are limited

- gaining the convenience of powdered ingredients (Adachi et al., 2004, Maisuthisakul and Gordon, 2012).

A possible disadvantage of the encapsulation system is the lower concentration of the bioactive compound in the microcapsule, however, the unique protection offered by the wall might compensate for this (Gouin, 2004).

The production of $W_1/O/W_2$ emulsions involves a two-step process: first, to obtain a W_1/O emulsion and second, to disperse the W_1/O droplets in a W_2 continuous phase. Emulsification techniques, such as colloid mills, rotor-stator systems and high pressure homogenizers, that apply high shear stresses to promote droplet break-up, are often used to produce $W_1/O/W_2$ emulsions. Mem-

Chapter 4

brane emulsification (ME) has proven to be an interesting alternative because it uses lower shear stresses than conventional emulsification technologies, being a key factor to reduce the release of W_1 droplets during the second emulsification step (van der Graaf et al., 2005). Other reasons to use ME rely on its low energy consumption, the good control of droplet size distribution, and the possibility to encapsulate heat sensitive compounds due to low mechanical stresses (Joscelyne and Trägårdh, 2000). In premix ME, large emulsion droplets are pushed several times through a microporous membrane where they break-up into smaller droplets (Nazir et al., 2010). At pressures above the critical pressure, large emulsion droplets are deformed and enter the membrane pores, due to wall shear stresses and droplet collisions, the droplets leave the membrane having sizes around the pore size of the membrane (Vladisavljević et al., 2004).

During the spray drying of double emulsions, $W_1/O/W_2$ emulsion and wall material are mixed, fed into the spray dryer and atomized with a nozzle (Augustin and Hemar, 2009). Drying of the atomized droplets leads to microcapsule formation. Spray drying is used to encapsulate heat sensitive compounds as the rapid water evaporation keeps the temperature of the core low. The retention of the core material during spray drying relies on the physical and chemical properties of the wall and core material, the performance of hydrophilic emulsifiers (e.g. film-forming ability) and the viscosity at high concentration of the wall materials (Madene et al., 2006).

Regarding the film-forming properties of the hydrophilic emulsifiers, soluble electrostatic protein–polysaccharides complexes are able to effectively adsorb on oil-water (O–W) interfaces, often improving the stability of O/W emulsions when compared to those stabilized with single proteins. The ability of those protein–polysaccharide complexes to form composite interfacial structures has suggested their use to enhance the capacity of emulsions for entrapping bioactive compounds in the disperse phase (Dickinson, 2008, 2011b, McClements et al., 2009). In terms of stability against environmental stresses, protein–polysaccharides complexes seem to reduce the impact of thermal processing or drying on emulsion stability, reducing the advers effects of the thermal treatment on the interfacial layers surrounding the oil droplets. Some protein–polysaccharide complexes used as emulsifiers are sodium caseinate–dextran sulfate (Jourdain et al., 2009), bovine serum albumin–dextran sulfate (Dickinson and Semenova, 1992), whey protein–carboxymethyl cellulose (Koupantsis and Kiosseoglou, 2009), whey protein–locust bean gum and whey protein–xanthan gum (Benichou et al., 2003).

The aim of this Chapter was to encapsulate a commercial procyanidin-rich extract in spray dried $W_1/O/W_2$ emulsions produced by premix ME. Besides, we

determined how the emulsion properties affected the characteristics of the final microcapsules, in terms of particle size distribution, encapsulation of procyanidins and microstructure of the solid capsules. Special attention was paid to investigate if the interfacial properties of the O/W_2 emulsions affected the microstructure of the redispersed microcapsules. To do so, whey protein isolate (WPI) and several WPI–polysaccharide complexes were used as hydrophilic emulsifiers to stabilize the $O–W_2$ interface: WPI–carboxymethyl cellulose, WPI–gum Arabic and WPI–chitosan. For producing the microcapsules, maltodextrin was the wall material added to $W_1/O/W_2$ emulsions prior the spray drying step.

4.2 Material and Methods

4.2.1 Materials

Vitaflavan Pur'expert (Purexpert, France), a water soluble commercial grape seed extract, with a reported total polyphenol content above 96% of which 22% are monomers, 19% are dimers and 56% are trimers up to pentamers, was the source of procyanidins encapsulated in the W_1 phase of the double emulsions. Vitaflavan was kindly provided by Quimidroga, S.A. Barcelona, Spain. The oil phase of the emulsions (O) was composed of crude sunflower oil, kindly provided by Cargill S.L.U. (Reus, Spain), and a 4%wt of polyglycerol polyricinoleate (PGPR) (Palsgaard Denmark), a very effective hydrophobic emulsifier.

To obtain the several WPI–polysaccharide complexes that were used as hydrophilic emulsifiers in the W_2 phase, solutions of WPI and each polysaccharide were prepared separately. Solutions (2.0%wt) were obtained by dissolving in distilled water and stirring for 2 h the following compounds: whey protein isolate (WPI) with a reported protein content of 98.1% on dry basis (BiPRO, lot no. JE 034-7-440-6, Davisco Foods International. Inc., Le Sueur, MN) and carboxymethyl cellulose sodium salt (CMC) (code: 332611000, Acros Organics), with a M_w of 250,000 and a degree of substitution (DS) of 0.7, and gum Arabic (GA) from acacia tree (SKU 69752, Sigma-Aldrich Quimica, S.L.). Solutions were kept overnight at 7°C.

A solution of 0.4%wt chitosan (Chi) of low molecular weight (SKU 448869, M_w 150,000, Sigma-Aldrich) was obtained after dissolving and stirring, for 2 h at room temperature, in acetic acid solution. Osmolality was adjusted by preparing all solutions in 0.01 M acetic acid (acetic acid 96%, Panreac) and 0.02%wt sodium azide (NaN_3, Sigma-Aldrich), from here on called acetic solution. For preparing the microcapsules, maltodextrin (SUK 419699, MD, Sigma-Aldrich), with a dextrose

Chapter 4

equivalent 16.5 – 19.5, was used as a wall material. A 75%wt MD solution was obtained after dissolving and stirring, at room temperature, in acetic acid solution.

4.2.2   Methods

Preparation of the WPI–polysaccharide soluble complexes

Aqueous solutions containing 2%wt of WPI were combined with GA, CMC or Chi solutions to obtain the soluble electrostatic complexes with the WPI:polysaccharide mass ratio shown in Table 4.1. All mixtures were made in acetic solution and the pH was adjusted for each WPI–polysaccharide complex according to Table 4.1 (Benichou et al., 2003). Initial WPI and polysaccharide solutions were transparent, upon mixing and pH change, mixtures became turbid without phase separation, suggesting soluble complex formation. To confirm the complex formation at those conditions of pH and WPI:polysaccharide mass ratio, Laser Doppler micro-electrophoresis (Zetasizer Nano ZS, Malvern Instruments), was used. To determine the ζ-potential of WPI, GA, Chi and WPI–CMC, WPI–GA, WPI–Chi complexes in solution, pH was adjusted to different values (Table 4.1) and samples were centrifuged at 1000 G for 30 min to remove impurities. After that, the ζ-potential distribution of each of them was measured. All reported ζ-potential values are an average of six measurements and were calculated by the Smoluchowski equation. All measured ζ-potential distributions were monomodal, confirming that all WPI–polysacharide complexes were truly formed (Table 4.1).

Table 4.1: Hydrophilic emulsifiers used to stabilize the O–W$_2$ interface (composition, pH, ζ-potential) and transmembrane pressure during premix ME

	hydrophilic emulsifier	pH	ζ-potential [mV]	ΔP_{tm} [kPa]
WPI	1.0%wt WPI	3.8	$+18.7 \pm 5.1$	175 ± 25
WPI–CMC	0.5%wt WPI$-$0.25%wt CMC	3.8	-24.3 ± 7.5	750 ± 50
WPI–GA	0.5%wt WPI$-$0.50%wt GA	4.8	-20.1 ± 4.4	250 ± 50
WPI–Chi	0.5%wt WPI$-$0.05%wt Chi	5.4	$+38.5 \pm 5.0$	300 ± 50

Production of $W_1/O/W_2$ emulsions by premix ME

$W_1/O/W_2$ emulsions were produced by first preparing a water-in-oil (W_1/O) emulsion that was subsequently dispersed in the outer water phase (W_2). The primary W_1/O emulsion was obtained by initially mixing the inner water phase (15 g) with the oil phase (35 g) by rotor-stator homogenization (Ultra Turrax, IKA$^{™}$ T18 basic) at 11,000 rpm for 5 min. The inner water phase contained 10%wt vitaflavan in 0.01 M acetic solution while the oil phase was crude sunflower oil with 4%wt of PGPR (lipophilic emulsifier). At these conditions we obtained a monodisperse W_1/O emulsion with a $d_{4,3}$ of 2.6 μm and a span factor of 1.0.

To finally disperse the (W_1/O) emulsion in W_2, we used a two-step emulsification process. First, a coarse emulsion was prepared by adding 40 g of W_1/O emulsion to 160 g of W_2 phase containing 0.01 M acetic solution and a hydrophilic emulsifier (see Table 4.1). The system was mixed with a magnetic stirrer at 1600 rpm for 5 min. Second, a fine dispersed emulsion was prepared by repeated premix ME. The coarse emulsion was loaded into a high-speed mini kit (SPG Technology Co., Japan) equipped with a hydrophilic Shirasu porous glass (SPG, SPG Technology Co., Japan) membrane of 10 μm pore size (membrane dimensions were 125 mm $\times$ 10 mm $\times$ 0.8 mm) and forced through the membrane with nitrogen gas, adjusting the transmembrane pressure for each emulsion (see Table 4.1). This procedure was performed up to 3 times, from cycle 1 to 3, to progressively reduce the mean droplet size and improve droplet size dispersion of the final double emulsion.

Finally, maltodextrin was added to W_2 to obtain an oil phase to wall material ratio of 1:3. To do so, 84 g of 75%wt maltodextrin water solution were added to 150 g of freshly prepared $W_1/O/W_2$ emulsion and gently stirred till homogeneously mixed. The final composition of the double emulsions prior to spray drying is shown in Table 4.2.

Table 4.2: Phase fractions of emulsions prior to spray drying, composition of each phase fraction W_1, Oil, W_2, and wall material (wm). Acetic solution contains 0.01 M acetic acid and 0.02%wt sodium azide.

fraction	phase	composition	medium
3.8%wt	W_1	vitaflavan (10%wt)	acetic solution
9.0%wt	Oil	PGPR (4%wt)	crude sunflower oil
51.3%wt	W_2	hydrophilic emulsifier	acetic solution
35.9%wt	wm	maltodextrin (75%wt)	acetic solution

Chapter 4

Spray drying of double emulsions

The double emulsions were spray dried using a Mini Spray Dryer B-290 (Büchi technology, Switzerland) that was equipped with a two fluid nozzle of 0.7 mm. The operation conditions in the spray dryer were air inlet and outlet temperatures of 170 and between 80 and 90°C, respectively, and an emulsion flow rate of 8 – 15 mL min^{-1}. Emulsions in the feed reservoir were gently stirred to ensure homogeneity of the oil droplet distribution. The yielded dried powder was collected from the cyclone and the recovery chamber, and was stored in airtight containers with nitrogen gas as headspace. Experiments were performed in duplicate.

Microstructure imaging

The outer morphology of the microcapsules was characterized by electronic microscopy. An environmental scanning electron microscope (FEI Quanta 600 ESEM) was used to analyze the surface morphology of the dried powders. The microcapsules were mounted on cylindrical stubs coated with conductive carbon tape to study their outer morphology. Digital images were taken at an accelerating voltage of 20 kV and magnification of ×900.

Optical microscopy (Leica DM 2500) was used to visualize the microcapsule structure after redispersion in acetic solution.

Droplet and microcapsule size distribution

Size distribution of both emulsion droplets and microcapsules was measured by laser diffraction (Mastersizer 2000, Malvern Instruments) supplemented with a Hydro 2000SM or a Scirocco 2000 dispersion unit, respectively. To measure droplet size distributions of: freshly prepared double emulsions (cycle 3) and redispersed microcapsules, Hydro 2000SM dispersion unit was filled with distilled water as continuous phase, stirring speed was set at 1400 rpm, and laser obscuration was between 10 – 15%. Refractive index (RI) of both phases (W_2 and W_1/O) was measured by a refractometer (Digital Abbe Refractometer-WAY–1S, 315). The refractive indices applied were 1.33 for distilled water and 1.46 for the W_1/O droplets, at 25°C. To determine the size distribution of microcapsules after spray drying, Scirocco 2000 dispersion unit used a vibration feed rate of 50% and dispersive air pressure of 1 bar.

The angular scattering intensity data was then analyzed, using the Mie theory of light scattering, to calculate the size of the droplets or microcapsules responsible for creating the scattering pattern. Mean droplet or particle size and dispersion

were calculated as the volume-weighted mean diameter ($d_{4,3}$) and the relative span factor (span). Each determination was performed in triplicate and the data were reported as averages.

Water activity of microcapsules

The water activity (a_w) of microcapsules was measured using an electric hygrometer (Novasina IC-500 AW-LAB, Novasina). A sample dish was carefully filled halfway with microcapsules, measurements were performed at room temperature and the results were recorded after the equilibrium was reached.

Moisture content of microcapsules

The moisture content of microcapsules was determined by the Karl Fischer titration method with a TitroMatic 1S Karl Fischer instrument (Crison Instruments S.A., Spain), using solvent and titrant for Karl Fischer (Aquametric, Panreac Spain). A sample of 0.2 g of microcapsules was dissolved in the solvent and was automatically titrated till the drift was below 30 μL min^{-1}. Moisture content was calculated through a water standard (Hydranal$^{®}$-Water Standard 10.0, Fluka) and expressed as mass per 100 g of powder (wet basis). Each determination was done in triplicate.

Total oil content of microcapsules

The total oil content of the microcapsules was analyzed gravimetrically by n-hexane extraction based on Richardson method (Richardson, 1985) and modified by Ramakrishnan et al. (2013) and expressed as mass per 100 g of powder (wet basis). A sample of 2 g microcapsules was dissolved in a solution containing 20 g of distilled water and 2 mL of ammonium hydroxide solution 25% (Sigma-Aldrich). The mixture was stirred for 20 min to ensure microcapsule redispersion and emulsion breaking. Hereafter, 35 mL of n-hexane 95% (Panreac) were added and the mixture was shaken for 3 min to completely dissolve the oil phase into the hexane. The mixture was left to phase separate then the organic fraction was vacuum evaporated at 60°C (Heidolph VV Micro rotary evaporator, Heidolph Instruments, Germany) and the remaining oil was weighted. The water phase was stored at 6 ± 2°C for further analysis of the procyanidin content.

Procyanidin content of microcapsules

The procyanidin content of microcapsules was determined by Folin-Ciocalteu's method (Singleton and Rossi, 1965). An aliquot of 50 μL, from the water phase previously obtained during the determination of total oil content, was diluted in 5 mL of distilled water and 1.5 mL of this were mixed with 20 μL of Folin-Ciocalteu's reagent (Panreac) and 20 μL of 30% NaOH solution. After 5 min, absorbance was measured spectroscopically (DR 5000 Hach Lange) at 660 nm. Concentration of procyanidin was calculated by a previously determined calibration curve with known amounts of Gallic Acid 1-hydrate (Panreac) as standard. Results were expressed as mass per kg of powder (wet basis).

Encapsulation efficiency of procyanidins in $W_1/O/W_2$ emulsions and microcapsules

Encapsulation of procyanidins in $W_1/O/W_2$ emulsions was expressed as the mass of procyanidins that remained encapsulated within the W_1 droplets over the total mass of procyanidins initially introduced in the inner water phase after 3 emulsification cycles (n = 3). It was assumed that, during the production of the double emulsions, the procyanidins mainly escape through the loss of inner water droplets (Vladisavljević et al., 2006b). Therefore encapsulation can be expressed as:

$$\frac{EEemulsion}{100} = \frac{m^0_{p,W_1} - m^n_{p,W_2}}{m^0_{p,W_1}} = \frac{m^0_{W_1} + m^0_{W_2} - m^n_{W_2}}{m^0_{W_1}} \qquad (4.1)$$

where m^0_{p,W_1} is the initial procyanidin mass in the inner water phase, m^n_{p,W_2} the procyanidin mass in the outer water phase after 3 cycles the premix ME, $m^0_{W_1}$ the initial mass of the inner water phase, $m^0_{W_2}$ the initial mass of the outer water phase, and $m^n_{W_2}$ the mass of the outer water phase after 3 cycles of premix ME. The concentration of procyanidins that is measured in the outer water phase can be calculated as:

$$m^n_{p,W_2} = C^n_{p,W_2}\left(m^0_{W_1}\left(1 - \frac{EEemulsion}{100}\right) + m^0_{W_2}\right) \qquad (4.2)$$

where C^n_{p,W_2} is the concentration of procyanidins in the outer water phase after 3 cycles of premix ME which was determined by Folin-Ciocalteu's reagent. Substitution of Equation 4.2 into 4.1 gives:

$$EEemulsion = \frac{m^0_{p,W_1} - C^n_{p,W_2}\left(m^0_{W_1} + m^0_{W_2}\right)}{m^0_{p,W_1} - C^n_{p,W_2}m^0_{W_1}} \times 100 \qquad (4.3)$$

Encapsulation of procyanidins in microcapsules was calculated as:

$$EE\mu capsule = \frac{C^{total}_{p,\mu capsule} - C^{wall}_{p,\mu capsule}}{C^{total}_{p,\mu capsule}} \times 100 \qquad (4.4)$$

where $C^{total}_{p,\mu capsule}$ is the procyanidin content in microcapsules and $C^{wall}_{p,\mu capsule}$ is the procyanidin content in the microcapsule wall.

To calulate $C^{wall}_{p,\mu capsule}$, first, microcapsules were redispersed with distilled water at room temperature, samples were gently agitated until no powder particles were visually evident. Subsequently, an aliquot of 1.5 mL of the redispersed microcapsules was centrifuged (Biocen 22R, rotor RT 223, Orto Alresa) at 15 G to separate W_2 phase from W_1/O phase and 50 μL of W_2 phase were diluted in 25 mL of distilled water. The aforementioned Folin-Ciocalteu's method was followed to determine the procyanidin content in the W_2 phase.

Statistical analysis

Data from moisture, total oil and procyanidin content of microcapsules and encapsulation efficiency of emulsions and microcapsules was analyzed using one-way analysis of variance (ANOVA) followed by the protected Fisher's LSD method to establish the significance of differences among the mean values at $p < 0.05$.

4.3   Results

4.3.1   Properties of spray dried double emulsions

The encapsulation of a water soluble extract of procyanidins was tackled by spray drying $W_1/O/W_2$ emulsions. Considering the limited storage stability of $W_1/O/W_2$ emulsions and the convenience of solid food ingredients, a spray drying step was performed to produce solid microcapsules. For obtaining the emulsions, we used the same formulation (see Table 4.2) but modifying the type and concentration of hydrophilic emulsifiers: single WPI versus three soluble WPI–polysaccharide complexes (see Table 4.1). Regarding the emulsification process,

rotor-stator homogenization combined with multistage premix ME (3 cycles) enabled to produce stable double emulsions. The type and pore size of the membrane was kept constant for all emulsifications while the transmembrane pressure was set up for each emulsion according to the kind of hydrophilic emulsifier (Table 4.1). During premix ME higher transmembrane pressures were required for WPI–polysaccharide complexes used as emulsifier, even though the total amount of emulsifier was equal or lower than that of WPI-stabilized emulsions, especially in the case of WPI–CMC they increased the viscosity of the W_2 phase.

After producing $W_1/O/W_2$ emulsions, microcapsules were obtained by adding wall material and subsequent spray drying. Maltodextrin was used as wall material with a 1:3 oil to wall material ratio and finally $W_1/O/W_2$ emulsions were spray dried using the same operating conditions for all emulsions. In terms of microcapsule final properties, we observed that moisture content ranged from 5.6% to 7.5% for WPI–polysaccharide spray dried emulsions (Table 4.3), showing that the presence of a polysaccharide in the emulsifier at these low concentrations slightly affects the drying behavior. In terms of a_w, we observed that microcapsules from emulsions stabilized with WPI–polysaccharide showed slightly lower values (between 0.26 and 0.29) than those of microcapsules from WPI stabilized emulsions (0.34), due to the lower capacity of proteins in binding water. Higher differences in oil content were determined among microcapsules from $W_1/O/W_2$ emulsions stabilized by different emulsifiers, even though we should consider that they were calculated in wet basis and, in turn, affected by the slight variations in moisture content.

Table 4.3: Water activity (a_w), moisture and oil content in microcapsules stabilized by various hydrophilic emulsifiers. Mean and standard deviation with a different letter (a–c) are significantly different ($p < 0.05$).

	a_w [-]	moisture [%]	oil [%]
WPI	0.34	6.2 ± 0.4^b	9.1 ± 0.5^c
WPI–CMC	0.28	5.6 ± 0.1^a	4.2 ± 0.5^a
WPI–GA	0.26	6.0 ± 0.3^{ab}	4.9 ± 1.0^{ab}
WPI–Chi	0.29	7.5 ± 0.2^c	6.6 ± 0.2^b

Table 4.4 shows the procyanidin content in microcapsules and in the microcapsule wall. Although the microcapsules with the highest procyanidin con-

Table 4.4: Procyanidin content in microcapsules and in the microcapsule wall and encapsulation efficiencies of procyanidins of freshly produced emulsions and microcapsules stabilized with various hydrophilic emulsifiers. Mean and standard deviation with a different letter (a–c) are significantly different ($p < 0.05$).

	emulsion	microcapsule		
	$EEemulsion$ [%]	$C_{p,\mu capsule}^{total}$ [g kg^{-1}]	$C_{p,\mu capsule}^{wall}$ [g kg^{-1}]	$EE\mu capsule$ [%]
WPI	68.0 ± 1.2^a	3.8 ± 0.2^a	0.9 ± 0.1^b	76.0 ± 8.9^a
WPI–CMC	71.8 ± 0.5^b	5.3 ± 0.2^b	1.3 ± 0.0^c	75.8 ± 5.9^a
WPI–GA	73.5 ± 2.7^b	3.8 ± 0.3^a	1.0 ± 0.0^b	72.5 ± 8.1^a
WPI–Chi	73.5 ± 1.8^b	3.6 ± 0.2^a	0.7 ± 0.0^a	79.9 ± 6.5^a

tent were those obtained from WPI–CMC stabilized emulsions (5.3 g kg^{-1}), they also presented the highest values of procyanidin content in the microcapsule wall (1.3 g kg^{-1}). $C_{p,\mu capsule}^{wall}$ measures the amount of 'free procyanidins' in spray dried emulsions and is defined as that part of procyanins that can be extracted with water after rehydrating solid microcapsules, that is, those procyanidins not retained in the W$_1$ phase. To better analyze if procyanidins were truly entrapped in the W$_1$ phase, we calculated the encapsulation efficiency of procyanidins in microcapsules (see equation 4.4) similarly to the oil encapsulation efficiency in single microcapsules, that is, reflecting the presence of 'free procyanidins' on the particle matrix within the powder. According to these results, we did not observe significant differences in the amount of encapsulated procyanidins regardless the emulsifier (WPI–polysaccharide complex or WPI) used. For all cases, $EE\mu capsule$ ranges from 72.5% to 79.9%, showing that this percentage of procyanidins was retained in W$_1$ after microcapsule rehydration. Values in the same range were obtained by Rodríguez-Huezo et al. (2004) when spray drying double emulsions containing carotenoids which had similar formulation to those used in the present work.

Particle size distribution showed important differences regarding the type of spray dried emulsion (Figure 4.1). Mean particle size ($d_{4,3}$) was 25.0, 18.7 and 50.1 μm for WPI, WPI–CMC and WPI–GA spray dried emulsions, respectively, while the span factor ranged from 1.6 to 5.7. Microcapsules from WPI–GA stabilized emulsions were very polydisperse with a flat peak in the region of 18 μm

and a heavy tail that moves up to 600 μm. Contrary, spray dried WPI–CMC emulsions show a monomodal and symmetric particle distribution with a narrow peak at about 18 μm.

All microcapsules exhibited an outer topography characterized by more or less spherical shapes, with surface dents and a high degree of integrity, that is, no cracks or pores could be observed in the outer surfaces. Typical images of microcapsules stabilized by different emulsifiers are shown in Figure 4.2. Apart from size and distribution, no significant differences on the external microstructure were detected regardless of the type of hydrophilic emulsifier.

4.3.2 Role of double emulsions on the microcapsule properties

Figure 4.1 shows how the microcapsule size measured by laser diffraction depends on the emulsion droplet size, considering that oil to wall material ratio was kept constant (1:3). Although the droplet size of double emulsion was around 9 μm after 3 cycles of premix ME regardless of the hydrophilic emulsifier, significant differences were found in the microcapsule size. While the microcapsule $d_{4,3}$ was 2.6 and 2.4 times that of droplet $d_{4,3}$ in $W_1/O/W_2$ emulsions stabilized by WPI and WPI–CMC, respectively, microcapsules from emulsions stabilized with WPI–GA showed a $d_{4,3}$ 4.8 times higher than that of the emulsions droplets. The differences observed with WPI–GA can be related to the behavior of emulsion droplets during spray drying, as it will be discussed below.

Besides the properties of freshly produced $W_1/O/W_2$ emulsions, the microstructure and droplet size distribution of rehydrated microcapsules were analyzed. In fact, the ability to form stable emulsions after rehydration is a relevant property of microcapsules in practical applications. Images in Figure 4.2 show how the rehydrated microcapsules keep the structure of double emulsions for the four hydrophilic emulsifiers, with inner W_1 droplets clearly visible. Similar results were obtained by Rodríguez-Huezo et al. (2004) after rehydrating microcapsules from multiple emulsions containing carotenoids.

Although the inner W_1 droplets were found in all the rehydrated microcapsules, the original $W_1/O/W_2$ emulsion was not fully reconstituted and polydisperse emulsions were obtained after rehydrating microcapsules from WPI–GA and WPI–Chi stabilized emulsions. The distribution of W_1/O droplets in both systems showed a bimodal distribution with two overlapping peaks; one in the region of 14 μm and a smaller one in the zone of 80 μm that led to a major increase in $d_{4,3}$ and span (Figure 4.1c and d). In contrast, W_1/O droplets of rehydrated microcapsules from

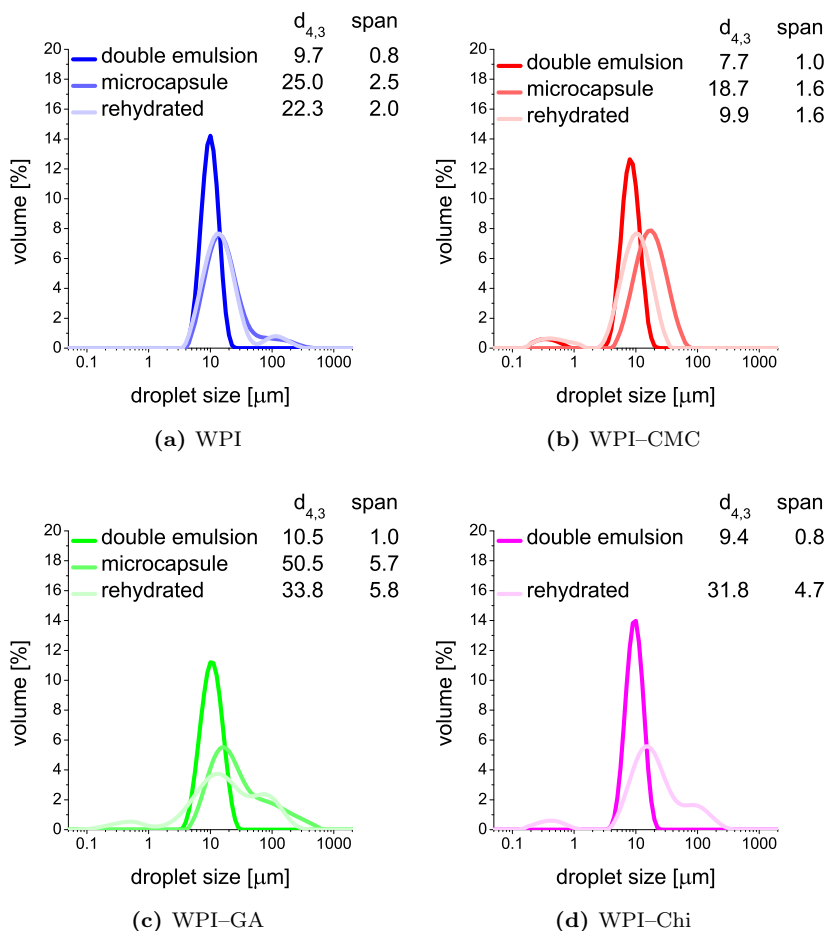Spray dried water-in-oil-in-water emulsions containing procyanidin-rich extracts

Figure 4.1: Size distributions at different stages of the microcapsule production stabilized by (a) 1.0%wt WPI, (b) 0.5%wt WPI−0.25%wt CMC, (c) 0.5%wt WPI−0.5%wt GA, and (d) 0.5%wt WPI−0.05%wt Chi. Size distributions of: 3rd cycle double emulsion premix membrane emulsification, double emulsion microcapsule, and redissolved microcapsule in acetic acid solution.

111

Chapter 4

WPI–CMC presented a monomodal distribution (Figure 4.1b) with a small shift in the oil droplet size, which had a minor impact on $d_{4,3}$ and span. Rehydrated microcapsules from WPI–CMC stabilized emulsions had $d_{4,3}$ values of 9.9 μm and a span of 1.6, just slightly higher than those of double emulsions right after premix ME ($d_{4,3}$ of 7.7 μm and a span of 1.0). In the W_1/O droplet size distribution of rehydrated microcapsules from WPI stabilized emulsions, the formation of some large particles could be observed.

As aforementioned, the progress of droplet stability along the microcapsule production, that is, after producing the emulsion, adding the wall material (maltodextrin) and further spray drying, determines the final properties of the rehydrated microcapsules. Regarding $W_1/O/W_2$ emulsions stabilized with WPI–GA, their lower stability compared with that of the other emulsions could be the reason of the high dispersion observed in the rehydrated microcapsules. In Chapter 3, the creaming rate of WPI–GA stabilized double emulsions showed that emulsions were quite unstable within some minutes after production (creaming velocity of 22.6 $\text{mm}\,\text{h}^{-1}$), bridge flocculation was suggested to occur. In the case of WPI–Chi stabilized emulsions, droplet instability can be caused by the addition of wall material, inducing depletion flocculation, in which depletion forces result from maltodextrin addition which would outweigh repulsive forces, leading to coalescence and thus to large droplet sizes. At those conditions a highly polydisperse emulsion was formed, as the droplet size distribution of the rehydrated microcapsules showed (see Figure 4.1d). Other authors observed depletion flocculation from non-adsorbed chitosan (Klinkesorn and Namatsila, 2009, Speiciene et al., 2007) and from maltodextrin (Gharsallaoui et al., 2012) under similar conditions.

Considering that a major property of dehydrated emulsions for consumer use is that the rehydrated microcapsules have the same droplet size distribution as the parent emulsions, WPI–CMC complex was the best emulsifier among the ones investigated. The reasons of its good performance seem to rely on its ability to prevent emulsion instability, what can be correlated to a thick interfacial layer (2.2 nm versus 0.6 nm of WPI) and a significant high surface charge (see ζ-potential in Table 4.1) resulting in steric hindrance and electrostatic repulsions as mechanisms of droplet stabilization. During atomization and drying droplets are forced in close proximity, which is the reason why creating short-range steric and electric repulsions between neighboring droplets has been suggested as an approach to prevent attractive interactions (Gharsallaoui et al., 2010) that may end up in flocculation and subsequent coalescence. In addition WPI–CMC significantly increased the viscosity of the continuous phase, an important factor to reduce creaming phenomena.

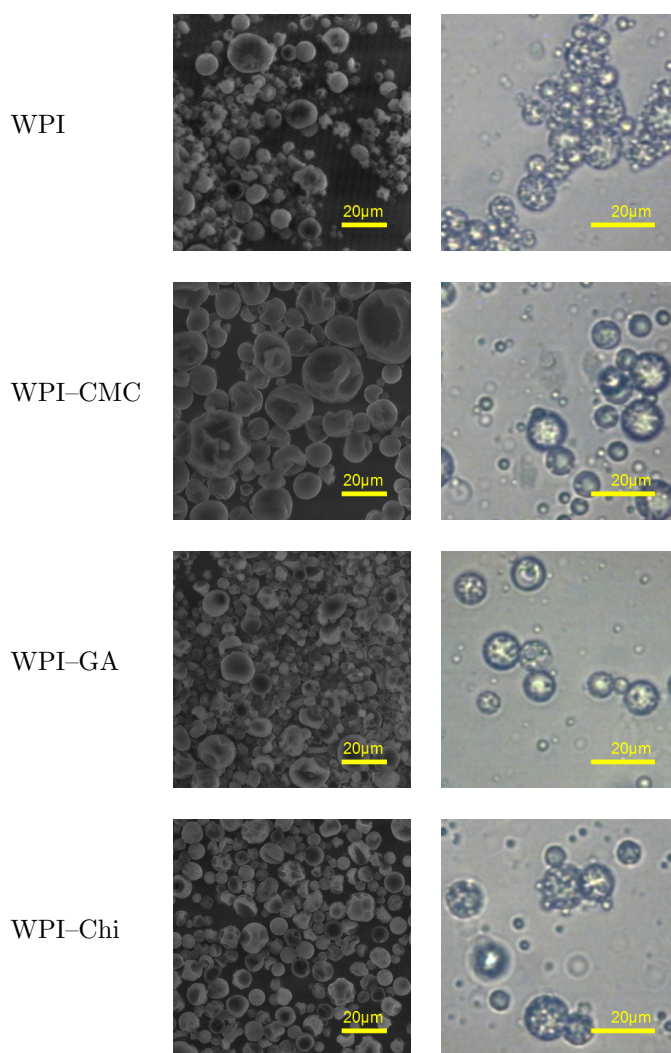Spray dried water-in-oil-in-water emulsions containing procyanidin-rich extracts

WPI

WPI–CMC

WPI–GA

WPI–Chi

Figure 4.2: Left hand side) ESEM images of microcapsules with a magnification of $900\times$, Right hand side) microscopic images of rehydrated microcapsules in acetic acid solution, for the four different hydrophilic emulsifiers.

Chapter 4

In terms of encapsulation efficiency, however, we observed that the $EE\mu capsule$ value did not show significant differences regardless of the hydrophilic emulsifier. When we analyze the procyanidin encapsulation during emulsification (Table 4.4), $W_1/O/W_2$ emulsions stabilized with any of the WPI–polysaccharide complexes led to significant higher values ($EEemulsion$ between 71.8% and 73.5%) than those stabilized with single WPI ($EEemulsion = 68\%$). Procyanidin release at this stage is mainly controlled by the escape of inner W_1 droplets as the size of W_1/O droplets is reduced in each premix ME cycle. Considering this, WPI–polysaccharide complexes slightly improved the procyanidin retention in W_1 during premix ME. In contrast, after spray drying and microcapsule formation, procyanidin migration is limited by the combined resistance of the oil phase and the interfacial O–W_2 layer within the powder.

The case of WPI–CMC stabilized emulsions and the further microcapsules shows that different mechanisms seem to determine the amount of procyanidins in the microcapsule and how procyanidins are distributed. Emulsions stabilized with WPI–CMC resulted in the highest droplet stability over the whole process of microcapsule production (see the droplet size distribution of the rehydrated microcapsules) and the highest value in procyanidin content in the microcapsules (Table 4.4), while $EE\mu capsule$ was not significantly higher than that showed by the other emulsifiers. According to this, it seems that to keep the emulsion monodisperse with a low droplet size facilitated the encapsulation of W_1/O droplets, being able to increase the total procyanidin content, which was also seen for single emulsions (Ramakrishnan et al., 2014). Nevertheless, the high interfacial area resulting from the narrow droplet size distribution acted as a promoter of procyanidin migration. The barrier properties of the oil phase and the interfacial O–W_2 layer with WPI–CMC complex mitigated this just partially, as the similar values of $EE\mu capsule$ obtained for the differently formulated microcapsules show. Considering all this, a strategy to improve the encapsulation efficiency of procyanidins should be considered to coat emulsion droplets with interfacial layers able to stabilize the emulsion over the entire production process and increase their capacity to retain procyanidins.

4.4   Conclusions

Double emulsions were produced by premix ME and subsequent spray drying enabled to encapsulate a procyanidin-rich extract in powder form. At the operating conditions, the emulsions stabilized with WPI or WPI–polysaccharide complexes

showed good resistance to dehydration so that they could be converted into powders, retaining procyanidins. Even though all the spray dried double emulsions recovered the structure of $W_1/O/W_2$ emulsions after rehydration, with a clearly differentiated W_1 phase, only rehydrated microcapsules from double emulsions stabilized by WPI–CMC were able to recover the droplet size distribution of the fresh ones. In this case, emulsions were able to keep their droplet stability over the whole production process, i.e. from emulsification to spray drying. Bridge flocculation of the $W_1/O/W_2$ emulsions stabilized with WPI–GA and depletion flocculation after addition of maltodextrin to the WPI–Chi stabilized emulsions are the suggested instability mechanisms that resulted in polydisperse droplets after microcapsule rehydration.

Results on encapsulation efficiency indicated that between 72.5% and 79.9% of the procyanidins in microcapsules were entrapped in inner W_1 droplets, regardless of the hydrophilic emulsifier. It has been shown that, WPI–CMC complex was able to truly stabilize the W_1/O droplets during the different stages of microcapsule production but it moderately retained the migration of procyanidins through the W_1–O interface.

According to this, we observed how small changes in hydrophilic emulsifiers have large influence on microcapsules and rehydrated microcapsules. These results suggest that interfacial properties of emulsions prior and during spray drying should be studied in order to increase microcapsule quality.

5

General conclusions and future work

5.1   General conclusions

Premix ME enabled to produce single and double emulsions stabilized with hydrophilic emulsifiers made of WPI–polysaccharide complexes and entrapping a bioactive compound. Regarding emulsion properties, they depended on the process conditions during premix ME, mainly, membrane pore size, transmembrane pressure and number of premix ME cycles, and also on the emulsion formulation. Considering that this project was focused on using protein–polysaccharide complexes due to their surface active and barrier properties, the differences in emulsion formulation were mainly based on the type of hydrophilic emulsifier. The structure of the interfacial layer, determined by the amount and composition of WPI–polysaccharide complex adsorbed at the oil-water interface, had a strong impact on emulsion stability and retention of the encapsulated compound.

When premix ME was applied to produce sunflower O/W emulsions with interfacial structures made of WPI and a WPI–CMC complex (**Chapter 2**), emulsion stability was different according to the composition and number of interfacial layers. Although SPR measurements confirmed the adsorption between the several layers, only O/W emulsions stabilized by one interfacial layer (either WPI or WPI–CMC complex) did not coalesce after preparation. Even though WPI emulsions showed a mean droplet size close to the pore membrane size (10 μm), a significant amount of much smaller droplets contribute to increase droplet dispersion. This seemed to affect emulsion stability during storage. Non-washed emulsions, containing free emulsifier in the bulk water phase, were much more stable than their washed counterpart, what suggests that reducing the non-adsorbed WPI in the water solution (either as a complex or isolated) by centrifugation did contribute to droplet flocculation and further coalescence. A redistribution of WPI and WPI–CMC complex at the droplet interface may be the reason of the much lower stability.

The oxidation rate of sunflower O/W emulsions strongly depended on the interfacial composition: TBARS in WPI–CMC stabilized emulsions increased much faster than in emulsions with WPI. Adsorption data at a hydrophobic interface and the electrical charge of the WPI–CMC complex suggest that it formed a thick but less dense interface than WPI with a negative charge able to attract any transition metal ion and promote lipid oxidation. This research suggests that the strategies to improve the oxidation stability of O/W emulsions by tailoring their interface should consider multi-layer arrangements, e.g. made of WPI, or protein–polysaccharide complexes having a positive electrical charge at the emulsion conditions, among others.

Chapter 5

In the case of $W_1/O/W_2$ emulsions entrapping a procyanidin-rich extract and stabilized by WPI–CMC, WPI–GA, or WPI–Chi (**Chapter 3**), the encapsulation of procyanidin was at least 70% at the end of the emulsification step, regardless the hydrophilic emulsifier used. Procyanidin encapsulation decreased with each premix ME cycle, mainly linked to the escape of the inner W_1 phase as a result of the break-up of W_1/O droplets. Even though no important differences in the polyphenol encapsulation were observed among emulsions stabilized with WPI–polysaccharide complexes, data about the shear stress in the membrane pores would help to better determine the effect of those on the break-out of inner W_1 droplet.

Stability of $W_1/O/W_2$ emulsions, encompassing creaming rate, droplet size distribution and polyphenol release during storage, was affected by the type of WPI–polysaccharide complex used as emulsifier. In the case of creaming rate, the viscosity imposed by each WPI–polysaccharide complex to the W_2 phase was a parameter to consider. The progress of the droplet size distribution during storage, in turn, was affected by pH, due to its influence on the surface charge of emulsion droplets as well as on the interactions between WPI and each polysaccharide. Hence, different windows of pH values, in which emulsions kept droplet size distribution stable, were identified for each WPI–polysaccharide complex. Furthermore, release rate constants during 14 days of storage ranged from 5.6 to 11.3 $\mu g\,mL^{-1}min^{-0.5}$ and depended more on the type of hydrophilic emulsifier than on pH environment. When the release rate constants were related to the thickness of the interfacial layer made of WPI–polysaccharides (obtained from SPRi measurements), we observed that thicker layers led to lower release rates. Further research on the relationship between the properties of tailor-made interfaces with the diffusion of entrapped bioactive compounds is required to optimize each.

Solid microcapsules, containing a procyanin-rich extract, were obtained by spray drying $W_1/O/W_2$ emulsions produced by premix ME (**Chapter 4**). At the operating conditions, the emulsions stabilized with WPI or WPI–polysaccharide complexes showed good resistance to dehydration so that they could be converted into powders, retaining procyanidins. Even though all the spray dried double emulsions recovered the structure of $W_1/O/W_2$ emulsions after rehydration, with a clearly differentiated W_1 phase, only rehydrated microcapsules from double emulsions stabilized by WPI–CMC were able to recover the droplet size distribution of the fresh ones. In this case, emulsions were able to keep their droplet stability over the whole production process, i.e. from emulsification to spray drying. Bridge flocculation of the $W_1/O/W_2$ emulsions stabilized with WPI–GA and depletion

flocculation after addition of maltodextrin to the WPI–Chi stabilized emulsions are the suggested instability mechanisms that resulted in polydisperse droplets after microcapsule rehydration. Results on encapsulation efficiency indicated that between 72.5% and 79.9% of the procyanidins in microcapsules were entrapped in the inner W_1 droplets, regardless the hydrophilic emulsifier. It has been shown that, WPI–CMC complex was able to truly stabilize the W_1/O droplets during the different stages of microcapsule production but it moderately retained the migration of procyanidins through the W_1/O interface. According to this, we observed how small changes in hydrophilic emulsifiers have large influence on microcapsules and rehydrated microcapsules. These results suggest that interfacial properties of emulsions prior and during spray drying should be studied in order to increase microcapsule quality.

For every type of encapsulation (single emulsion, double emulsion and spray dried double emulsion) a tailor-made hydrophilic emulsifier is required to comply with the type of protection needed, the addenda used and the desired site of delivery.

5.2   Future work

The oxidation behavior of sunflower O/W emulsions stabilized with several WPI and CMC interfaces showed (**Chapter 2**) that a thin compact positive WPI layer could better protect against oil oxidation than a thick non-compact negative WPI–CMC layer. These results suggested that the fast oxidation observed in O/W emulsions stabilized WPI–CMC complex was mainly caused by the negative charge of the droplet interface. Although WPI–Chi complexes have a narrow range of environmental conditions in where they can effectively protect the emulsion droplet (depletion flocculation easily occurs), they can form thick positively charged interfaces. Therefore, WPI–Chi could be a good candidate to protect emulsion against oil oxidation. Another approach would be to produce a layer-by-layer interface with an external layer made of positively charged WPI. Regarding the use of multi-layer systems to stabilize O–W interfaces, further research should be undertaken to investigate the properties at the interface of WPI in combination with other polysaccharides. Even though SPRi adsorption measurements showed that WPI–CMC interfacial layers were less dense than WPI layers, it would be interesting to consider other WPI–polysaccharide complexes that, upon layer-by-layer deposition, could form denser interfaces able to successfully stabilize emulsion droplets.

The effect of the environmental conditions, such as pH, on the interfacial properties of WPI and WPI–polysaccharide complexes could be further investigated by means of SPRi. These measurements would provide insight on how pH affects the thickness and density of the interfacial layers and about the mechanisms controlling the emulsion stability.

Fourier-Transform Infrared Microspectroscopy (ATR-IRMS) is a novel technique that could have several applications in the frame of the present project: i) to quantify the amount of proteins and polysaccharides adsorbed at the O–W interface and ii) to monitor oil oxidation in emulsions and solid microcapsules. A promising start had been made, where the main problem was sample preparation, in particular, water evaporation from the emulsions when a sample was deposited on a slide which led to instable emulsions, but on the other hand to avoid the large effect of water on the FTIR signal.

As stated in Chapter 1, encapsulation systems to entrap sensitive compounds can i) protect them from environmental effects, ii) be used as delivery system, and iii) mask undesired sensory attributes. In this research we mainly focussed on the first, protection, while delivery and masking did not have our focus. Since the to be protected compounds often have an off-taste, such as fish oil and procyanidin, continuation of the research could increase its focus on masking off-flavors. Masking off-flavours can be achieved by protecting the encapsulation system from specific environmental effects, namely saliva. Saliva is an aqueous solution of salts, proteins and enzymes which can deteriate emulsions leading to delivery of the sensitive compounds. A saliva model could help to simulate and investigate the stability of emulsions under these conditions.

Concerning the stability of procyanidins entrapped in the double emulsions and solid microcapsules (**Chapters 3** and **4**), analytical determinations shoud be performed to establish if the chemical composition of the mixture of monomers up to pentamers present in the procyanidin-rich extract evolve during emulsification and/or drying and further storage.

122

References

S. Adachi, H. Imaoka, H. Ashida, H. Maeda, and R. Matsuno. Preparation of microcapsules of W/O/W emulsions containing a polysaccharide in the outer aqueous phase by spray-drying. *European Journal of Lipid Science and Technology*, 106(4):225–231, 2004.

S. L. Anna, N. Bontoux, and H. A. Stone. Formation of dispersions using "flow focusing" in microchannels. *Applied Physics Letters*, 82(3):364–366, 2003.

T. Aoki, E. A. Decker, and D. McClements. Influence of environmental stresses on stability of O/W emulsions containing droplets stabilized by multilayered membranes produced by a layer-by-layer electrostatic deposition technique. *Food Hydrocolloids*, 19(2):209–220, 2005.

M. Augustin and Y. Hemar. Nano- and micro-structured assemblies for encapsulation of food ingredients. *Chemical Society Reviews*, 38(4):902–912, 2009.

A. Benichou, A. Aserin, and N. Garti. Double emulsions stabilized by new molecular recognition hybrids of natural polymers. *Polymers for Advanced Technologies*, 1031(10–12):1019–1031, 2003.

A. Benichou, A. Aserin, and N. Garti. Double emulsions stabilized with hybrids of natural polymers for entrapment and slow release of active matters. *Advances in Colloid and Interface Science*, 108–109:29–41, 2004.

F. Bernheim, M. Bernheim, and K. Wilbur. The reaction between thiobarbituric acid and the oxidation products of certain lipides. *Journal of biological chemistry*, 174(1):257–264, 1948.

S. Bjerregaard, I. Söderberg, C. Vermehren, and S. Frokjaer. Formulation and evaluation of release and swelling mechanism of a water-in-oil emulsion using factorial design. *International Journal of Pharmaceutics*, 193(1):1–11, 1999.

L. Booysen, L. Kalombo, E. Brooks, R. Hansen, J. Gilliland, V. Gruppo, P. Lungenhofer, B. Semete-Makokotlela, H. Swai, A. Kotze, A. Lenaerts, and L. Du Plessis. In vivo/in vitro pharmacokinetic and pharmacodynamic study of spray-dried poly-(DL-lactic-*co*-glycolic) acid nanoparticles encapsulating rifampicin and isoniazid. *International Journal of Pharmaceutics*, 444(1–2):10–17, 2013.

M. Bos and T. van Vliet. Interfacial rheological properties of adsorbed protein layers and surfactants: a review. *Advances in Colloid and Interface Science*, 91 (3):437–471, 2001.

M. M. Bradford. A rapid and sensitive method for the quantitation of microgram quantities of protein utilizing the principle of protein–dye binding. *Analytical Biochemistry*, 72(1–2):248–254, 1976.

H. Breisig, J. Hoppe, T. Melin, and M. Wessling. On the droplet formation in hollow-fiber emulsification. *Journal of Membrane Science*, 467(0):109–115, 2014.

M. Brückner, M. Bade, and B. Kunz. Investigations into the stabilization of a volatile aroma compound using a combined emulsification and spray drying process. *European Food Research and Technology*, 226(1–2):137–146, 2007.

I. Capek. Degradation of kinetically-stable O/W emulsions. *Advances in Colloid and Interface Science*, 107(2–3):125–155, 2004.

R. Chanamai and D. McClements. Comparison of gum arabic, modified starch, and whey protein isolate as emulsifiers: Influence of pH, $CaCl_2$ and temperature. *Journal of Food Science*, 67(1):120–125, 2002.

C. Charcosset. Preparation of emulsions and particles by membrane emulsification for the food processing industry. *Journal of Food Engineering*, 92(3):241–249, 2009.

R. Charoen, A. Jangchud, K. Jangchud, T. Harnsilawat, E. A. Decker, and D. J. McClements. Influence of interfacial composition on oxidative stability of oil-in-water emulsions stabilized by biopolymer emulsifiers. *Food Chemistry*, 131(4): 1340–1346, 2012.

B. Chen, D. J. McClements, D. A. Gray, and E. A. Decker. Stabilization of soybean oil bodies by enzyme (laccase) cross-linking of adsorbed beet pectin coatings. *Journal of Agricultural and Food Chemistry*, 58(16):9259–9265, 2010.

C. Cooper, P. Dubin, A. Kayitmazer, and S. Turksen. Polyelectrolyte–protein complexes. *Current Opinion in Colloid & Interface Science*, 10(1–2):52–78, 2005.

K. Damianou and V. Kiosseoglou. Stability of emulsions containing a whey protein concentrate obtained from milk serum through carboxymethylcellulose complexation. *Food Hydrocolloids*, 20(6):793–799, 2006.

C. de Kruif, F. Weinbreck, and R. de Vries. Complex coacervation of proteins and anionic polysaccharides. *Current Opinion in Colloid & Interface Science*, 9(5): 340–349, 2004.

K. Desai and H. Park. Recent developments in microencapsulation of food ingredients. *Drying Technology*, 23(7):1361–1394, 2005.

E. Dickinson. Properties of emulsions stabilized with milk proteins: Overview of some recent developments. *Journal of Dairy Science*, 80(10):2607–2619, 1997.

E. Dickinson. Hydrocolloids at interfaces and the influence on the properties of dispersed systems. *Food Hydrocolloids*, 17(1):25–39, 2003.

E. Dickinson. Interfacial structure and stability of food emulsions as affected by protein–polysaccharide interactions. *Soft Matter*, 4(5):932–942, 2008.

E. Dickinson. Hydrocolloids as emulsifiers and emulsion stabilizers. *Food Hydrocolloids*, 23(6):1473–1482, 2009.

E. Dickinson. Mixed biopolymers at interfaces: Competitive adsorption and multilayer structures. *Food Hydrocolloids*, 25(8):1966–1983, 2011a.

E. Dickinson. Mixed biopolymers at interfaces: Competitive adsorption and multilayer structures. *Food Hydrocolloids*, 25(8):1966–1983, 2011b.

E. Dickinson and E. Parkinson. Heat-induced aggregation of milk protein-stabilized emulsions: sensitivity to processing and composition. *International Dairy Journal*, 14(7):635–645, 2004.

E. Dickinson and M. G. Semenova. Emulsifying properties of covalent protein–dextran hybrids. *Colloids and Surfaces*, 64(3-4):299–310, 1992.

T. Driessen and R. Jeurissen. A regularised one-dimensional drop formation and coalescence model using a total variation diminishing (TVD) scheme on a single eulerian grid. *International Journal of Computational Fluid Dynamics*, 25(6):333–343, 2011.

B. E. Dybowska. Whey protein-stabilized emulsion properties in relation to thermal modification of the continuous phase. *Journal of Food Engineering*, 104(1):81–88, 2011.

A. Edris and B. Bergnståhl. Encapsulation of orange oil in a spray dried double emulsion. *Nahrung/Food*, 45(2):133–137, 2001.

M. Evans, I. Ratcliffe, and P. Williams. Emulsion stabilisation using polysaccharideprotein complexes. *Current Opinion in Colloid & Interface Science*, 18(4):272–282, 2013.

J. Fang, P. Wang, X. Du, and D.-M. Zhu. Detailed analysis of quartz crystal microbalance and surface plasmon resonance spectroscopy in probing molecular adsorption onto solid-liquid interfaces. *Journal of Physical Chemistry C*, 113 (36):16121–16127, 2009.

Z. Fang and B. Bhandari. Encapsulation of polyphenols – a review. *Trends in Food Science & Technology*, 21(10):510–523, 2010.

M. Fivash, E. M. Towler, and R. J. Fisher. BIAcore for macromolecular interaction. *Current Opinion in Biotechnology*, 9(1):97–101, 1998.

J. Flanagan and H. Singh. Microemulsions: A potential delivery system for bioactives in food. *Critical Reviews in Food Science and Nutrition*, 46(3):221–237, 2006.

K. Frank, E. Walz, V. Gräf, R. Greiner, K. Köhler, and H. Schuchmann. Stability of anthocyanin-rich W/O/W-emulsions designed for intestinal release in gastrointestinal environment. *Journal of Food Science*, 77(12):N50–N57, 2012.

T. Fuchigami, M. Toki, and K. Nakanishi. Membrane emulsification using sol-gel derived macroporous silica glass. *Journal of Sol-Gel Science and Technology*, 19 (1–3):337–341, 2000.

N. Garti. Double emulsions – scope, limitations and new achievements. *Colloids and Surfaces A: Physicochemical and Engineering Aspects*, 123–124:233–246, 1997.

M. J. Geerken, R. G. Lammertink, and M. Wessling. Interfacial aspects of water drop formation at micro-engineered orifices. *Journal of Colloid and Interface Science*, 312(2):460–469, 2007.

A. Gharsallaoui, G. Roudaut, O. Chambin, A. Voilley, and R. Saurel. Applications of spray-drying in microencapsulation of food ingredients: An overview. *Food Research International*, 40(9):1107–1121, 2007.

A. Gharsallaoui, K. Yamauchi, O. Chambin, E. Cases, and R. Saurel. Effect of high methoxyl pectin on pea protein in aqueous solution and at oil / water interface. *Carbohydrate Polymers*, 80(3):817–827, 2010.

A. Gharsallaoui, G. Roudaut, L. Beney, O. Chambin, A. Voilley, and R. Saurel. Properties of spray-dried food flavours microencapsulated with two-layered membranes : Roles of interfacial interactions and water. *Food Chemistry*, 132 (4):1713–1720, 2012.

B. Gibbs, S. Kermasha, I. Alli, and C. Mulligan. Encapsulation in the food industry: A review. *International Journal of Food Sciences and Nutrition*, 50(3): 213–224, 1999.

L. Giorno, N. Li, and E. Drioli. Preparation of oil-in-water emulsions using polyamide 10 kDa hollow fiber membrane. *Journal of Membrane Science*, 217 (1–2):173–180, 2003.

L. Giorno, R. Mazzei, M. Oriolo, G. D. Luca, M. Davoli, and E. Drioli. Effects of organic solvents on ultrafiltration polyamide membranes for the preparation of oil-in-water emulsions. *Journal of Colloid and Interface Science*, 287(2):612–623, 2005.

M. Girard, S. Turgeon, and P. Paquin. Emulsifying properties of whey protein–carboxymethylcellulose complexes. *Journal of Food Science*, 67(1):113–119, 2002.

M. Gonthier, J. Donovan, O. Texier, C. Felgines, C. Remesy, and A. Scalbert. Metabolism of dietary procyanidins in rats. *Free Radical Biology and Medicine*, 35(8):837–844, 2003.

S. C. Gopinath. Biosensing applications of surface plasmon resonance-based biacore technology. *Sensors and Actuators B: Chemical*, 150(2):722–733, 2010.

S. Gouin. Microencapsulation: Industrial appraisal of existing technologies and trends. *Trends in Food Science and Technology*, 15(7–8):330–347, 2004.

S. V. D. Graaf, C. G. P. H. Schroën, R. G. M. V. D. Sman, and R. M. Boom. Influence of dynamic interfacial tension on droplet formation during membrane emulsification. *Journal of Colloid and Interface Science*, 277(2):456–463, 2004.

D. Grigoriev and R. Miller. Mono- and multilayer covered drops as carriers. *Current Opinion in Colloid & Interface Science*, 14(1):48–59, 2009.

J. M. C. Gutteridge. Aspects to consider when detecting and measuring lipid peroxidation. *Free Radical Research Communications*, 1(3):173–184, 1986.

D. Guzey and D. McClements. Formation, stability and properties of multilayer emulsions for application in the food industry. *Advances in Colloid and Interface Science*, 128:227–248, 2006.

A. Hafner, J. Filipović-Grčić, D. Voinovich, and I. Jalsenjak. Development and in vitro characterization of chitosan-based microspheres for nasal delivery of promethazine. *Drug Development and Industrial Pharmacy*, 33(4):427–436, 2007.

J. Hammerstone, S. Lazarus, and H. Schmitz. Procyanidin content and variation in some commonly consumed foods. *Journal of Nutrition*, 130(8 Suppl):2086S–2092S, 2000.

P. Hansen, J. Hidalgo, and I. Gould. Reclamation of whey protein with carboxymethylcellulose. *Journal of Dairy Science*, 54(6):830–834, 1971.

P. He, S. Davis, and L. Illum. Sustained release chitosan microspheres prepared by novel spray drying methods. *Journal of Microencapsulation*, 16(3):343–355, 1999.

Y. Hemar, L. Cheng, C. Oliver, L. Sanguansri, and M. Augustin. Encapsulation of resveratrol using water-in-oil-in-water double emulsions. *Food Biophysics*, 5 (2):120–127, 2010.

W. I. Higuchi. Analysis of data on the medicament release from ointments. *Journal of Pharmaceutical Sciences*, 51(8):802–804, 1961.

J. Hoppe and T. Melin. A new technology for producing mono-disperse macroemulsions. *Journal of Membrane Science*, 303(1–2):100–111, 2007.

K. Hosoya, M. Bendo, N. Tanaka, Y. Watabe, T. Ikegami, H. Minakuchi, and K. Nakanishi. An application of silica-based monolithic membrane emulsification technique for easy and efficient preparation of uniformly sized polymer particles. *Macromolecular Materials and Engineering*, 290(8):753–758, 2005.

R. Jiménez-Alvarado, C. Beristain, L. Medina-Torres, A. Román-Guerrero, and E. Vernon-Carter. Ferrous bisglycinate content and release in $W_1/O/W_2$ multiple emulsions stabilized by protein-polysaccharide complexes. *Food Hydrocolloids*, 23(8):2425–2433, 2009.

R. A. L. Jones. *Soft Condensed Matter*. Oxford University Press, 2002.

S. M. Joscelyne and G. Trägårdh. Food emulsions using membrane emulsification: conditions for producing small droplets. *Journal of Food Engineering*, 39(1): 59–64, 1999.

S. M. Joscelyne and G. Trägårdh. Membrane emulsification – a literature review. *Journal of Membrane Science*, 169(1):107–117, 2000.

L. S. Jourdain, M. E. Leser, C. Schmitt, M. Michel, and E. Dickinson. Stability of emulsions containing sodium caseinate and dextran sulfate: Relationship to complexation in solution. *Food Hydrocolloids*, 22(4):647–659, 2008.

L. S. Jourdain, C. Schmitt, M. E. Leser, B. S. Murray, and E. Dickinson. Mixed layers of sodium caseinate + dextran sulfate: Influence of order of addition to oil–water interface. *Langmuir*, 25(16):10026–10037, 2009.

Z. Ju and A. Kilara. Properties of gels induced by heat, protease, calcium salt, and acidulant from calcium ion-aggregated whey protein isolate. *Journal of Dairy Science*, 81(5):1236–1243, 1998.

L. Jung, C. Campbell, T. Chinowsky, M. Mar, and S. Yee. Quantitative interpretation of the response of surface plasmon resonance sensors to adsorbed films. *Langmuir*, 14(19):5636–5648, 1998.

M. S. Katsuda, D. McClements, L. H. S. Miglioranza, and E. A. Decker. Physical and oxidative stability of fish oil-in-water emulsions stabilized with β-lactoglobulin and pectin. *Journal of Agricultural and Food Chemistry*, 56(14): 5926–5931, 2008.

Y. Kawashima, T. Hino, H. Takeuchi, T. Niwa, and K. Horibe. Shear-induced phase inversion and size control of water/oil/water emulsion droplets with porous membrane. *Journal of Colloid and Interface Science*, 145(2):512–523, 1991.

R. Kaye, T. Purewal, and H. Alpar. Simultaneously manufactured nano-in-micro (SIMANIM) particles for dry-powder modified-release delivery of antibodies. *Journal of Pharmaceutical Sciences*, 98(11):4055–4068, 2009.

U. Klinkesorn and Y. Namatsila. Influence of chitosan and NaCl on physicochemical properties of low-acid tuna oil-in-water emulsions stabilized by non-ionic surfactant. *Food Hydrocolloids*, 23(5):1374–1380, 2009.

U. Klinkesorn, P. Sophanodora, P. Chinachoti, E. A. Decker, and D. J. Mc-Clements. Characterization of spray-dried tuna oil emulsified in two-layered interfacial membranes prepared using electrostatic layer-by-layer deposition. *Food Research International*, 39(4):449–457, 2006.

I. Kobayashi, M. Nakajima, K. Chun, Y. Kikuchi, and H. Fujita. Silicon array of elongated through-holes for monodisperse emulsion droplets. *AIChE Journal*, 48(8):1639–1644, 2002a.

I. Kobayashi, M. Yasuno, S. Iwamoto, A. Shono, K. Satoh, and M. Nakajima. Microscopic observation of emulsion droplet formation from a polycarbonate membrane. *Colloids and Surfaces A: Physicochemical and Engineering Aspects*, 207(1–3):185–196, 2002b.

T. Koupantsis and V. Kiosseoglou. Whey protein–carboxymethylcellulose interaction in solution and in oil-in-water emulsion systems. effect on emulsion stability. *Food Hydrocolloids*, 23(4):1156–1163, 2009.

I. Kralova and J. Sjöblom. Surfactants used in food industry: A review. *Journal of Dispersion Science and Technology*, 30(9):1363–1383, 2009.

A. Kubo, H. Shinmori, and T. Takeuchi. Atrazine-imprinted microspheres prepared using a microfluidic device. *Chemical letters*, 35(6):588–589, 2006.

M. Lane, F. Brennan, and O. Corrigan. Comparison of post-emulsification freeze drying or spray drying processes for the microencapsulation of plasmid DNA. *Journal of Pharmacy and Pharmacology*, 57(7):831–838, 2005.

S. Laplante, S. L. Turgeon, and P. Paquin. Emulsion stabilizing properties of various chitosans in the presence of whey protein isolate. *Carbohydrate Polymers*, 59(4):425–434, 2005a.

S. Laplante, S. L. Turgeon, and P. Paquin. Effect of pH, ionic strength, and composition on emulsion stabilising properties of chitosan in a model system containing whey protein isolate. *Food Hydrocolloids*, 19(4):721–729, 2005b.

F. Leal-Calderon, F. Thivilliers, and V. Schmitt. Structured emulsions. *Current Opinion in Colloid & Interface Science*, 12(4–5):206–212, 2007.

T. Learoyd, J. Burrows, E. French, and P. Seville. Sustained delivery of salbutamol and beclometasone from spray-dried double emulsions. *Journal of Microencapsulation*, 27(2):162–170, 2010.

I. Lesschaeve and A. Noble. Polyphenols: factors influencing their sensory properties and their effects on food and beverage preferences. *The American journal of clinical nutrition*, 81(1 Suppl):330S–335S, 2005.

M. Liang, R. Liu, W. Qi, R. Su, Y. Yu, L. Wang, and Z. He. Interaction between lysozyme and procyanidin: Multilevel structural nature and effect of carbohydrates. *Food Chemistry*, 138(2–3):1596–1603, 2013.

S. S. Lim, M. Y. Baik, E. A. Decker, L. Henson, L. M. Popplewell, D. J. McClements, and S. J. Choi. Stabilization of orange oil-in-water emulsions: A new role for ester gum as an Ostwald ripening inhibitor. *Food Chemistry*, 128(4):1023–1028, 2011.

G. D. Luca, A. Sindona, L. Giorno, and E. Drioli. Quantitative analysis of coupling effects in cross-flow membrane emulsification. *Journal of Membrane Science*, 229(1–2):199–209, 2004.

R. Lutz and A. Aserin. *Multiple Emulsions Stabilized by Biopolymers*, pages 85–120. John Wiley & Sons, Inc., 2007.

R. Lutz, A. Aserin, L. Wicker, and N. Garti. Release of electrolytes from W/O/W double emulsions stabilized by a soluble complex of modified pectin and whey protein isolate. *Colloids and Surfaces B: Biointerfaces*, 74(1):178–185, 2009.

A. Madene, M. Jacquot, J. Scher, and S. Desobry. Flavour encapsulation and controlled release – a review. *International Journal of Food Science and Technology*, 41(1):1–21, 2006.

P. Maisuthisakul and M. Gordon. Influence of polysaccharides and storage during processing on the properties of mango seed kernel extract (microencapsulation). *Food Chemistry*, 134(3):1453–1460, 2012.

D. McClements. Theoretical analysis of factors affecting the formation and stability of multilayered colloidal dispersions. *Langmuir*, 21(21):9777–9785, 2005.

D. McClements and E. Decker. Lipid oxidation in oil-in-water emulsions: Impact of molecular environment on chemical reactions in heterogeneous food systems. *Journal of Food Science*, 65(8):1270–1282, 2000.

D. McClements, E. Decker, Y. Park, and J. Weiss. Structural design principles for delivery of bioactive components in nutraceuticals and functional foods. *Critical Reviews in Food Science and Nutrition*, 49(6):577–606, 2009.

D. J. McClements. Nanoemulsions versus microemulsions: terminology, differences, and similarities. *Soft Matter*, 8(6):1719, 2012.

D. J. McClements, E. A. Decker, and J. Weiss. Emulsion-based delivery systems for lipophilic bioactive components. *Journal of Food Science*, 72(8):109–124, 2007.

G. Muschiolik. Multiple emulsions for food use. *Current Opinion in Colloid & Interface Science*, 12(4–5):213–220, 2007.

A. Nazir, K. Schroën, and R. Boom. Premix emulsification: A review. *Journal of Membrane Science*, 362(1–2):1–11, 2010.

N. Neirynck, P. V. der Meeren, S. B. Gorbe, S. Dierckx, and K. Dewettinck. Improved emulsion stabilizing properties of whey protein isolate by conjugation with pectins. *Food Hydrocolloids*, 18(6):949–957, 2004.

T. Nisisako and T. Torii. Microfluidic large-scale integration on a chip for mass production of monodisperse droplets and particles. *Lab on a chip*, 8(2):287–93, 2008.

S. Ogawa, E. A. Decker, and D. J. McClements. Influence of environmental conditions on the stability of oil in water emulsions containing droplets stabilized

by lecithinchitosan membranes. *Journal of Agricultural and Food Chemistry*, 51 (18):5522–5527, 2003.

K. Pays, J. Giermanska-Kahn, B. Pouligny, J. Bibette, and F. Leal-Calderon. Double emulsions: how does release occur? *Journal of Controlled Release*, 79 (1–3):193–205, 2002.

S. Peng and R. Williams. Controlled production of emulsions using a crossflow membrane: Part i: Droplet formation from a single pore. *Chemical Engineering Research and Design*, 76(8):894–901, 1998.

M. Pinent, M. Blay, M. Bladé, M. Salvadó, L. Arola, and A. Ardévol. Grape seed-derived procyanidins have an antihyperglycemic effect in streptozotocin-induced diabetic rats and insulinomimetic activity in insulin-sensitive cell lines. *Endocrinology*, 145(11):4985–4990, 2004.

S. Prigent, A. Voragen, G. van Koningsveld, A. Baron, C. Renard, and H. Gruppen. Interactions between globular proteins and procyanidins of different degrees of polymerization. *Journal of Dairy Science*, 92(12):5843–5853, 2009.

S. Ramakrishnan, M. Ferrando, L. Aceña Muñoz, S. De Lamo-Castellví, and C. Güell. Fish oil microcapsules from O/W emulsions produced by premix membrane emulsification. *Food and Bioprocess Technology*, 6(11):3088–3101, 2013.

S. Ramakrishnan, M. Ferrando, L. Aceña Muñoz, M. Mestres, S. De Lamo-Castellví, and C. Güell. Influence of emulsification technique and wall composition on physicochemical properties and oxidative stability of fish oil microcapsules produced by spray drying. *Food and Bioprocess Technology*, 7(7): 1959–1972, 2014.

G. Richardson. *Standard methods for the examination of dairy products*. Washington, DC: American Public Health Association, 1985.

M. Rodríguez-Huezo, R. Pedroza-Islas, L. Prado-Barragán, C. Beristain, and E. Vernon-Carter. Microencapsulation by spray drying of multiple emulsions containing carotenoids. *Journal of Food Science*, 69(7):E351–E359, 2004.

J. M. Rodríguez Patino and A. M. Pilosof. Protein–polysaccharide interactions at fluid interfaces. *Food Hydrocolloids*, 25(8):1925–1937, 2011.

C. Santos-Buelga and A. Scalbert. Proanthocyanidins and tannin-like compounds
- nature, occurrence, dietary intake and effects on nutrition and health. *Journal
of the Science of Food and Agriculture*, 80(7):1094–1117, 2000.

C. Schmitt and S. L. Turgeon. Protein/polysaccharide complexes and coacervates
in food systems. *Advances in Colloid and Interface Science*, 167(1–2):63–70,
2011.

C. Schmitt, C. Sanchez, S. Desobry-Banon, and J. Hardy. Structure and techno-
functional properties of protein-polysaccharide complexes: A review. *Critical
Reviews in Food Science and Nutrition*, 38(8):689–753, 1998.

V. Schröder, O. Behrend, and H. Schubert. Effect of dynamic interfacial tension
on the emulsification process using microporous, ceramic membranes. *Journal
of Colloid and Interface Science*, 202(2):334–340, 1998.

M. Semenova. Thermodynamic analysis of the impact of molecular interactions on
the functionality of food biopolymers in solution and in colloidal systems. *Food
Hydrocolloids*, 21(1):23–45, 2007.

Y. Serfert, J. Schröder, A. Mescher, J. Laackmann, K. Rätzke, M. Shaikh,
V. Gaukel, H.-U. Moritz, H. Schuchmann, P. Walzel, S. Drusch, and
K. Schwarz. Spray drying behaviour and functionality of emulsions with β-
lactoglobulin/pectin interfacial complexes. *Food Hydrocolloids*, 31(2):438–445,
2013.

F. Shahidi and M. Naczk. *Phenolics in food and nutraceuticals*. CRC press, 2003.

M. Shima, M. Tanaka, T. Fujii, K. Egawa, Y. Kimura, S. Adachi, and R. Matsuno.
Oral administration of insulin included in fine W/O/W emulsions to rats. *Food
Hydrocolloids*, 20(4):523–531, 2006.

H. D. Silva, M. A. Cerqueira, and A. A. Vicente. Nanoemulsions for food appli-
cations: Development and characterization. *Food and Bioprocess Technology*, 5
(3):854–867, 2012.

V. Singleton and J. A. Rossi. Colorimetry of total phenolics with phosphomolybdic-
phosphotungstic acid reagents. *American Journal of Enology and Viticulture*,
16(3):144–158, 1965.

P. Sipos, A. Szabó, I. Erõs, and P. Szabó-Révész. A dsc and raman spectroscopic
study of microspheres prepared with polar cosolvents by different techniques.
Journal of Thermal Analysis and Calorimetry, 94(1):109–118, 2008.

S. Somavarapu, S. Pandit, G. Gradassi, M. Bandera, E. Ravichandran, and O. Alpar. Effect of vitamin E TPGS on immune response to nasally delivered diphtheria toxoid loaded poly(caprolactone) microparticles. *International Journal of Pharmaceutics*, 298(2):344–347, 2005.

K. Sotoyama, Y. Asano, K. Ihara, K. Takahashi, and K. Doi. Water/oil emulsions prepared by the membrane emulsification method and their stability. *Journal of Food Science*, 64(2):211–215, 1999.

V. Speiciene, F. Guilmineau, U. Kulozik, and D. Leskauskaite. The effect of chitosan on the properties of emulsions stabilized by whey proteins. *Food Chemistry*, 102(4):1048–1054, 2007.

B. Sperber, H. Schols, M. C. Stuart, W. Norde, and A. Voragen. Influence of the overall charge and local charge density of pectin on the complex formation between pectin and β-lactoglobulin. *Food Hydrocolloids*, 23(3):765–772, 2009.

S. Sugiura, M. Nakajima, and M. Seki. Preparation of monodispersed emulsion with large droplets using microchannel emulsification. *Journal of the American Oil Chemists' Society*, 79(5):515–519, 2002.

J. Surh, G. Vladisavljević, S. Mun, and D. McClements. Preparation and characterization of water/oil and water/oil/water emulsions containing biopolymer-gelled water droplets. *Journal of Agricultural and Food Chemistry*, 55(1):175–184, 2007.

K. Suzuki, I. Fujiki, and Y. Hagura. Preparation of corn oil/water and water/corn oil emulsions using PTFE membranes. *Food Science and Technology International, Tokyo*, 4(2):164–167, 1998.

H. Tawfeek, S. Khidr, E. Samy, S. Ahmed, M. Murphy, A. Mohammed, A. Shabir, G. Hutcheon, and I. Saleem. Poly(glycerol adipate-co-ω-pentadecalactone) spray-dried microparticles as sustained release carriers for pulmonary delivery. *Pharmaceutical Research*, 28(9):2086–2097, 2011.

H. Tawfeek, A. Evans, A. Iftikhar, A. Mohammed, A. Shabir, S. Somavarapu, G. Hutcheon, and I. Saleem. Dry powder inhalation of macromolecules using novel PEG-co-polyester microparticle carriers. *International Journal of Pharmaceutics*, 441(1–2):611–619, 2013.

C. Thongkaew, M. Gibis, J. Hinrichs, and J. Weiss. Polyphenol interactions with whey protein isolate and whey protein isolatepectin coacervates. *Food Hydrocolloids*, 41(0):103–112, 2014.

T. Thorsen, R. W. Roberts, F. H. Arnold, and S. R. Quake. Dynamic pattern formation in a vesicle-generating microfluidic device. *Physical Review Letters*, 86(18):4163–4166, 2001.

V. B. Tolstoguzov. Functional properties of food proteins and role of protein–polysaccharide interaction. *Food Hydrocolloids*, 4(6):429–468, 1991.

L. Tshweu, L. Katata, L. Kalombo, and H. Swai. Nanoencapsulation of water-soluble drug, lamivudine, using a double emulsion spray-drying technique for improving hiv treatment. *Journal of Nanoparticle Research*, 15(11):1–11, 2013.

V. Tsukruk and V. Bliznyuk. Adhesive and friction forces between chemically modified silicon and silicon nitride surfaces. *Langmuir*, 14(2):446–455, 1998.

S. Turgeon, C. Schmitt, and C. Sanchez. Protein–polysaccharide complexes and coacervates. *Current Opinion in Colloid & Interface Science*, 12(4–5):166–178, 2007.

P. B. Umbanhowar, V. Prasad, and D. A. Weitz. Monodisperse emulsion generation via drop break off in a coflowing stream. *Langmuir*, 16(2):347–351, 2000.

A. S. Utada, E. Lorenceau, D. R. Link, P. D. Kaplan, H. A. Stone, and D. A. Weitz. Monodisperse double emulsions generated from a microcapillary device. *Science*, 308(5721):537–541, 2005.

S. van der Graaf, C. Schroën, and R. Boom. Preparation of double emulsions by membrane emulsification–a review. *Journal of Membrane Science*, 251(1–2):7–15, 2005.

E. van der Zwan, K. Schroën, K. van Dijke, and R. Boom. Visualization of droplet break-up in pre-mix membrane emulsification using microfluidic devices. *Colloids and Surfaces A: Physicochemical and Engineering Aspects*, 277(1–3):223–229, 2006.

K. C. van Dijke, K. Schroën, A. van der Padt, and R. Boom. EDGE emulsification for food-grade dispersions. *Journal of Food Engineering*, 97(3):348–354, 2010.

G. Vladisavljević, J. Surh, and D. McClements. Effect of emulsifier type on droplet disruption in repeated shirasu porous glass membrane homogenization. *Langmuir*, 22(10):4526–4533, 2006a.

G. T. Vladisavljević and R. A. Williams. Recent developments in manufacturing emulsions and particulate products using membranes. *Advances in Colloid and Interface Science*, 113(1):1–20, 2005.

G. T. Vladisavljević, M. Shimizu, and T. Nakashima. Preparation of monodisperse multiple emulsions at high production rates by multi-stage premix membrane emulsification. *Journal of Membrane Science*, 244(1–2):97–106, 2004.

G. T. Vladisavljević, M. Shimizu, and T. Nakashima. Production of multiple emulsions for drug delivery systems by repeated SPG membrane homogenization: Influence of mean pore size, interfacial tension and continuous phase viscosity. *Journal of Membrane Science*, 284(1–2):373–383, 2006b.

L. Wen and K. D. Papadopoulos. Effects of osmotic pressure on water transport in $W_1/O/W_2$ emulsions. *Journal of Colloid and Interface Science*, 235(2):398–404, 2001.

G. Williamson and C. Manach. Bioavailability and bioefficacy of polyphenols in humans. ii. review of 93 intervention studies. *The American journal of clinical nutrition*, 81(1 Suppl):243S–255S, 2005.

J. Yamakoshi, S. Kataoka, T. Koga, and T. Ariga. Proanthocyanidin-rich extract from grape seeds attenuates the development of aortic atherosclerosis in cholesterol-fed rabbits. *Atherosclerosis*, 142(1):139–149, 1999.

N. Yamazaki, K. Naganuma, M. Nagai, G. Ma, and S. Omi. Preparation of W/O (waterinoil) emulsions using a PTFE (polytetrafluoroethylene) membrane – a new emulsification device. *Journal of Dispersion Science and Technology*, 24(2): 249–257, 2003.

F. Yuan, Y. Gao, E. Decker, and D. McClements. Modulation of physicochemical properties of emulsified lipids by chitosan addition. *Journal of Food Engineering*, 114(1):1–7, 2013.

B. Zeeb, M. Gibis, L. Fischer, and J. Weiss. Influence of interfacial properties on ostwald ripening in crosslinked multilayered oil-in-water emulsions. *Journal of Colloid & Interface Science*, 387(1):65–73, 2012.

J. Zhu and D. Barrow. Analysis of droplet size during crossflow membrane emulsifi-
cation using stationary and vibrating micromachined silicon nitride membranes.
Journal of Membrane Science, 261(1–2):136–144, 2005.

Rikkert Berendsen

Doctoral Thesis